Hydrology of the Sudanian Savannah in West Africa, Burkina Faso

THÈSE N^{O} 6011 (2014)

PRÉSENTÉE LE 17 JANVIER 2014

À LA FACULTÉ DE L'ENVIRONNEMENT NATUREL, ARCHITECTURAL ET CONSTRUIT
LABORATOIRE DE MÉCANIQUE DES FLUIDES DE L'ENVIRONNEMENT
PROGRAMME DOCTORAL EN ENVIRONNEMENT

ÉCOLE POLYTECHNIQUE FÉDÉRALE DE LAUSANNE

POUR L'OBTENTION DU GRADE DE DOCTEUR ÈS SCIENCES

PAR

Theophile MANDE

acceptée sur proposition du jury:

Prof. F. Golay, président du jury
Prof. M. Parlange, Dr A. Repetti, directeurs de thèse
Prof. A. Berne, rapporteur
Prof. G. G. Katul, rapporteur
Prof. N. C. van de Giesen, rapporteur

ÉCOLE POLYTECHNIQUE
FÉDÉRALE DE LAUSANNE
Suisse
2013

À mes parents : Feu Mande Saïdou Emmanuel et Zoungrana Tiga Félicité

Acknowledgements / Remerciements

‘‘Un proverbe mossi (ethnie du Burkina) dit : Qu’il est difficile voire impossible de ramasser de la farine avec un seul doigt : ‘‘**Nougbi yendé ka wouk’d zoome yé’’**. Je veux donc humblement remercier toutes les personnes qui ont participé de près ou de loin à la préparation et à l’exécution de ce magnifique voyage qu’est la thèse de doctorat.

Je tiens tout d’abord à remercier mes directeurs de thèse Marc B Parlange et Alexandre Repetti. Ils ont été pour moi les personnes qui m’ont appris à me lever, à marcher et même à courir dans le monde complexe et exigeant de la recherche. Leurs confiances, leurs soutiens et leurs conseils avisés m’ont permis d’atteindre cette étape. Je vous serai éternellement reconnaissant.

À mes collègues de laboratoire : Marie José Pellaud « la maman » de l’EFLUM, qui comme une bonne maman a su bien prendre soin de nous. Profites de ta retraite bien méritée, tu vas beaucoup nous manquer. Jacques Golay, pour ton aide dans la conception, la réalisation et la calibration du matériel scientifique. Francesco Ciocca, Raphaël Mutzner, Hendrik Huwald et Marc Diebold pour nos excellents rapports (scientifiques et sociaux) recevez mes remerciements. Je tiens très particulièrement à adresser mes vives remerciement à deux personnes : Holly Jayne Oldroyd, merci pour ta disponibilité permanente, ton soutien indéfectible et tes innombrables bons actes à mon égard (conseils, relectures et correction de ma thèse, résumés, posters). Steven Weijs pour ton encadrement, tes conseils, corrections et pour ta grande disponibilité scientifique et sociale sans lesquels cette thèse n’aurait pas vu le jour, ‘‘Merci, Baarka, Tak’’.

Merci aux professeurs invités Gaby Katul et Jozsef Szilagyi avec qui j’ai entretenu des échanges scientifiques très fructueux qui ont produit d’excellents résultats. Aux professeurs Yacouba Hamma (2iE), Blaise Somé (Université de Ouagadougou) et au docteur Bruno Barbier (Cirad-2iE) pour la confiance que vous avez placé en ma personne en acceptant d’être mes référents et surtout pour vos nombreux conseils ; recevez mes remerciements.

Je ne pourrais finir sans remercier mes collègues de projet (Info4Dourou) il s’agit : Natalie Ceperley ma collègue, ami et complice de recherche. Je te remercie pour ta patience, tes conseils (précieux) et surtout pour ta grande expérience de terrain qui a permis de nous sortir de problèmes à de multiples reprises, reçois mes salutations distinguées. À mes collègues de terrain Kouakou Yao désiré et Yonli Dramane, à la population de Tambarga et environnant, à Ouoba Mamadou maire de la commune de Madjoari, Kaboré Seydou et son Epouse. Aux nombreux étudiants stagiaires, Bachelors et Masters qui ont participé à cette riche expérience de recherche dont les contributions sont d’une très grande richesse. Veuillez tous trouvé en ces lignes ma reconnaissance et mes sincères remerciements.

Je tiens particulièrement à exprimer ma gratitude à ma famille, celle qui a beaucoup souffert de la séparation. Il s’agit de ma femme **Eilfried Lidwine Fatoumata** et mes fils **Wendkuni Emmanuel Stephane** et **Kiswendsida Brendan Johan**, merci pour votre patience et votre soutien inconditionnel sans lesquels je n’aurais pu finir cette thèse.

Sachant qu’aucune œuvre scientifique de qualité n’est réalisable sans le soutien d’institutions fortes.- Je terminerai mes propos en remerciant l’École Polytechnique Fédérale de Lausanne (EPFL), l’Institut International d'Ingénierie de l’Eau et de l’Environnement (2iE) et le KFPE pour leurs financements et leurs supports divers.

Mi maakubikaama

Tanbaliga dogu tie naani n ki tia ki soangi kelima un ye yaa diema nni, Bulicina Faso naa biani leni ŋinboanciangu. Laa dogu pia u pakiceli yaala n tie ku siagu leni li fali yaa kani. Mi taŋinbaama yabingu bi mi waalu ŋuadinni ŋan ye naani leni yaa yogunu yo.

Laa taŋinbaama puasindisindima kpendinni laa dogu niba po mi yepaagima kelima bi jiema leni bi ŋantaadikuandi kuli ŋa ku siagu kpaabu kane. Tanbaliga dogu nni pia ku ŋintibidigu ke ku fanma pundi cilometidikaare 4. Laa ŋintibidigu yaa kani, bi bugini/caani yaa masina n baa yaa wangi mi taŋinbaama n da maama leni laa taŋima n koa naani. Lani yaa po, ŋali 2009 binli, bi den taani a masina n puuni yaa laabaali kuli (lani n tie ki tinga, mi taŋinwangima (metewo) yaa kani).

Li binli 2010 ki gedi 2012 binli yaa siadi nni, bi den taani i laabaali kuli ki bua ki kpaagi ki bandi mi taŋinbaama n cuoni maama. Yaa tuonsoantiadi n den todi ke bi laa i laabaali tie : ku taŋinwangigu (sensorkopi), taŋinsanilie (deverisuari), caanaanii leni wulitonbiigidilie.

Bi diidi ki sua ke ku wuligu (mi wulitonma) n kpendinni Tanbaliga taamu. Lani n teni ke u yensiinu taamu ki yen waagi ki mi , ama ki nan yen wuli mi taŋima boncianla. Mi taŋima yabi ku ŋintibidigu kunu (li fuali n ye naani yaa po) ki cie a yaa piadi (i kuani nni). Ki taaga n yabi ku ŋintibidigu kunu yeni bua ki yedi ke mi wulitonma yabi laa fuule ki cie. Yaala n cuani lani mo tie li fuali leni ki tinge. Mi wulitonma yaa yabidi, mi yen fii ki do tanpoli ki ban tongi a tawala ki taaga n mi.

Yaala n baa taani ki teni ki taaga n cua lebida. Li ŋuani nni u yogunu leni u kaanu n tie maame. Lani yaa po tabuolilie n ye : ku siagu cilima yaa taamu leni ku siagu siiga yaa yaamu. Ku siagu cilima (a taŋinbaana) yogunu yen sua ke ki tinga kuoni ke ku tinŋingbangu foagi leni tanpoli. Lani n teni ke ku siagu cilima yaa taamu ŋuadini leni mi taŋima yabingu ke ku siagu siiga yaa taamu mo ŋuadini leni ki tinga soakpelima.

Ki tinga tiipo ŋingbandi ŋua ki tuatua ti liedi po yo. Ku taŋincendigu yaa ŋuudi, laa ŋima yen cili ki gbieni yaa ŋingbangu n ye tanpoli, laa ŋingbangu mo yaa gbie kun tindi ki gbieni yaa ŋingbangu n ye tiipo. Ŋingbandilie siiga kuli pia ku tanbibugiligu. Tanpoli ŋingbangu ŋima yen tagini laa tanbibugiligu kane ki kuodi ki gbieni ku ŋingbanliegu. Li baa ŋuaŋuadi yene u fuanu ŋima n baa ki kali tiipo(km 2.8).

A ŋinpudima moko pia ŋanŋua yaa sanbile. Ku tiŋaagu li ŋinpudinli ŋima yee yabi. Laa ŋima baa yaa wadi waamu waamu ki ban pundi u yensiinu (h 13). Li yenbigidili yaa pundi, mi ŋima yen guani ki yaa pugidi waamu waamu ki ban pundi li yenbaanli yogunu (h6). Bonla bonlilie n cedi ke li tie yeni: minaa ŋima yen ŋuudi ki kua tiipo ki ban kali ku ŋingbangu nni mine mo n kpandi ki tua wulima ki do tanpoli. Yaa ŋima n ye tinga ki kua tiipo yen yabi yabi boncianla a sakuana yogunu. Yaa ŋima yen tua wulima mo yen yabi ku siagu siige. Mi lingima puoli ti sua ke mi ŋinwulima yeni n yen ban joani ki gaa yaa fanma tanpoli dagininni ku ŋintibidigu fanma 0,6%. Laa ŋinwulima fanma tanpoli po dani nani tiipo li ŋinbuli, li gaanilindima leni ku ŋintibidigu buosoanga yaa fanma. Lani yaa kaani kane ke mi ŋima yabi ki kpandi ŋinwulima kelima mi yenwulitonma n pia u paalu laa fuuna nne. Li puoli po, ti diidi ki la ki taaga leni ti ŋingbandi n tuugi maama. Laa kpaagima puoli ti sua ke li pia yaa sanbila n baa todi Tanbaliga kpaabu n baa u paalu. Lani n tie ki gbi a caaŋuama lan fidi ki todi a kpakpaala n moa ki paadi ti taŋinpoadi.

A MABIBENGA : Burkina Faso, mi taŋima, mi wulitonma; li daala; nni taŋincendigu; mi ŋima n lebidi ki tua wulima; mi ŋima ŋuudima;ku kpaangu

Résumé

Le village de Tambarga, situé dans une zone semi-aride d'un pays enclavé, le Burkina Faso, subit de plein fouet les aléas de la saisonnalité de l'hydrologie locale. La pluviométrie à Tambarga est très variable, tant dans l'espace que dans le temps. Cette variabilité affecte la qualité de vie des populations qui est dépendante de l'agriculture pluviale. Le bassin versant de Tambarga (4km^2 de surface) a été équipé d'instruments afin de suivre la pluviométrie et ses dérivés (les ruissellements de surface, les écoulements de base) ainsi que l'effet de l'évaporation sur le bilan hydrologique. Par conséquent depuis 2009, les paramètres du sol, de même que les variables hydrologiques et météorologiques, ont été collectées à haute définition spatiale et temporelle. Les mesures pour cette étude ont été faites au cours des saisons des pluies de 2010 à 2012 à l'aide d'un réseau de stations météorologiques autonomes (Sensorscope), de deux déversoirs, de huit puits piézométriques et de deux stations de mesure de flux de chaleurs.

Les évènements pluvieux à Tambarga sont déclenchés par les mécanismes de convection du flux de chaleur sensible. Les pluies en cours de journée sont convectives et caractérisées par leurs courtes durées et leurs fortes intensités. En général on observe une pluviométrie

supérieure de 10 à 30% dans la partie amont du bassin (forêt de type soudanienne) que dans la partie avale du bassin (terrain agricole). L'abondance de pluie dans la partie amont du bassin est due à la forte production en flux de chaleur sensible de cette partie du bassin. Les facteurs biotiques (index du feuillage végétal) et abiotiques (drainage des sols) permettent de comprendre la forte production de flux de chaleur sensible dans la zone de forêt de type soudanienne comparativement à la zone agricole du bassin. Cette forte production en chaleur sensible contrôle le développement de la couche atmosphérique et par conséquent augmente la probabilité d'événements de pluie de type convectif, qui sont consécutifs au croisement de la couche mixte atmosphérique avec la couche de condensation.

Les réponses hydrologiques aux évènements de pluie varient spatio-temporellement et sont caractérisées par deux types d'hydrographes de crues : l'hydrographe à pic unique et l'hydrographe à deux pics. En début de saison, quand le sol est sec et le niveau de la nappe profonde, la réponse du bassin à un évènement pluvieux est caractérisée par un hydrographe à un seul pic. Cet hydrographe à un pic évolue en hydrographe à deux pics avec l'installation complète de la saison des pluies et la recharge de la nappe.

Les hydrographes à un pic dépendent plus de l'intensité de pluie tandis que les hydrographes à double pic sont corrélés avec l'humidité antécédente du sol. Les écoulements de surface commencent avec la recharge des nappes perchées qui, après leur remplissage, génèrent des écoulements dans des sections du cours d'eau. Les écoulements dus à la nappe perchée située en amont s'infiltrent dans un premier dans l'aquifère situé entre les deux nappes perchées qui agit comme une zone de stockage dans laquelle toutes les eaux en amont s'infiltrent. La recharge complète de cet aquifère permet l'interconnexion entre les deux nappes perchées et le début des écoulements continus sur l'ensemble du cours d'eau (2.8 km).

Les écoulements de base dans le cours d'eau suivent un modèle d'écoulement journalier particulier. Ce modèle se caractérise par des débits d'écoulement importants tôt le matin (6 :00), débits qui décroissent progressivement jusqu'au environ de 13 :00 pour reprendre une tendance inverse et atteindre leur niveau du matin aux environs de 18 :00. Ce comportement de l'écoulement est commandé principalement par deux phénomènes : l'infiltration dans le lit de la rivière et l'évaporation dans la rivière et ses abords. L'infiltration dans le lit du cours d'eau est plus prononcée en début de saison tandis que l'évaporation dans la rivière et ses alentours reprend le contrôle tard dans la saison quand le réseau de nappes souterraines est

connecté. La validation du contrôle par l'évaporation du modèle de l'écoulement de base tard dans la saison nous a permis de définir la surface siège de l'évaporation, qui correspond à 0.6% de la surface du bassin et est équivalente en terme de surface à la zone composée de la rivière, de sa partie riparienne et des zones humides du bassin. Ces zones sont sujettes à une forte évaporation de par leur exposition aux intenses rayons solaires de la région. Pour terminer cette étude, un simple modèle hydrologique pluie-débit a été développé avec les informations obtenues sur les principales variables du bilan hydrologique. Le modèle a permis de tester des solutions alternatives pour une meilleure production agricole. Ces tests suggèrent le stockage souterrain de l'eau accompagné de puits profonds comme pouvant être une alternative agricole pour réduire la vulnérabilité de population de Tambarga à la pluviométrie.

Mots clés: Burkina Faso, pluie convective, flux de chaleur sensible, hydrographes de crue, écoulement journalière, évaporation, infiltration, hystérésis, production agricole.

Abstract

As in all semi-arid regions, Tambarga, a small village surrounded by national parks in the landlocked country of Burkina Faso, is affected by the seasonality of the local hydrology. Seasonal and spatial variability of rainfall shapes the livelihoods of rural farmers who depend mainly on rain-fed agriculture. We instrumented the Tambarga catchment (area=~4 km^2) to investigate the rainfall patterns, the resulting hydrologic processes (surface runoff, base flow) and the evaporation effects on the local water balance. Thus, we have measured hydrological, meteorological and soil parameters at high spatial and temporal resolution over the catchment since 2009. Data for this research were acquired from the 2010 to 2012 rainy seasons using a network of automatic wireless weather stations (SensorScope stations), two weirs, eight piezometric wells, and two surface energy balance stations.

Rain at Tambarga is triggered by the convective mechanism, which is mainly controlled by the sensible heat flux. The daytime rain events at Tambarga are convective and are characterized by their high intensities and short durations. An overall increase in rainfall of 10-30% is observed in the savannah forest when compared to the agricultural field from 2010 to 2012. Biotic (leaf area index) and abiotic (well drained soil) factors, causing enhanced sensible heat flux at the savannah site, lead to an increased predisposition toward convective rainfall.

The hydrologic processes concomitant to the rain events were identified over the basin and intermittent responses of streamflow were isolated. The rise of the perched water tables located in the upstream and downstream regions of the basin generated two separate flows in the riverbed after the first rain. The intermediate zone operates like a deep storage tank, and by filling, it creates a connection between the two perched water tables. This connection induces a continuous flow throughout the 2.8 km of the stream. The hydrologic response at the basin outlet is observed to alternate between two different states over the course of the season. At the start of the rainy season, when the soils are very dry and the groundwater level is deep, a typical single-peak hydrograph is observed. This evolves into a double-peak hydrograph when the rainy season is completely established. The single-peak hydrograph is correlated with rainfall intensity, while the double-peak hydrograph is also correlated with the antecedent soil moisture condition. The baseflow, meanwhile, occurs when the groundwater level is higher than the riverbed at certain locations in the basin.

In contrast, during dry days (no rain) the baseflow exhibits a diurnal flow pattern. This diurnal pattern consists of decreased flow rate from sunrise (6:00 A.M.) to 1:00 P.M. and flow rate recovery to its previous level from 1:00 P.M. to sunset (6:00 P.M.). The diurnal pattern of the streamflow was found to be derived both from infiltration in the riverbed and evaporation over the river edges. The infiltration process dominates during the beginning of the season. While late in the season, when the groundwater network is interconnected and its overall level is higher than the riverbed elevation, evaporation controls the diurnal pattern. An evaporation contributing area is defined when the diurnal pattern is controlled by the evaporation. This area is about 0.6% of the basin area and could be rationally represented by the riparian area and the outlet wetland. Given the importance of rainfall-runoff processes over this catchment, a water balance was completed based on a simple lumped model. This model allowed for testing some water management strategies to improve agricultural production. Its implementation suggests that storing water underground for irrigation purpose with deeper wells is a way to achieve better agricultural productivity and therefore, reduce the vulnerability of the local people.

Keywords: Burkina Faso, convective rainfall, sensible heat flux, hydrograph peak, diurnal pattern, evaporation, infiltration, hysteresis, water management strategies.

Contents

Introduction

In the context of current environmental change, the main challenge for poor African countries, such as Burkina Faso is to find ways to stimulate and sustain economic growth in the face of natural resource depletion. Economic growth in West Africa is undeniably dependent on the main activity, rain-fed agriculture, which employs up to 70% of the population. Rain-fed agriculture is highly sensitive to environmental variability. Tambarga village, commune de Madjoari in the South Eastern Burkina Faso is experiencing, as other villages, the consequences of the climate change. Green economy was proposed at the Rio+20 conference as being a way to mitigate the impacts of climate change and achieve sustainable growth. However, this requires a prior understanding and characterization of each environmental variable affected by climate change, such as land cover, rainfall, runoff, storage, evaporation etc. The current advancement of monitoring equipment allows assessing at finer scales the temporal and spatial variability of hydro-meteorological data, which are necessary to understand the environment change and to stimulate sustainable agriculture.

The effects of climate change on the environmental variables could lead to severe and unpredictable events, such as rainfall onset shifts, dry spells, floods and droughts (Balme et al. 2006). These effects are more pronounced in water limited areas, such as Tambarga. "L'eau c'est la vie", meaning "water that is life", is nowadays an absolutely true sentence in Tambarga, where water resources have become insufficient. Therefore, we need to insure the access to water by the local people, which could be done through understanding the water cycle at a local scale. The water balance is the way used by the scientific community to assess the water cycle.

The experimental watershed around the village of Tambarga, in the Singou River basin (~2500 km^2), Southeastern Burkina Faso was equipped to study the local hydrological and micrometeorological processes. Tambarga is one of eight villages of the Madjaori commune 400 km southeast of Ouagadougou. Madjoari is bordered by the regions of Pama (North), Logobou (West), and Benin in the South and East. The commune is part of a hunting-protected zone, with important wildlife, vegetation, and water resources. The latter are a source of conflict between the local population and the resource managers. While the population strives to satisfy their everyday needs without being subject to rules, policy makers implemented important restrictions in response to current climate change impact to better

protect the rare resources of the country. However, farmers are under pressure to increase crop yields without expanding their agricultural area to supply their family given the important birth-rate of 5.3% in the region (Commune Rurale de Madjoari 2009).

The basin (4 km^2) is shaped by an ephemeral stream (~3 km) which flows continuously between July and October toward the Pendjari River. The rainfall regime is mono-modal with a single rainy season (May to October) followed by a dry season (November to April). The basin receives more than 1000 mm/year of rain and the temperature ranges from 45°C in April to around 25°C in October with an average wind speed of about 5m/s predominantly from the southwest. The watershed could be subdivided into two hydrological units based on the land use and soil type. The upper basin (mean altitude of ~320 m.a.s.l.) is a type of savannah forest on undisturbed sandy soil with scattered stones surrounding several mesa-shaped rock platforms, while the lower part is an agricultural area (~220 m.a.s.l. mean altitude) with highly disturbed sandy soil and no rocks. Agriculture is the main source of living for Tambarga producing mainly corn, millet, cotton and rice where rice is growing mainly around the stream outlet and millet elsewhere.

This thesis is part of the project Info4dourou (Codev-EPFL) aiming to combine research and development goals with the intention of pairing cutting edge scientific investigation with improvement of local resource management capacity. A workshop focusing on four issues (water, forest, village, and habitat) was held in February 2009 at Konkombouri Ranch in collaboration with local stakeholders, which has allowed us to align the project goals with the local population's needs. Therefore, since 2009 hydrometric and meteorological data were collected and are used in this thesis for exploring the water balance over the Tambarga basin. As a first step, the water balance was completed through analysis of its main components, which are precipitation, streamflow and evaporation.

1- Water balance

The water in the world follows a certain pathway, called the water cycle or hydrological cycle. This pathway consists mainly of three steps: precipitation, streamflow and evaporation. The water balance is evaluated mathematically with the conservation of mass principle derived from Lavoisier (1976) and previously reported in the Greek literature during the 4th century. The mass equation in the water balance is

$$R = P - E, \qquad (1)$$

where R is the streamflow, P is the precipitation and E is the evaporation. However, a more detailed soil water balance could be defined by integrating other components, such as infiltration and recharge, which act within R, and transpiration and interception, which act within E. The soil water balance equation is

$$nZ_r \frac{ds(t)}{dt} = P(t) - I(t) - Q[s(t), t] - E[s(t)] - L[s(t)], \quad (2)$$

where n is porosity, Zr is active soil depth, s(t) is relative soil moisture, P(t) is the rainfall rate, *I*(t) is canopy interception, *Q(s(t),t)* is the runoff, *E[s(t)]* is evapotranspiration and *L[s(t)]* is leakage. The soil water balance is more precise and allows for quantifying all of the balance components at one precise location in the basin.

a. Precipitation

Precipitation is the way in which water falls to the ground or is intercepted by plant canopies. Precipitation is composed of either solid, liquid or water vapor, such as snow, hail, rain, drizzle and dew (Hewlett 2003; Beven 2004; Wilfried Brutsaert 2005). Precipitation can be generated by the meeting of dry and wet air masses, the convective movement of heat, the orographic effects on air masses and the displacement of tropical systems (Brutsaert 2005). Rain, the principle form of precipitation in Tambarga, is well known for varying drastically in space and time. In 2011 around 500 mm of rain was reported at Tambarga, while almost 12000 mm was recorded in Colombia, Puerto Lopez de Micay (http://www.geoclimat.org01/). In addition, at Tambarga a temporal variability of rain was observed between 2010 and 2011, when about 50% less rain fell. Several other factors influenced the rainfall pattern, such as the natural and anthropogenic pressure on the land cover, which impacts significantly the rainfall

pattern at both local and continental scales (Kanae et al. 2001; Roger et al. 2001; Pielke et al. 2007; Juang et al. 2007), the dependence on higher temperature for extreme precipitation (Lenderink and van Meijgaard 2008; Berg et al. 2013), soil moisture patterns (Findell and Eltahir 1999; J. Y. Juang et al. 2007; de Arellano, van Heerwaarden, and Lelieveld 2012), CO2 levels (Hennessy et al. 1997; Chase et al. 2001; Pall et al. 2007; de Arellano et al. 2012) and global deforestation (Werth and Avissar 2002). Each factor could lead to damaging consequences for people, mainly in the water limited areas. For this study, the rain was collected using tipping buckets connected at Sensorscope weather stations. After falling, rain is transformed into streamflow and evaporation which are the other two crucial components of the water balance.

b. Streamflow

Streamflow is the process by which water moves from point to point in or over the land. Streamflow can account for up to 30-35% of the precipitation in the world (Brutsaert, 2005). The streamflow is mainly partitioned between storm runoff (Horton 1933) and subsurface flow (Freeze 1972). Several methods exist, such as hydrograph separation and isotope analysis, which allows quantifying each component based on the water's age. In general, the streamflow is demonstrated by a hydrograph, which is a function of the type of rain, soil and land covers (Onda et al. 2001; Casenave and Valentin 1992; Karambiri et al. 2011; Burt and Butcher 1985). The hydrograph is the representation of the flow behavior at some point in the basin. It exhibits, depending on location and the period, either a single or a double-peak hydrograph. The double-peak hydrograph is well known in hydrology and was found by Burt and Butcher (1985) in England, Dubreuil (1985) and Masiyandima et al. (2003) in Ivory coast, Anderson and Burt (1978) in the USA and Onda (1994) in Japan.

Water flow in streams is the first source of recharge for open natural and artificial water bodies, such as reservoirs, dams, rivers, lakes and seas. However, extreme streamflows, which have become more frequent nowadays, could induce floods with severe consequences for humans and infrastructure. Therefore, accurately assessing the streamflow pathway and discharge is important for development. Several methods are proposed in the literature to quantify the discharge. For this study, V-notch weirs equipped with automatic pressure transducers were used to measure discharge at fine time scales.

c. Evaporation

Evaporation is the process by which water is vaporized and returned to the atmosphere. The evaporation takes places over open surfaces of water (dams, reservoirs, rivers, ponds, etc) and through soil and plants. The amount of water evaporated is variable and is space and time dependent. It depends also on the rainfall type, wind speed, land cover characteristics and availability in evaporative energy (Brutsaert 1982). Evaporation accounts for 60-65% of the overall precipitation in the world (Brutseart, 2005). In some desert regions, the evaporation rate could reach 100% of the precipitation rate, which could lead to dramatic consequences for human, plant and animal life. At Kompienga, a catchment near Tambarga, the evaporation was found to consume 71% of the available surface energy (Bagayoko et al. 2007). The evaporation played an important role in the Tambarga local hydrology. The evaporation influenced the baseflow pattern by exhibiting a typical diurnal streamflow pattern during the dry period inside the rainy season. Therefore, accurate evaluation of the evaporation rate is critical. Several methods exist to quantify the evaporation rate, but the eddy covariance technique tends to be the most accurate available method. This method is used in the current thesis to quantify the evaporation.

The main goal of this work is to study the hydrology of a semi-arid region that experiences high spatial and temporal variability of environment variables, such as rainfall, streamflow and evaporation. Quantification of these main components of the water balance and their drivers is the way chosen to perform this work. We investigated the water cycle through the rainfall and its resulting streamflow hydrograph. A particular attention was devoted to the diurnal streamflow drivers and their correlations with evaporation. Finally, some potential water management strategies with the ability to improve the agricultural productivity for Tambarga's local population were implemented.

The first chapter investigates the rainfall occurrence and distribution over the small Tambarga basin, which is characterized by two landscapes, an agricultural field (AF) and a savannah forest (SF). The focus of this chapter is to explain the main causes of enhanced rainfall observed over SF versus AF within this region. These two areas experience similar synoptic scale weather patterns, but significantly differ in land-cover properties.

A model for predicting the time evolution of the mixed layer (ML) height combined with a model for predicting the lifting condensation level (LCL) were implemented for tracking the

convective rainfall (Brutsaert 1982; Juang et al. 2007; Juang et al. 2007). The ML model is driven by measured sensible heat flux, while the LCL model is driven by measured mean air temperature and relative humidity. The thermodynamic encroachment hypothesis was used to parameterize the sensible heat flux at the top of the ML (Stull 1988; Kim and Entekhabi 1998). The convective rainfall events are identified by following the crossing of the LCL and ML heights coinciding with the start of the rain. The daytime rain events are convective and produce 10-30% more rain in SF when compared to AF. The sensible heat flux is driven by biotic (leaf area index) and abiotic (drainage) effects, and was found to be the main driver of the rain spatial variability.

The second chapter presents the response of the basin to rain events. The hydrograph patterns were dissected by highlighting their process occurrences and drivers. During the rainy season, the hydrograph shifts between two forms, single and double-peak hydrographs. The double-peak hydrograph has been found in several studies, but the explanation remains unclear (Burt and Butcher 1985; Dubreuil 1985; Y Onda 1994; Masiyandima et al. 2003a). At Tambarga, the shapes of the hydrographs are a function of the rain intensity and the groundwater recharge. However, a special attention should be paid in the analysis of hydrograph peaks so as not to confuse the double-peak hydrograph induced by the bimodality of the rain event and the one induced by the delayed flow. Assessing the particular shapes allows for better streamflow modeling and forecasting.

In complement to the previous, the third chapter is focused on studying the baseflow, the main component of the surface runoff. The baseflow exhibits a particular diurnal pattern during the dry days. This pattern consists of a decreased flow rate in morning and flow rate recovery during the afternoon. This diurnal pattern is generated by two drivers, infiltration in the riverbed and evaporation along the riparian zone. The correlation between the diurnal flow rate cycle and the evaporation has allowed for estimating an evaporation control area based on a simple and intuitive method. A hysteresis relationship was also highlighted between the water loss in the stream and the evaporation measured in the agricultural field. This hysteresis relationship is suitable for daily evaporation partitioning.

Finally, the last chapter proposes water management strategies for agricultural purposes. Almost 100% of Tambarga's population works in agriculture. This working period lasts for four to five months, which is not efficient enough to achieve food security. For this reason, a simple lumped rainfall-runoff hydrological model was developed and used to implement

irrigation scenarios through dams and wells for better productivity. The underground storage of the water seems to be a way for both reducing dry spells, which damage the production during the season, and increasing dry period production through irrigation. This model is still under development, and a compilation of the results from our detailed study of the rainfall, runoff and baseflow generation processes will be used to fix and improve the model.

References

Anderson, M. G, and T. P Burt. 1978. "The Role of Topography in Controlling Throughflow Generation." *Earth Surface Processes* 3 (4) (October 1): 331–344. doi:10.1002/esp.3290030402.

Bagayoko, F., S. Yonkeu, J. Elbers, and N. van de Giesen. 2007. "Energy Partitioning over the West African Savanna: Multi-year Evaporation and Surface Conductance Measurements in Eastern Burkina Faso." *Journal of Hydrology* 334 (3-4): 545–559.

Balme, M., T. Vischel, T. Lebel, C. Peugeot, and S. Galle. 2006. "Assessing the Water Balance in the Sahel: Impact of Small Scale Rainfall Variability on Runoff: Part 1: Rainfall Variability Analysis." *Journal of Hydrology* 331 (1–2) (November 30): 336–348. doi:10.1016/j.jhydrol.2006.05.020.

Berg, Peter, Christopher Moseley, and Jan O. Haerter. 2013. "Strong Increase in Convective Precipitation in Response to Higher Temperatures." *Nature Geoscience* 6 (3) (March): 181–185. doi:10.1038/ngeo1731.

Beven, K. J. 2004. *Rainfall-runoff Modelling: The Primer*. John Wiley and Sons.

Brutsaert, W. 1982. *Evaporation into the Atmosphere: Theory, History and Applications*. Springer.

Brutsaert, W. 2005. *Hydrology: An Introduction*. Cambridge University Press.

Burt, T.P., and D.P. Butcher. 1985. "On the Generation of Delayed Peaks in Stream Discharge." *Journal of Hydrology* 78 (3–4) (June 20): 361–378. doi:10.1016/0022-1694(85)90113-1.

Casenave, A., and C. Valentin. 1992. "A Runoff Capability Classification-System Based on Surface-Features Criteria in Semiarid Areas of West Africa." *Journal of Hydrology* 130 (1-4) (January): 231–249. doi:10.1016/0022-1694(92)90112-9.

Chase, T. N., R. A. Pielke, T. G. F. Kittel, M. Zhao, A. J. Pitman, S. W. Running, and R. R. Nemani. 2001. "Relative Climatic Effects of Landcover Change and Elevated Carbon Dioxide Combined with Aerosols: A Comparison of Model Results and Observations." *Journal of Geophysical Research: Atmospheres* 106 (D23): 31685–31691. doi:10.1029/2000JD000129.

De Arellano, J. V,, C. C. van Heerwaarden, and J. Lelieveld. 2012. "Modelled Suppression of Boundary-layer Clouds by Plants in a CO2-rich Atmosphere." *Nature Geoscience* 5 (10) (October): 701–704. doi:10.1038/ngeo1554.

Dubreuil, P.L. 1985. "Review of Field Observations of Runoff Generation in the Tropics." *Journal of Hydrology* 80 (3–4) (October 15): 237–264. doi:10.1016/0022-1694(85)90119-2.

Findell, K. L., and E.A. B. Eltahir. 1999. "Analysis of the Pathways Relating Soil Moisture and Subsequent Rainfall in Illinois." *Journal of Geophysical Research: Atmospheres* 104 (D24): 31565–31574. doi:10.1029/1999JD900757.

Freeze, R. A. 1972. "Role of Subsurface Flow in Generating Surface Runoff: 2. Upstream Source Areas." *Water Resources Research* 8 (5): 1272–1283. doi:10.1029/WR008i005p01272.

Hennessy, K. J., J. M. Gregory, and J. F. B. Mitchell. 1997. "Changes in Daily Precipitation Under Enhanced Greenhouse Conditions." *Climate Dynamics* 13 (9) (September 1): 667–680. doi:10.1007/s003820050189.

Hewlett, John D. 2003. *Principles of Forest Hydrology*. University of Georgia Press.

Horton, R. E. 1933. "The Role of Infiltration in the Hydrologic Cycle." *Transactions-American Geophysical Union* 14 (June): 446–460.

Juang, J.Y., A. Porporato, P.C. Stoy, M.S. Siqueira, A.C. Oishi, M. Detto, H.S. Kim, and G.G. Katul. 2007. "Hydrologic and Atmospheric Controls on Initiation of Convective Precipitation Events." *Water Resour. Res* 43 (3): W03421.

Juang, J.Y.I.H., G.G. Katul, A. Porporato, P.C. Stoy, M.S. Siqueira, M. Detto, H.S. Kim, and R. Oren. 2007. "Eco-hydrological Controls on Summertime Convective Rainfall Triggers." *Global Change Biology* 13 (4): 887–896.

Kanae, S., T. Oki, and K. Musiake. 2001. "Impact of Deforestation on Regional Precipitation over the Indochina Peninsula." *Journal of Hydrometeorology* 2 (1) (February): 51–70. doi:10.1175/1525-7541(2001)002<0051:IODORP>2.0.CO;2.

Karambiri, H., García Galiano, S. G, J. D Giraldo, H. Yacouba, B. Ibrahim, B. Barbier, et al. 2011. "Assessing the Impact of Climate Variability and Climate Change on Runoff in West Africa: The Case of Senegal and Nakambe River Basins, Assessing the Impact of Climate Variability and Climate Change on Runoff in West Africa: The Case of Senegal and Nakambe River Basins." *Atmospheric Science Letters, Atmospheric Science Letters* 12, 12 (1, 1) (January 1): 109, 109–115, 115. doi:10.1002/asl.317, 10.1002/asl.317.

Kim, C. P., and D. Entekhabi. 1998. "Feedbacks in the Land-Surface and Mixed-Layer Energy Budgets." *Boundary-Layer Meteorology* 88 (1) (July 1): 1–21. doi:10.1023/A:1001094008513.

Lenderink, G., and E. van Meijgaard. 2008. "Increase in Hourly Precipitation Extremes Beyond Expectations from Temperature Changes." *Nature Geoscience* 1 (8) (August): 511–514. doi:10.1038/ngeo262.

Masiyandima, M. C, N. van de Giesen, S. Diatta, P. N. Windmeijer, and T. S Steenhuis. 2003. "The Hydrology of Inland Valleys in the Sub-humid Zone of West Africa: Rainfall-runoff Processes in the M'bé Experimental Watershed." *Hydrological Processes* 17 (6) (April 30): 1213–1225. doi:10.1002/hyp.1191.

Onda, Y. 1994. "Contrasting Hydrological Characteristics, Slope Processes and Topography Underlain by Paleozoic Sedimentary Rocks and Granite." *Transactions, Japanese Geomorphological Union* 15: 49–65.

Onda, Yuichi, Yosuke Komatsu, Maki Tsujimura, and Jun-ichi Fujihara. 2001. "The Role of Subsurface Runoff through Bedrock on Storm Flow Generation." *Hydrological Processes* 15 (10): 1693–1706. doi:10.1002/hyp.234.

Pall, P., M. R. Allen, and D. A. Stone. 2007. "Testing the Clausius–Clapeyron Constraint on Changes in Extreme Precipitation Under CO2 Warming." *Climate Dynamics* 28 (4) (March 1): 351–363. doi:10.1007/s00382-006-0180-2.

Pielke, R. A., J. Adegoke, A. Beltrán-Przekurat, C. A. Hiemstra, J. Lin, U. S. Nair, D. Niyogi, and T. E. Nobis. 2007. "An Overview of Regional Land-use and Land-cover Impacts on Rainfall." *Tellus B* 59 (3): 587–601. doi:10.1111/j.1600-0889.2007.00251.x.

Pielke, R. A. 2001. "Influence of the Spatial Distribution of Vegetation and Soils on the Prediction of Cumulus Convective Rainfall." *Reviews of Geophysics* 39 (2): 151–177. doi:10.1029/1999RG000072.

Stull, R. B. 1988. *An Introduction to Boundary Layer Meteorology*. New York: Springer.

Werth, D., and R. Avissar. 2002. "The Local and Global Effects of Amazon Deforestation." *Journal of Geophysical Research: Atmospheres* 107 (D20): LBA 55–1–LBA 55–8. doi:10.1029/2001JD000717.

Chapter 1: Suppressed convective rainfall by agricultural expansion in southeastern Burkina Faso

Abstract

With the 'green economy' being promoted as a path to sustainable development and food security within the African continent, the influx of agricultural land is proliferating at a rapid pace often replacing natural savannah forests. Our investigation calls attention to potential the adverse impacts of agricultural land influx on rainfall occurrences in water limited areas such as West Africa, where agriculture is primarily rain-fed. Using field observations complemented by model calculations in southeastern Burkina Faso, the main causes of a 10-30% suppressed rainfall recorded over agricultural fields when referenced to natural savannah forests are explained. Measurements and model runs reveal that the crossing of the mixed layer height and lifting condensation levels, a necessary condition for rainfall occurrence, was 30% more frequent above the natural savannah forest. This increase in crossing statistics was primarily explained by increases in measured sensible heat flux above the savannah forest rather than differences in lifting condensation heights.

1.1 Introduction

Because of economic incentives and food security needs, West Africa is experiencing an unprecedented rapid expansion in agricultural land (http://lca.usgs.gov/lca/africalulc/results.php#burkinafaso_lulc). Prototypical of this expansion is Burkina Faso, where natural savanna forests (SF) occupied some 60% of the land area in 1975. By 2000, this fraction dropped to 50% and presently is less than 45%. These reductions are principally due to cropland expansion, which increased from 15% in 1975 to 23% in 2000, and are currently expanding at a rate exceeding 2% per year. The croplands are primarily fed by rainfall. The southern portion of Burkina Faso is still covered by large areas of SF vegetation, but there are many growing incursions of agricultural fields (AF) into this region, which can have unintended adverse impacts on convective rainfall, the focus of this work. Data were collected in the southeastern portion of Burkina Faso over three years at AF and SF sites using twelve advanced weather monitoring Sensorscope stations and two eddy flux towers. Measured variables include sensible and latent heat fluxes, mean air temperature and air humidity, shortwave and net radiation by

eddy-covariance, as well as precipitation measured with a network of raingages spatially distributed within AF and SF (see Methods). The rainy season is characteristic of a Sudanian climate beginning in May and ending in October(Bagayoko et al. 2007; Ceperley, Repetti, and Parlange 2012). The rainfall is short in duration, intense, and occurs mostly during daytime primarily due to convective activities.

1.2 Results

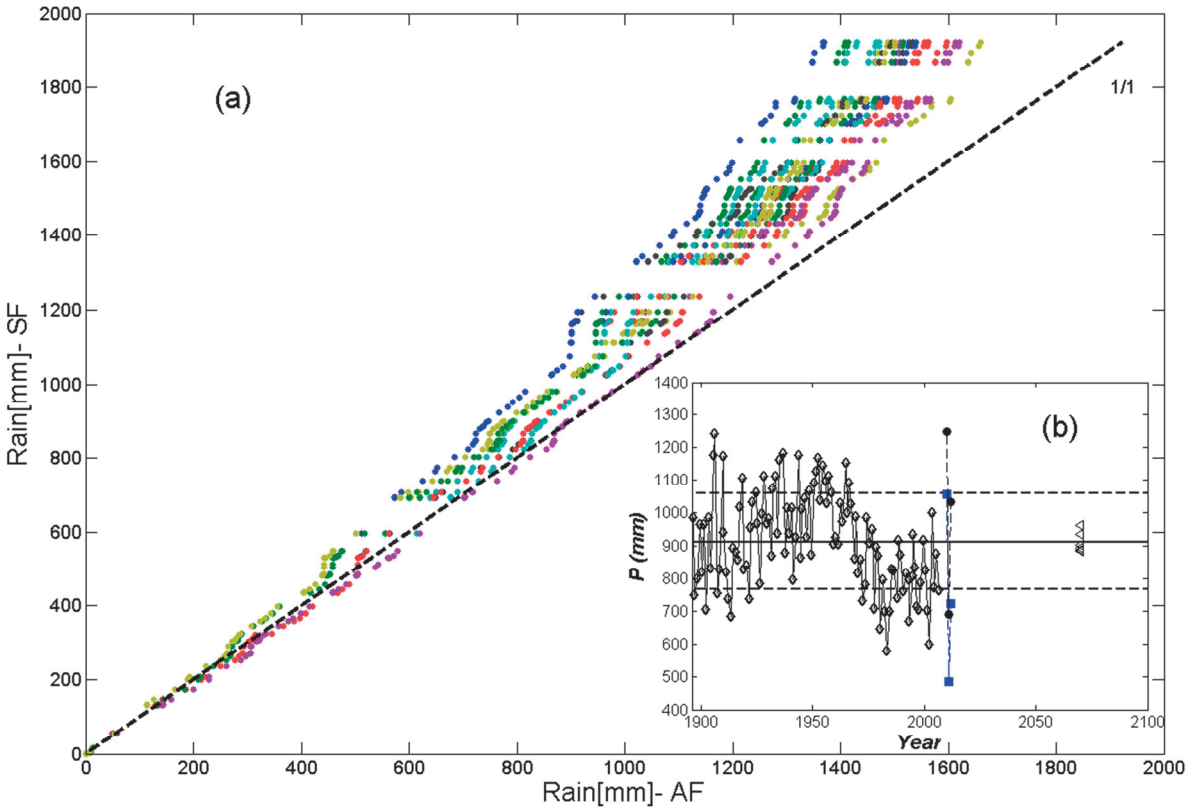

Figure 1.1: (a) Comparison of the daytime cumulative precipitation between three rain gauges of the savannah forests and all combinations of three rain gauges over six over the agricultural field. (b) Rainfall variability for past and future in relation to land-cover effect. Diamonds are from a long-term record for the Southwest Sahel region (1886-2006), triangles are model projections for the Sahel region in a double atmospheric CO2 scenario for different climate models, and annual rainfall at SF (rectangle) and AF (circle) for the study period. All the rain gages are identical and manufactured by Decagon.

Figure 1.1 shows a comparison between cumulative daytime precipitation from all the stations at the AF and SF sites for all three years along with reported annual rainfall across the entire southwest Sahel as well as climate projections for year 2100 for CO_2 doubling shown as an inset. The rain gage network at the SF documented a 10 - 30 % higher daytime precipitation when compared to the AF site for years with severe droughts and wet years. These site differences are statistically significant and not connected to errors or biases in tipping bucket gage measurements because the double-mass analysis in Figure 1.1 shows all

gages at SF recorded higher rainfall than any gage at AF. The measured difference in annual precipitation between AF and SF are larger than the temporal standard deviation in the 100-year annual precipitation fluctuations reported for the entire southwest Sahel(Mahé and Paturel 2009) (from 1896 to 2006, shown in Figure 1.1) and exceeds all climatic change projections (in 2100) reported for the Sahel region(Hulme et al. 2001) in a doubled atmospheric CO_2 concentration scenario. It can be surmised from Figure 1.1 that replacing SF with AF reduces rainfall; what is not evident from Figure 1.1 is the precise pathway leading to such reduction. It has been known for some time that land cover impacts convective rainfall occurrence and amounts at local and continental scales(Kanae, Oki, and Musiake 2001; Roger A. Pielke 2001; Findell and Eltahir 2003; Koster et al. 2004; Koster et al. 2006; Santanello, Friedl, and Ek 2007; R. A. Pielke et al. 2007; J. Y. I. H. Juang et al. 2007; Mölg et al. 2012). Describing the initiation and amounts of convective rainfall remains a daunting scientific task(Muller et al. 2009; Tao et al. 2012), but its predisposition can be 'distilled' to a minimum necessary crossing of the mixed layer height (h) and lifting condensation level (H_{LCL}). The mixed layer is a region where the air column thickness (=h) expands due to heating from the land surface and heating caused by entrained air originating from the free troposphere. The time-evolution of h depends on the diurnal history of surface sensible heat flux, while the evolution of H_{LCL} primarily depends on the diurnal variations in mean air temperature and mean air relative humidity(J. Y. I. H. Juang et al. 2007; J. Y. Juang et al. 2007; Siqueira, Katul, and Porporato 2009; de Arellano, van Heerwaarden, and Lelieveld 2012). This minimum necessary condition of h crossing H_{LCL} is employed here so as to assess whether replacing SF with AF explains the reductions in convective rainfall patterns using southeastern Burkina Faso as a prototypical system. It is demonstrated that upon replacing SF by AF at spatial scales(Avissar and Schmidt 1998) much larger than h lowers h but does not appreciably impact H_{LCL} during the wet season. The suppression of sensible heat flux resulting from an SF to AF conversion leads to a reduction in the crossing probability of h and H_{LCL}. It is further shown that the reason why H_{LCL} is not appreciably impacted by land cover is that the water vapor source within the ML is not originating from the land surface during the wet season. Furthermore, measured differences in surface water vapor fluxes are not large as these surface water vapor fluxes do not deviate appreciably from their near-wet surface evaporation values. On the other hand, converting SF to AF significantly lowers the surface sensible heat flux thereby lowering the h and the concomitant crossing statistics, considered next. A one-dimensional slab model(J. Y. Juang et al. 2007; J. Y. I. H. Juang et al. 2007)

coupled to an encroachment closure hypothesis linking *h* to measured sensible heat flux time series is employed at the two sites. The slab model neglects advection and subsidence(Stull 1988; Garcia, Cancillo, and Cano 2002; J. Y. Juang et al. 2007; J. Y. I. H. Juang et al. 2007) but was shown to be effective at reproducing mixed-layer heights rates(Pino, Vilà-Guerau de Arellano, and Kim 2006). The H_{LCL} was estimated from diurnal variation of measured mean air temperature, air humidity, and atmospheric pressure.

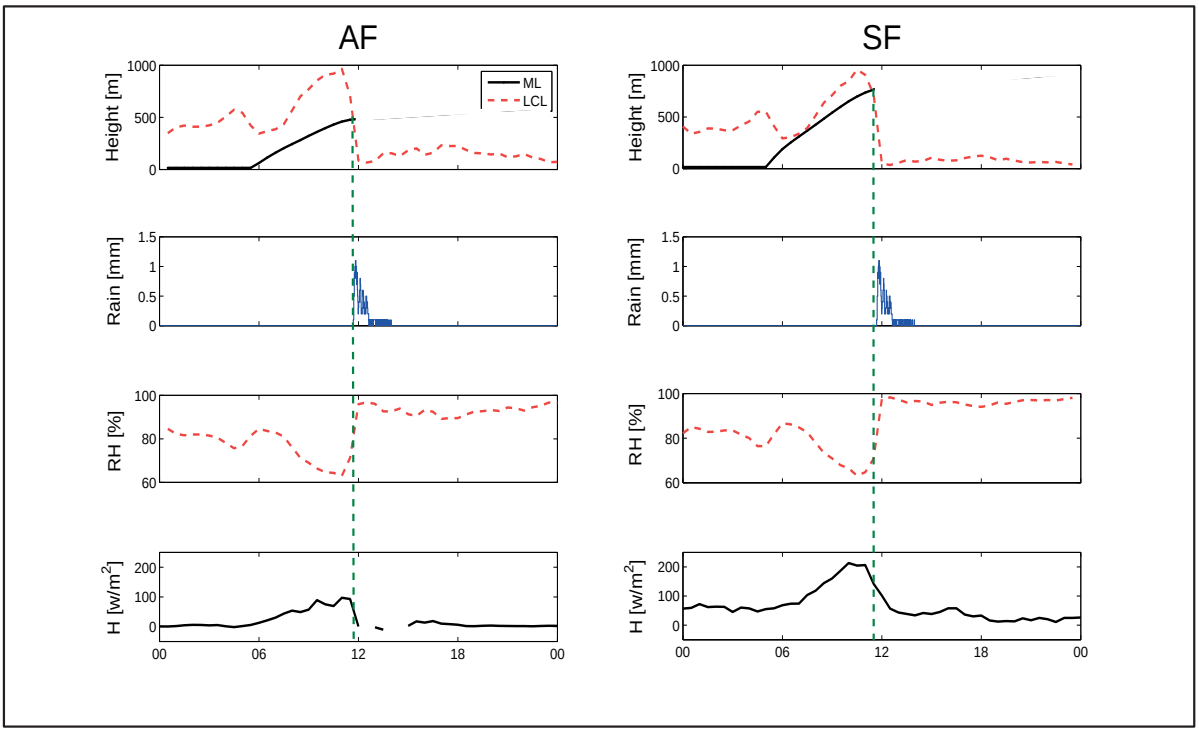

Figure 1.2: July 2nd 2010 – Evidence of the triggering convective rainfall over AF (left panel) and SF (right panel). More examples and details can be found in the appendix.

Figure 1.2 shows an emblematic case of modeled *h* and H_{LCL} evolution during the day using the measured sensible heat flux time series, and the mean air temperature and relative humidity as input (see supplementary material) at AF and SF. Shortly after modeled *h* intersects H_{LCL}, rainfall is measured by the tipping bucket gage network at both sites. When air parcels are lifted by the thermals controlling *h* and reach H_{LCL}, condensation proceeds in regions of negatively buoyant overshoots within these thermals. If the overshoot kinetic energy is sufficiently large, additional lifting of condensing air parcels occurs. Latent heat is released from the lifted air parcels and their potential temperature becomes sufficiently warmer than their surrounding thereby allowing them to become positively buoyant and propelling further ascent. This height defines the so-called level of free convection, which is

higher than H_{LCL}. The parcels may continue to rise buoyantly until they eventually become cooler than their surrounding atmosphere at which point the so-called limit of convective rise is reached. Any residual inertia in the parcels might propel them to further rise eventually terminating their ascent at the cloud top (Stull 1988; Emanuel, David Neelin, and Bretherton 1994). Once clouds develop, condensation nuclei are required to allow for rapid growth in water droplets. If these droplets reach sufficient size to precipitate and repenetrate the unsaturated air below the cloud base without completely re-evaporating before reaching the ground surface, rainfall at the surface is detected. After the h - H_{LCL} crossing, this entire process can be completed on time scales ranging from minutes to few hours. At SF and AF sites, when rainfall was recorded by the tipping bucket gage network, the fraction of events occurring within 3 hours after the h and H_{LCL} crossing exceeded 96%. There were no events in our analysis in which rainfall occurred without being preceded by an h - H_{LCL} crossing. Having demonstrated that the crossing of h and H_{LCL} is a necessary condition for rainfall occurrence, it is now used to diagnose whether land cover explains the measured rainfall differences between AF and SF reported in Figure 1.1. The computed H_{LCL} using measured mean air temperature and mean relative humidity are similar at both sites. Moreover, similarity in computed H_{LCL} suggests that the external water vapor source entrained or advected into the boundary layer dictates the mean air relative humidity within the ML at both sites, not the water vapor sources from the land-surface. In fact, the latent heat (LE) fluxes measured at both sites are comparable and do not appreciably deviate from their wet-surface value given by the Priestley-Taylor equation(Priestley and Taylor 1972). It can be surmised from Figure 1.3 that land cover differences do not appreciably impact H_{LCL} in the wet season, presumably due to the weak land-surface controls on the water vapor concentration within the mixed layer column. However, the measured sensible heat flux at SF is some 1.4 times larger than its counterpart at AF (Figures 1.2 and 1.3). Model calculations show that this excess sensible heat leads to some 30% more frequent h - H_{LCL} crossing, which is commensurate with the extra rainfall recorded at SF when compared to AF. Moreover, the higher sensible heat flux at SF is consistent with higher probability of rainfall occurrence or yield (~37% at SF versus 23% at AF) following the h-H_{LCL} crossing. Higher sensible heat flux at SF ensures that uplifted air parcels within thermal plumes have sufficient kinetic energy to become positively buoyant and be propelled to the level of free convection thereby yielding more rainfall.

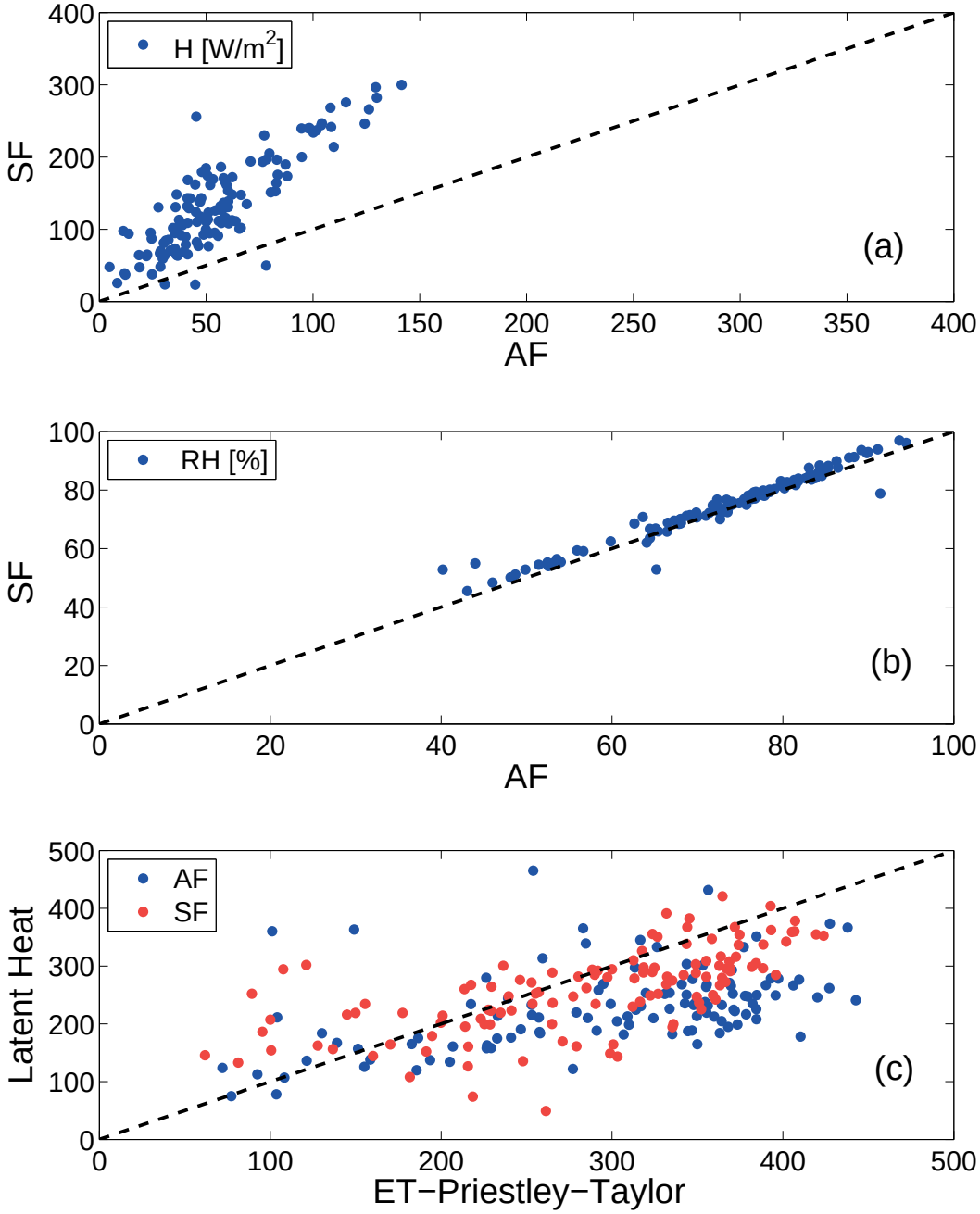

Figure 1.3: (a) Sensible heat flux, (b) Relative Humidity and (c) Latent Heat vs Priestley Taylor. All these variables were computed both on AF and SF.

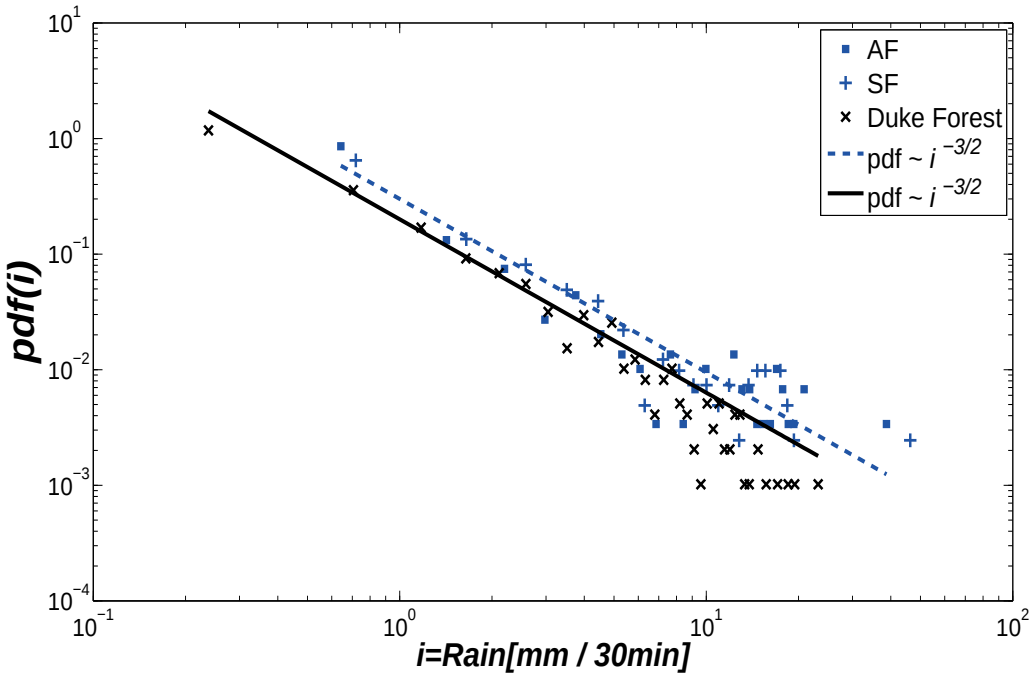

Figure 1.4: Rainfall *pdf* of AF, SF and Duke Forest summertime data.

Figure 1.4 shows that the probability density function (pdf) of measured rainfall intensity i at both sites exhibiting a near power-law regime. When a $pdf(i) = Ci^{\alpha}$ is fitted to the rainfall data at AF and SF, an exponent $\alpha = -3/2$ is computed for the range of i covered by the measurements here. This α is comparable to α reported from an 8-year record at a site dominated by summertime convective rainfall (near Durham, North Carolina, USA), also shown in Figure 1.4. This similarity in α across SF and AF (and other convectively dominated rainfall sites) precludes orographic effects as being the culprit explaining the differences in mean rainfall due to some 100 m elevation difference between the AF and SF sites. It also did not escape our attention that when $i \in [i_{min}, +\infty]$, the ensemble mean rainfall intensity $< i >$ normalized by the minimum intensity i_{min} detected by the tipping bucket gage (=0.2 mm) and given by $< i > / i_{min} = (-\alpha - 1)/(-\alpha - 2)$, is statistically divergent for $\alpha = -3/2$. In practice, this mathematical divergence is unlikely to persist because the maximum intensity is bounded by the finite precipitable water in clouds. That is, physical limits on maximum precipitable water ensures that the 'fat-tailed' power-law in Figure 1.4 will be censored thereby eliminating the divergence issue in the $pdf(i)$. To conclude, the main reason why the daily mean rainfall at SF is larger than AF is due to the more frequent crossings between ML and LCL associated with elevated sensible heat flux at SF.

Agricultural field expansion in West Africa could have unintended consequences which could affect dramatically the life quality for these low-income countries. Agriculture is mainly rainfed and contributes to 34% of the GDP and involves 70% of the population (Rio+20). In water limited areas, rainfall is the most crucial climatic parameter(IPCC 2002; Pall, Allen, and Stone 2007) impacting directly the quality of life. Given the United Nations Millennium Development Goals argue for green economy policies understanding land cover change and its impact on the spatial and temporal rainfall dynamics is fundamental. The effect of land cover change on precipitation pattern at larger scales has been reported in several studies (Avissar and Schmidt 1998; R. A. Pielke et al. 2007; Chase et al. 2001; Mölg et al. 2012; Pall, Allen, and Stone 2007). Our study has shown the potential impact of the land cover change on the precipitation pattern at local scales of kilometer. Land use signature on the convective rainfall mechanism is highlighted by water vapor controlled by regional forcing while the sensible heat flux is locally controlled with a 40% increase between AF and SF. Land use change does not only include the vegetation cover but also the soil properties (e.g. plowing and the removing of stones) and subsequent consequences for water movement, drainage and local energy balance. The local sensible heat flux enhances the likelihood of crossing between the ML and LCL, as demonstrated here with our field observations and precipitation convective models with hence a consequence of more frequent rain events in the SF. Future research will focus on the occurrence and the partitioning of extreme events at small scales and their potential consequences mainly in arid and semi-arid areas which recently experienced more frequent flood events. This future research will yield valuable insights in the context of environmental change.

1.3 Methods

The experiments were conducted around the village of Tambarga (11°26'42.79"N, 1°13'32.09"E), Kompienga city, southeastern Burkina Faso characterized by a semi-arid climate alternating between dry and wet seasons. Two sites - SF and AF - were chosen for micrometeorological measurements as prototypical of how agricultural land influx might be replacing natural savannah forests in the region. The SF is a mosaic of grassland, shrub woodlands and dense large trees situate at an elevation of about 100 m above AF. AF is a large agroforestry field used for millet and rice plantation during the rainy season. The soil in the AF is loamy sand with an impermeable clay layer at about one meter deep while SF soils are shallower and mainly sandy loam (<40cm) mixed with small stones and distributed rocks. The presence of rocks, caves and canyons on SF leads to enhance sensible heat flux because high soil drainage prevents near surface soil moisture accumulation. The soil at the AF is poorly drained. Meteorological data were acquired with SensorScope (Ss) wireless environmental monitoring stations and Eddy Correlation (EC) towers distributed over SF and the adjacent AF. The Ss measures mean wind speed, and direction[2 m], air temperature and relative humidity[1.5 m], precipitation [0.5 m], incoming solar radiation[2 m],, skin temperature [1 m] and soil moisture at different depths[0.05, 0.1, 0.2, 0.4 m]. All variables were sampled or summed every 5 minutes and averaged or summed every 30 minutes. Three Ss stations were situated within the SF and 6 Ss stations were distributed within the AF to capture some of the spatial and temporal variability at each site, especially precipitation. The EC station included a 3-dimensional sonic anemometer (CSAT3, Campbell Scientific, Logan UT) and an infrared gas analyzer (Licor7500, Licor, Lincoln, NE) situated at 2m above the ground surface along with a net radiometer (Kipp and Zonen, Delft, The Netherlands). The sampling frequency was 20 Hz and the averaging period was 30 minutes for all EC variables; post-processing utilized the planar fit technique[27] to minimize errors caused by the sonic anemometer tilt.

1.4 Supplementary Material

Model formulation: The ML height h was determined from a mixed-layer slab model and by adopting the encroachment closure for potential temperature T_p [22,28,29]

and by ignoring the contribution of heat sources and sinks within the ML to yield,

$$\frac{dh}{dt} = \frac{H_s - H_t}{\rho C_p \gamma},$$

where H_s is the measured sensible heat flux at the surface, H_t is the entrainment flux modeled as $H_t = -\beta H_s$, ρ is the mean air density, C_p is the specific heat capacity of dry air at constant pressure, and $\gamma = g/C_p$ is the lapse rate approximated by its dry adiabatic value, g(9.8 m s^{-2}) is the gravitational acceleration, and β is a constant that varies between 0.2 and 0.4, with a mean of 0.3 Kim and Entekhabi (1998) selected here. To solve this differential equation, an initial condition of $h(0)$ =15 m was set when H_s switches from negative (night) to positive (day). For the LCL, denoted by H_{LCL},

$$H_{LCL} = \frac{RT}{Mg} log\left(\frac{P_s}{P_{LCL}}\right),$$

where R is the Universal gas constant (=8.314 J mol^{-1} K), M is the molecular weight of dry air (~29 g mol^{-1}), T (K) is the mean air temperature, P_s is the local surface atmospheric pressure (kPa), and P_{LCL} (kPa) can be calculated from the hydrostatic approximation,

$$\frac{P_s}{P_{LCL}} = \left(\frac{T_{LCL}}{T}\right)^{3.5},$$

where $T_{LCL}$is the saturation temperature at the H_{LCL} given by (Stull, 1994)

$$T_{LCL} = 55 + \frac{2840}{3.5\ln(T) - ln\left(\frac{P_s r}{0.622 + r} - 7.108\right)},$$

where r is the near-surface water vapor mixing ratio derived from the measured air relative humidity.

References

Avissar, R., and T. Schmidt. 1998. “An Evaluation of the Scale at Which Ground-Surface Heat Flux Patchiness Affects the Convective Boundary Layer Using Large-Eddy Simulations.” *Journal of the Atmospheric Sciences* 55 (16) (August 15): 2666–2689. doi:10.1175/1520-469(1998)055<2666:AEOTSA>2.0.CO;2.

Bagayoko, F., S. Yonkeu, J. Elbers, and N. van de Giesen. 2007. “Energy Partitioning over the West African Savanna: Multi-Year Evaporation and Surface Conductance Measurements in Eastern Burkina Faso.” *Journal of Hydrology* 334 (3-4): 545–559.

Ceperley, N, A. Repetti, and M. Parlange. 2012. “Application of Soil Moisture Model to Marula (Sclerocarya Birrea): Millet (Pennisetum Glaucum) Agroforestry System in Burkina Faso.” In *Technologies and Innovations for Development*, edited by Jean-Claude Bolay, Magali Schmid, Gabriela Tejada, and Eileen Hazboun, 211–229. Paris: Springer Paris. http://www.springerlink.com/index/10.1007/978-2-8178-0268-8_15.

Chase, T. N., R. A. Pielke, T. G. F. Kittel, M. Zhao, A. J. Pitman, S. W. Running, and R. R. Nemani. 2001. “Relative Climatic Effects of Landcover Change and Elevated Carbon Dioxide Combined with Aerosols: A Comparison of Model Results and Observations.” *Journal of Geophysical Research: Atmospheres* 106 (D23): 31685–31691. doi:10.1029/2000JD000129.

De Arellano, J. V., C. C. V. Heerwaarden, and J. Lelieveld. 2012. “Modelled Suppression of Boundary-Layer Clouds by Plants in a CO2-Rich Atmosphere.” *Nature Geoscience* 5 (10) (October): 701–704. doi:10.1038/ngeo1554.

Emanuel, K.A., J. D. Neelin, and C. S. Bretherton. 1994. “On Large-Scale Circulations in Convecting Atmospheres.” *Quarterly Journal of the Royal Meteorological Society* 120 (519): 1111–1143. doi:10.1002/qj.49712051902.

Findell, K. L., and E. A. B. Eltahir. 2003. “Atmospheric Controls on Soil Moisture–Boundary Layer Interactions. Part I: Framework Development.” *Journal of Hydrometeorology* 4 (3) (June): 552–569. doi:10.1175/1525-7541(2003)004<0552:ACOSML>2.0.CO;2.

Garcia, J. A., M. L. Cancillo, and J. L. Cano. 2002. “A Case Study of the Morning Evolution of the Convective Boundary Layer Depth.” *Journal of Applied Meteorology* 41 (10) (October): 1053–1059.

Hulme, M., R. Doherty, T. Ngara, M. New, and D. Lister. 2001. “African Climate Change: 1900-2100.” *Climate Research* 17 (2) (August 15): 145–168. doi:10.3354/cr017145.

IPCC. 2002. “IPCC Workshop on Changes in Extreme Weather and Climate Events”. Beijing, China: INTERGOVERNMENTAL PANEL ON CLIMATE CHANGE.

Juang, J.Y., A. Porporato, P.C. Stoy, M.S. Siqueira, A.C. Oishi, M. Detto, H.S. Kim, and G.G. Katul. 2007. “Hydrologic and Atmospheric Controls on Initiation of Convective Precipitation Events.” *Water Resour. Res* 43 (3): W03421.

Juang, J.Y.I.H., G.G. Katul, A. Porporato, P.C. Stoy, M.S. Siqueira, M. Detto, H.S. Kim, and R. Oren. 2007. “Eco-Hydrological Controls on Summertime Convective Rainfall Triggers.” *Global Change Biology* 13 (4): 887–896.

Kanae, S., T. Oki, and K. Musiake. 2001. “Impact of Deforestation on Regional Precipitation over the Indochina Peninsula.” *Journal of Hydrometeorology* 2 (1) (February): 51–70. doi:10.1175/1525-7541(2001)002<0051:IODORP>2.0.CO;2.

Koster, R. D., P. A. D., Z. Guo, G. Bonan, E. Chan, P. Cox, C. T. Gordon, et al. 2004. “Regions of Strong Coupling Between Soil Moisture and Precipitation.” *Science* 305 (5687) (August 20): 1138–1140. doi:10.1126/science.1100217.

Koster, R. D., Y. C. S., Z. Guo, P. A. Dirmeyer, G. Bonan, K. W. Oleson, E. Chan, et al. 2006. “GLACE: The Global Land–Atmosphere Coupling Experiment. Part I: Overview.” *Journal of Hydrometeorology* 7 (4) (August): 590–610. doi:10.1175/JHM510.1.

Mahé, G., and J-E. Paturel. 2009. “1896–2006 Sahelian Annual Rainfall Variability and Runoff Increase of Sahelian Rivers.” *Comptes Rendus Geoscience* 341 (7) (July): 538–546. doi:10.1016/j.crte.2009.05.002.

Mölg, T., M. Großhauser, A. Hemp, M. Hofer, and B. Marzeion. 2012. “Limited Forcing of Glacier Loss through Land-Cover Change on Kilimanjaro.” *Nature Climate Change* 2 (4) (April): 254–258. doi:10.1038/nclimate1390.

Muller, C. J., L. E. Back, P. A. O’Gorman, and Kerry A. Emanuel. 2009. “A Model for the Relationship between Tropical Precipitation and Column Water Vapor.” *Geophysical Research Letters* 36 (16): n/a–n/a. doi:10.1029/2009GL039667.

Nicholson, S. E. 2013. "The West African Sahel: A Review of Recent Studies on the Rainfall Regime and Its Interannual Variability." *ISRN Meteorology* 2013: 1–32. doi:10.1155/2013/453521.

Pall, P., M. R. Allen, and D. A. Stone. 2007. "Testing the Clausius–Clapeyron Constraint on Changes in Extreme Precipitation under CO2 Warming." *Climate Dynamics* 28 (4) (March 1): 351–363. doi:10.1007/s00382-006-0180-2.

Pielke, R. A., J. Adegoke, A. Beltrán-Przekurat, C. A. Hiemstra, J. Lin, U. S. Nair, D. Niyogi, and T. E. Nobis. 2007. "An Overview of Regional Land-Use and Land-Cover Impacts on Rainfall." *Tellus B* 59 (3): 587–601. doi:10.1111/j.1600-0889.2007.00251.x.

Pielke, R. A. 2001. "Influence of the Spatial Distribution of Vegetation and Soils on the Prediction of Cumulus Convective Rainfall." *Reviews of Geophysics* 39 (2): 151–177. doi:10.1029/1999RG000072.

Pino, D., J. de Arellano, and Si-Wan Kim. 2006. "Representing Sheared Convective Boundary Layer by Zeroth- and First-Order-Jump Mixed-Layer Models: Large-Eddy Simulation Verification." *Journal of Applied Meteorology and Climatology* 45 (9) (September): 1224–1243. doi:10.1175/JAM2396.1.

Priestley, C. H. B., and R. J. Taylor. 1972. "On the Assessment of Surface Heat Flux and Evaporation Using Large-Scale Parameters." *Monthly Weather Review* 100 (2) (February): 81–92. doi:10.1175/1520-0493(1972)100<0081:OTAOSH>2.3.CO;2.

Santanello, J.A., Mark A. Friedl, and Michael B. Ek. 2007. "Convective Planetary Boundary Layer Interactions with the Land Surface at Diurnal Time Scales: Diagnostics and Feedbacks." *Journal of Hydrometeorology* 8 (5) (October): 1082–1097. doi:10.1175/JHM614.1.

Siqueira, M., G.G. Katul, and A. Porporato. 2009. "Soil Moisture Feedbacks on Convection Triggers: The Role of Soil–Plant Hydrodynamics." *Journal of Hydrometeorology* 10 (1) (February): 96–112. doi:10.1175/2008JHM1027.1.

Stull, R. B. 1976. "Mixed-Layer Depth Model Based on Turbulent Energetics." *Journal of the Atmospheric Sciences* 33 (7) (July): 1268–1278. doi:10.1175/1520-0469(1976)033<1268:MLDMBO>2.0.CO;2.

Stull, R. B. 1988. *An Introduction to Boundary Layer Meteorology*. New York: Springer.

Stull, R. B. 1994. "A Convective Transport Theory for Surface Fluxes." *Journal of the Atmospheric Sciences* 51 (1) (January): 3–22. doi:10.1175/1520-0469(1994)051<0003:ACTTFS>2.0.CO;2.

Tao, W., J-P. Chen, Zhanqing Li, Chien Wang, and Chidong Zhang. 2012. "Impact of Aerosols on Convective Clouds and Precipitation." *Reviews of Geophysics* 50 (2): doi:10.1029/2011RG000369.

Wilczak, J. M., S. P. Oncley, and S. A. Stage. 2001. "Sonic Anemometer Tilt Correction Algorithms." *Boundary-Layer Meteorology* 99 (1) (April 1): 127–150. doi:10.1023/A:1018966204465.

Chapter 2 : Stream response to a rain event in semi-arid region, Burkina Faso

Abstract

Water and energy balances at small spatial scale are generally not easy to close because their variables are difficult to estimate and their drivers are continuously changing and are site dependent. Despite the large advances on stream flow hydrograph studies (from the physical hydrograph separation technique to isotope analysis via geochemical methods), the mechanism of double peak hydrograph generation remains a vexing problem mainly for ephemeral streams. The Tambarga basin in southeastern Burkina Faso (4 km^2) was instrumented with two weirs, eight wells and an environmental wireless sensors network to assess the spatial and temporal distribution of rainfall, soil moisture, discharge and recharge, aiming to shed light on the hydrograph peaks drivers. Data to address this issue were collected during the 2010 and 2012 rainy seasons.

The hydrograph peak is a result of a complex interplay between several factors (soil moisture, rain intensity, infiltration and percolation processes, recharge, land cover and land use). However, observational data suggest that its pattern is mainly function of recharge and rainfall intensity. Typical single peak and double peak hydrograph responses were observed, respectively, at the two outlets of sub-basins of the Tambarga watershed. The single peak hydrograph occurs during unimodal, short and intensive rain events (>15 mm/hour) with an average lag time of about forty minutes. The double peak hydrographs could be subdivided in two classes. First, a quick primary peak induced solely by the bimodal rainfall pattern, identifiable nowadays because of the advent of finer temporal scales in advanced monitoring equipment, followed by a large, second peak induced by the delayed flow occurs when the water table is at least at riverbed height concomitantly with a long and less intense rain event (approx. 1.5 mm/hour), which enhances the infiltration. The lag time is, on average, 1.3 days for the large double peak hydrograph. The large double peak lag time is correlated with the antecedent soil moisture state in the riparian area while the single peak did not show any correlation. The double peak hydrographs are more pronounced in the agricultural field than in the upstream savannah forest. Additionally, the relative influence of the summer drought observed in 2011 is noticeable in the flow pattern. The evidence is highlighted by an increase (45%) and decrease (30%) of the lag time in 2012 with respect to 2010 for the single peak and

the double peak hydrographs. The factors causing these particular hydrograph patterns for semi-arid ephemeral stream flow are discussed hereafter. Future studies should focus on assessing the impact of drought on the stream flow hydrograph pattern.

KEY WORDS: Rain; Stream flow; Hydrograph peak; Groundwater; Lag time; Drought; Burkina Faso.

2.1 Introduction

In hydrology, before any modeling may be performed, the hydrologist needs to assess precisely the rainfall-runoff hydrograph patterns and their main physical drivers. The accuracy of a hydrological model depends on the understanding of flow dynamics in the unchanneled and channeled state. Rain-fed agriculture in sub-Saharan Africa (70% of the region's population) is facing several seasonal uncertainties such as timing of the onset of the rain season, and spatial and temporal distribution of rainfall and discharge, and is exacerbated by the present climate change associated with numerous natural calamities. These calamities have drastic impacts on local economy and consequently on life quality. It is then urgent to acquire tools, which are capable to forecast these uncertainties and better plan their consequences.

A common method to achieve this goal consists of measuring and evaluating all inputs involved in these processes, however this is not always possible. This method is by far the simplest, but its application is often difficult and impractical if not impossible (Wilfried Brutsaert 2005). However, identifying the flow pathways and accurately quantifying each hydrological variable and its time evolution is imperatively required prior to modeling or implementing water management strategies.

The subsurface flow, overland flow and infiltration excess runoff are well known to be the main contributors to stream flow (Dunne and Black 1970; Brutsaert and Nieber 1977; Dubreuil 1985; Casenave and Valentin 1992; Chevallier and Planchon 1993; Brutsaert 2005; McDonnell 2009). The hydrograph is used as a way to represent the stream flow rate as a function of time. Several categories of hydrographs have been reported in the literature, e.g. storm hydrographs, flood hydrographs, annual hydrographs, direct runoff hydrographs, effective runoff hydrographs, and raster hydrographs.

The hydrograph shape depends on various quantities such as the soil type, land use, land cover, and rainfall type (Boeye and Verheven 1992). Two dominant shapes of hydrographs

have been reported in the literature; (a) single peak hydrographs and (b) double or delay peak hydrographs (Anderson and Burt 1978). Recently, field evidence has shown that double peak hydrographs are mainly driven by recharge and controlled by subsurface flow (Chevallier and Planchon 1993; Masiyandima et al. 2003). Subsurface flow has been identified as the major contributor to discharge (Dubreuil 1985; van de Giesen et al. 2000; Masiyandima et al. 2003; Burt and Butcher 1985), and has been established as the main component in the runoff generation process (Sklash and Farvolden 1979; Pearce, et al. 1986; Onda et al. 2001). However, the subsurface flow depends largely on the soil properties and the local topography (Freeze 1972). Therefore, the presence of steep slopes, depression storages, springs and ponds play a significant role in the double peak hydrograph mechanism (Onda et al. 2004; Onda 1994; Komatsu and Onda 1996).

Rainfall is the main driver of hydrograph peaks in the West African semi-arid region, and therefore, its correlation with hydrograph peaks has been established by several studies since the early work of Horton (1933). In West Africa rainfall events are short (less than few hours), intense, and driven by convective systems (Mathon et al. 2002; Bagayoko et al. 2007). Tambarga, a Sudanian Savannah region, receives on average around 1000 mm of rain per year. The rainy season typically lasts 4 to 5 months, and the rain events are characterized by their brevity and their high intensity (duration < 1 hour, mean intensity ~15mm/hour). The hydrograph shape depends on the characteristics of the rain event. Therefore, according to the type of rain events, two kinds of hydrographs could be identified: The single peak hydrograph pattern is induced by the storm runoff and the double peak hydrograph by delayed subsurface flow. However, the double peak hydrograph could be generated by the bimodal pattern of the rainfall event (Zillgens et al. 2007). The figure 2.6 depicts a typical second peak hydrograph due to the bimodal rain event. Nevertheless, the rain intensity also plays a role on the generation of the delayed second peak as it enhances the infiltration when it is lower than the soil saturated hydraulic conductivity.

Soil water content, which depends on soil properties, rainfall, evapotranspiration, and water table level, contributes to the stream flow and sometimes corresponds to the main component of the second peak (Richey et al. 1998). However, the moistening process which controls the soil water content is valid only over a specific spatial and temporal scale (Finnerty et al. 1997; Mathon et al., 2002; Beven 2004). Anderson and Burt (1978) showed a correlation between soil moisture and delay flow peak by comparing times of occurrence of the maximum water pressure in the ponds and the delay flow peak. McGlynn et al. (2004) demonstrated that the

riparian groundwater level is correlated with the stream flow hydrograph pattern. At Tambarga the occurrence of the second peak coincides with the rise of the groundwater level to a depth that is higher than the riverbed (Figure 2.2, 2.3).

In hydrology the lag time (LT) is the time between the peak of rainfall and the peak of runoff hydrograph (Figure 2.5,2.6) .The double peak (LT) is approximately 30 times longer than that from a single peak, which is consistent with observation by Dunne (1978) who reported a LT of double peak 40 times the LT of the single peak.

The stream flow generation processes investigated since Pierre Perrault in 1674 ("On the Origin of Springs") have allowed for better hydro-meteorological predictions nowadays. However, ephemeral stream flow hydrograph peak generation in semi-arid region remains a misunderstood topic (Hihara and Susuki 1988; Mahé et al. 2000; Masiyandima et al. 2003). The objective of this study is to investigate hydrograph peak generation processes through a combined analysis of the antecedent soil moisture, rain intensity, water table level, and the lag time to shed a light on the single and double hydrograph peak drivers for an ephemeral stream in West Africa.

2.2 Study site and method

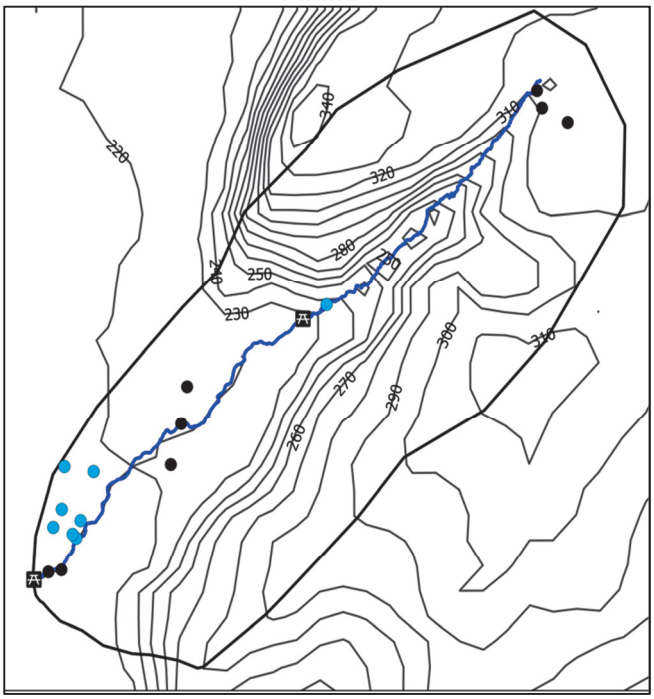

Figure 2.1: Tambarga Basin topographic map with two weirs (black squares), eight wells (light blue dots) and eight micro-meteorological stations (black dots).

For this study the region of Kompienga, Southeastern Burkina Faso was selected. The Tambarga experimental basin (~4km^2) is subdivided into two sub-basins (by the topographic line 230m msl) according to the land use.

Hydro-meteorological data were collected since April 2009. Specifically, nine (9) wireless SensorScope stations (Ingelrest et al, 2010), two weirs and eight wells were installed to monitor the full annual cycle of hydrological observations (Figure 2.1).

SensorScope stations allow measuring rainfall, soil moisture, air temperature and humidity, wind speed and direction, and skin temperature. These stations are energy autonomous and data are available in real time (data transmission through GPRS). Soil moisture probes were installed at different depths, at 15 and 30cm depth in 2009, and at 5, 10, 20, 40 cm in 2011, to measure soil temperature, moisture and electrical conductivity. Rainfall was measured using tipping bucket rain gauges with accuracies ranging between 0.1 mm (Précis Mécanique, Bezons, France) to 0.254 mm (Davis Instruments, Hayward, CA) per tips. With the gaol of reducing environmental and technical effects on the measurements, the number of rain gauge per site was increased in 2011 from one to two. Two v-notch weirs were installed at the basin outlet and the upper sub-basin (1.564 km upstream), respectively. This configuration aimed at capturing the variability in spatial flow and discharge over two sub-basins, which feature different land uses. The groundwater level was recorded by means of eight wells (six existing wells and two new hand-dug wells in the riverbed). The wells were initially measured twice per week and afterwards every 5 minutes using pressure transducers in the two hand-dug wells.

For this study, a set of 43 rainfall events and their corresponding stream flow hydrographs during the 2010 and 2012 rainy seasons were selected at two locations over the test site. The hydrographs are divided into two sets: Thirty-six single peak hydrographs and seven double peak hydrographs. The hydrograph peaks occurred both on the upper and lower basin. Results are presented in the following section.

2.3 Discussion

Tambarga has received more than hundred rain events in 2010 and 2012, where 90% resulted in a single peak hydrograph and 10% in a double peak hydrograph. The rain events are characterized by their shortness and their high intensity leading to an increasing direct runoff. As mentioned by Masiyandima et al. (2003), the infiltration rates are generally high and the storm duration short in the sub-humid zone in West Africa (Ivory coast). Nonetheless, the relatively weak Hortonian runoff contribution observed during the rainy season is attributed to the highest infiltration and evaporation rate.

The groundwater outflow pattern changes according to the timescale of observations; in Tambarga the change is more obvious at daily and seasonal scale. At the seasonal scale two phases are identified; depletion of the water table during the dry period and recharge during

the rainy season. During the dry period the rainfall contributes to groundwater recharge, then during the rainy season the recharge stage is subdivided into two periods. During the first period (May-July) the water level is stable with very sparse rain recharge, and during the second period (August - October) the groundwater recharges quickly (Figure 2.2). This recharge occurs concomitantly with the onset of less intense and longer rain events.

The flow in the river in Tambarga is seasonal, flashy, and occurs only during the rainy season. During the dry period (November to April) there is no stream flow in the river bed and the groundwater level depletes. Stream flow starts with the rainy season (May to October) and can be divided into periodical quick rainfall-runoff responses (May-July) and continuous groundwater base flow (August-October). The base flow takes place when the wet season with frequent rainfall events is fully established. During this period, the continuous flow over the entire river reach at Tambarga is governed by groundwater (Figures 2.2 and 2.3). Which suggest a strong relationship between groundwater elevation and basin discharge as reported by McGlynn et al., [2004].

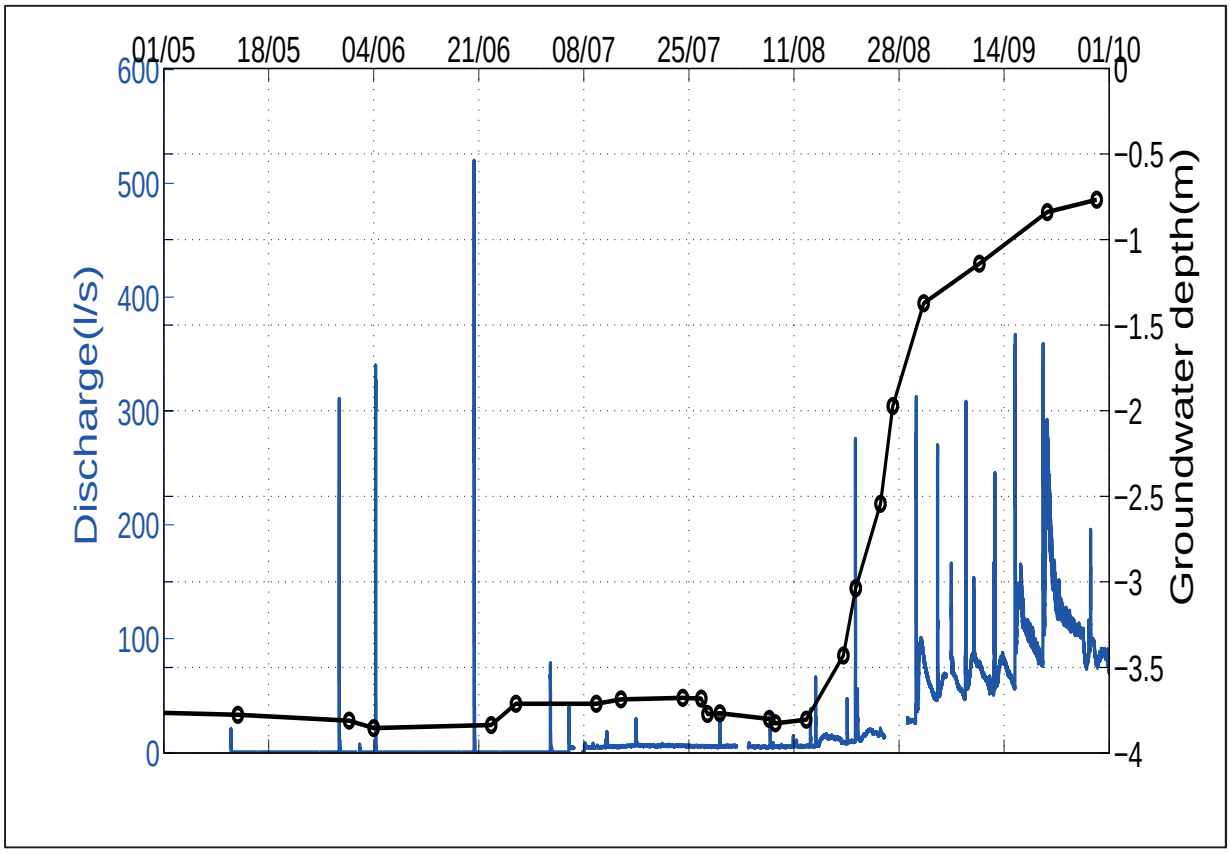

Figure 2.2: Evolution of stream flow (blue line) and groundwater level (black line) from May through September 2010.

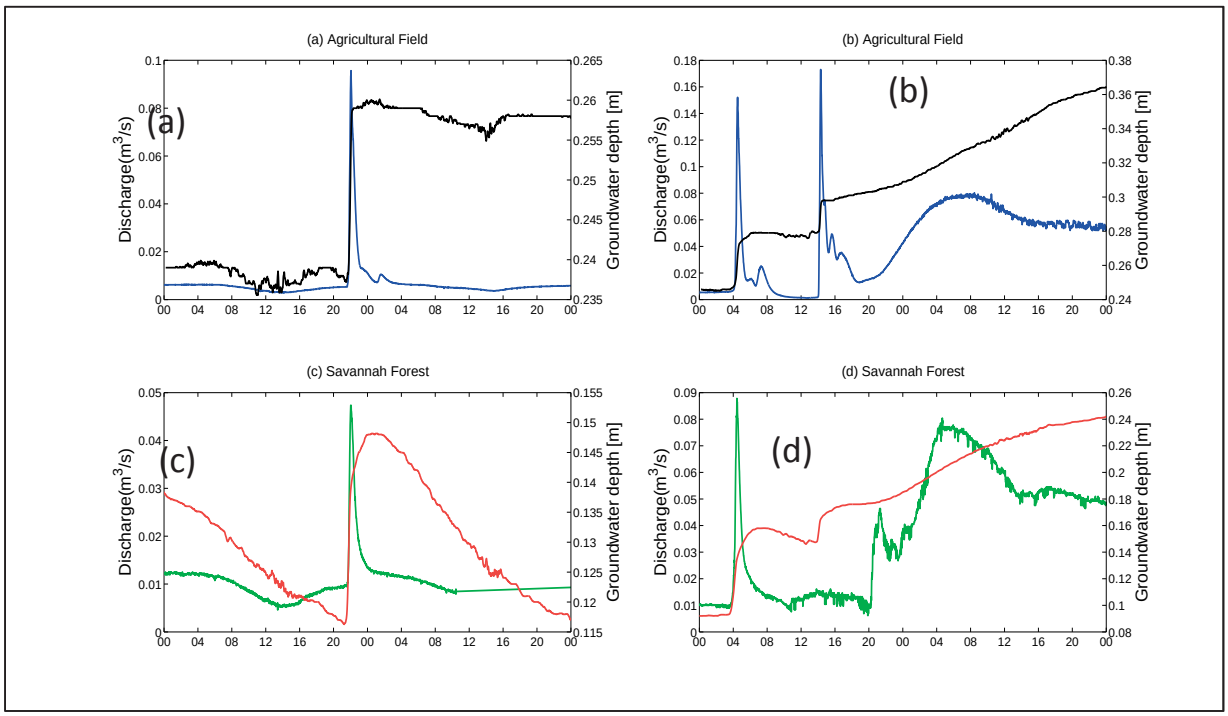

Figure 2.3: Stream discharge (blue and green lines) and groundwater depth (black and red lines) during a single peak event (panels a,b) and double peak event (panels c,d); a time period of 48 hours is shown.

In the Tambarga basin three permanent and several temporal springs were found over the rainy season. The temporal springs appear simultaneously with the groundwater recharge. The appearance of temporal springs is known to be a good indicator for assessing the river network and the level of groundwater recharge (Onda et al. 2006; Komatsu and Onda 1996; Onda et al. 2001).

The hydrologic response at the basin outlet is observed to shift between two forms (single and double peak hydrograph) over the course of the season. The Hortonian runoff is generated by the high rainfall intensities and the delayed stream flow response with respect to rain events, leading to a temporal variation in discharge in the stream (Malard, et al., 1999). At the start of the rainy season, when the soils are very dry with a low groundwater level, a typical single peak hydrograph is observed during the rain event. The single peak hydrograph evolves into a double peak hydrograph with the establishment of base flow (Figure 2.3, 2.4), which occurs when the groundwater rise is close to the riverbed (Figures 2.2, 2.3). In similar cases (Anderson and Burt 1978; Chevallier and Planchon 1993; Masiyandima et al. 2003) it was noted that the second discharge peak coincided with the highest rise of groundwater.

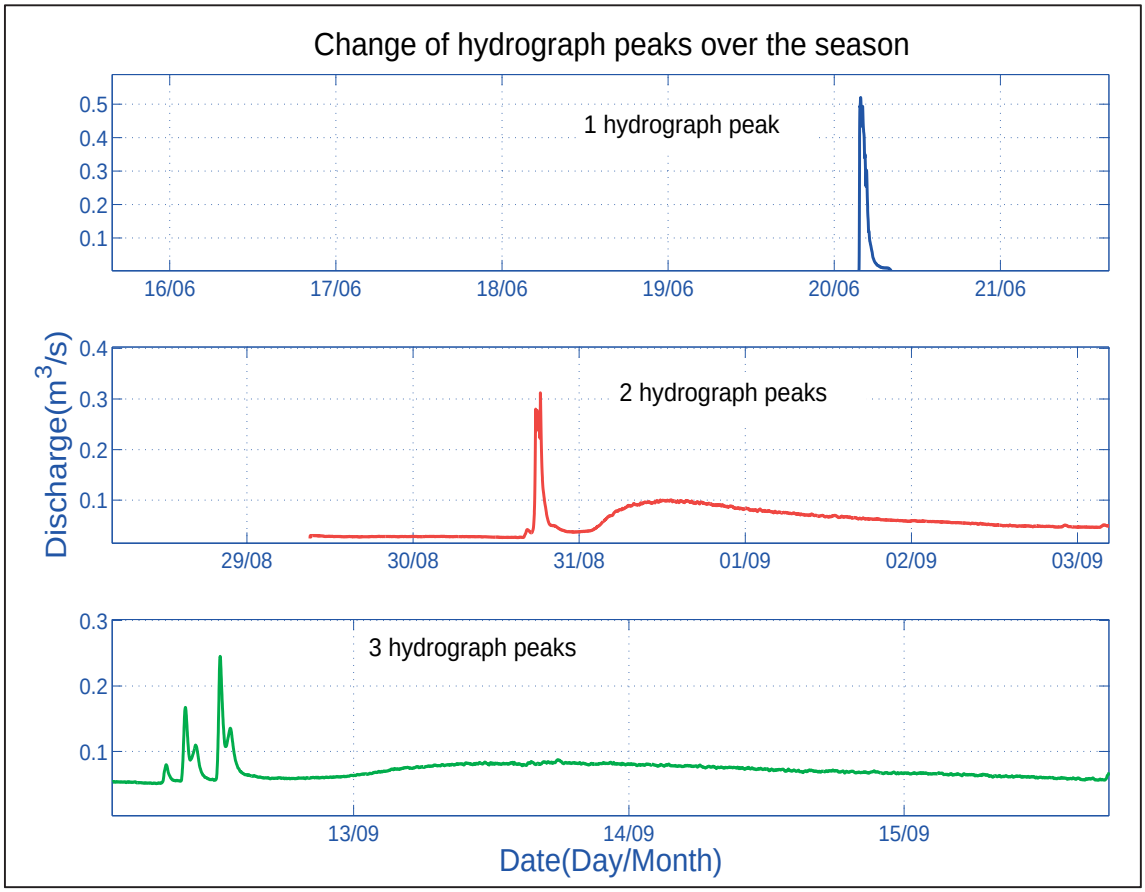

Figure 2.4: Examples of typical hydrograph peak patterns for 2010 season at the Tambarga basin. Single peak lasts less than hour while double peak is more than a day.

The lag time, i.e. the time between the peak of rainfall and the peak of runoff hydrograph (Figures 2.5, 2.6), is both important for flood prediction (Dubreuil, 1985) and a good indicator for characterizing hydrograph peaks (Haga et al. 2005). Despite its importance, it is mainly theoretically assessed through a simple linear relation (Dubreuil, 1985).

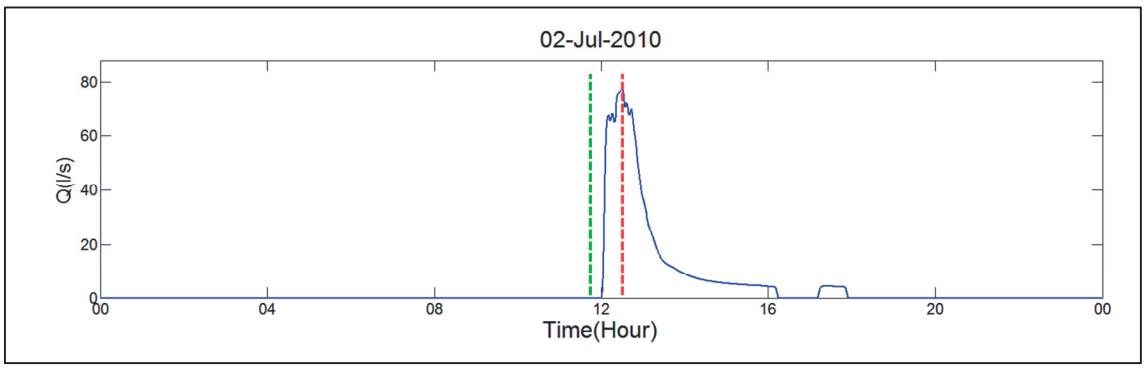

Figure 2.5: Examples of single peak lag times. Green line denotes the peak of rainfall; red line indicates the hydrograph peak time. The single peak lag time corresponds to the time between the green line and the red line.

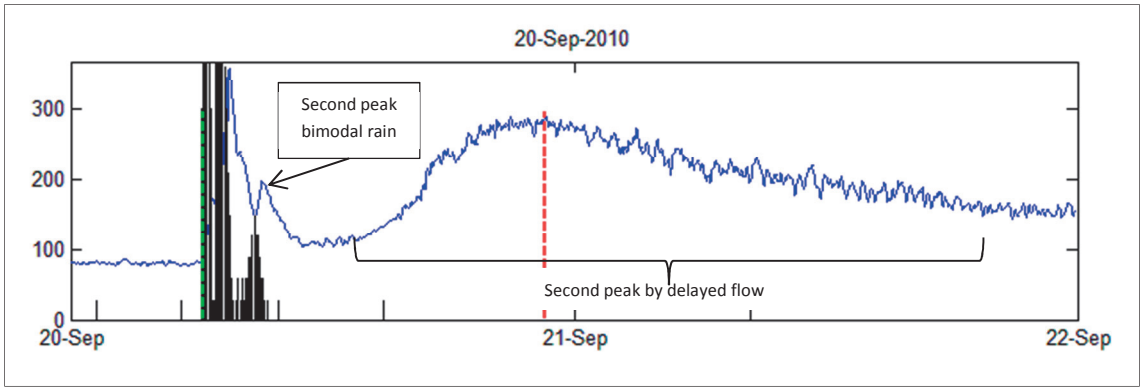

Figure 2.6: Illustration of a typical Second peak in the hydrograph (blue line) induced by the bimodal rainfall pattern (black). The green line marks the beginning of the rainfall; the red line indicates the second peak in discharge. The double peak lag time corresponds to the time between the green line and the red line.

The lag time for the single hydrograph peak is about half an hour regardless the antecedent soil moisture condition (Figure 2.7 (c-d), 2.9 (a)). The large rain intensity supersedes potential soil moisture effects. During the single peak event, the groundwater level experiences a quick recharge and subsequent decline after the event (Figure 2.3 (a,c)) while during the double peak occurrence the groundwater level being already at the river height is continuously increasing (Figure 2.3 (b, d)). Lateral inflow seems to be the preferential pathway for the water to enter the stream.

The first peak occurs during the storm, is caused by Hortonian runoff that is independent of the antecedent soil moisture condition (Figure 2.9 (a)). This single peak is mainly controlled by the rain intensity being larger than the saturated hydraulic conductivity most of the time. In Tambarga two variants of rain patterns are observable: unimodal and bimodal events. The unimodal rain events lead to a single peak hydrographs while bimodal rain events lead at short term to a double peak hydrograph (Figure 2.6).

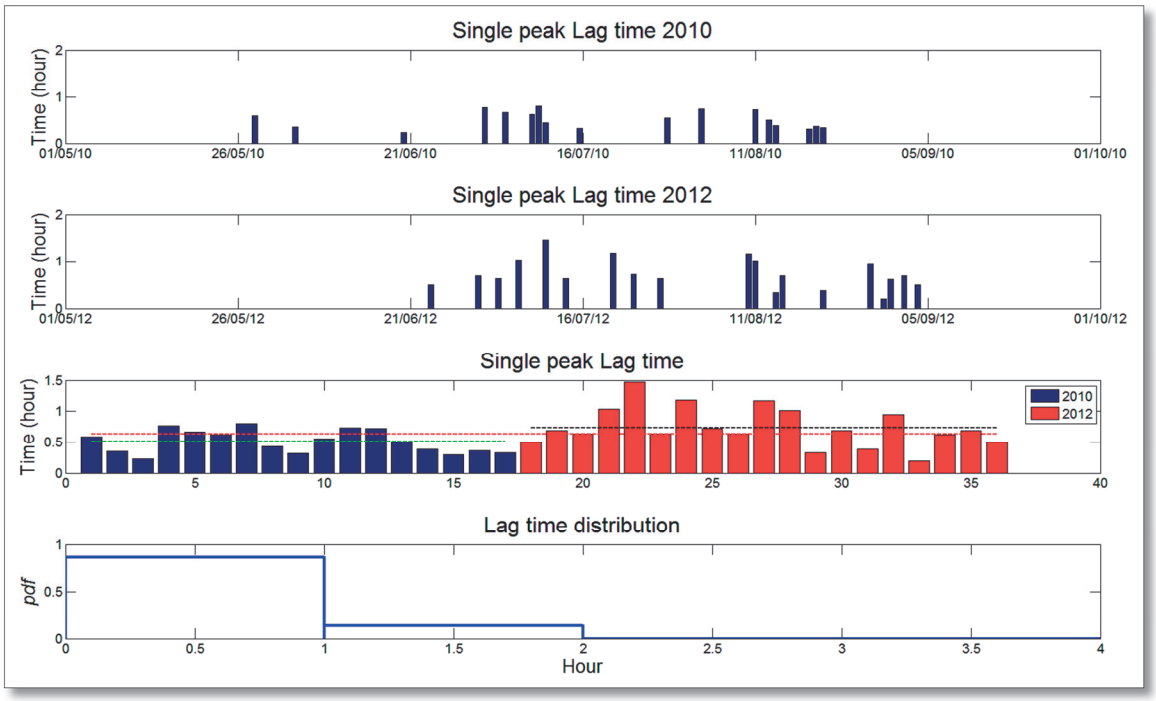

Figure 2.7: Lag time of the single hydrograph peak for the lower basin in 2010 (a) and 2012 (b). Panel (c) shows the lag time pattern in 2010 and 2012 and (d) presents the respective probability density function.

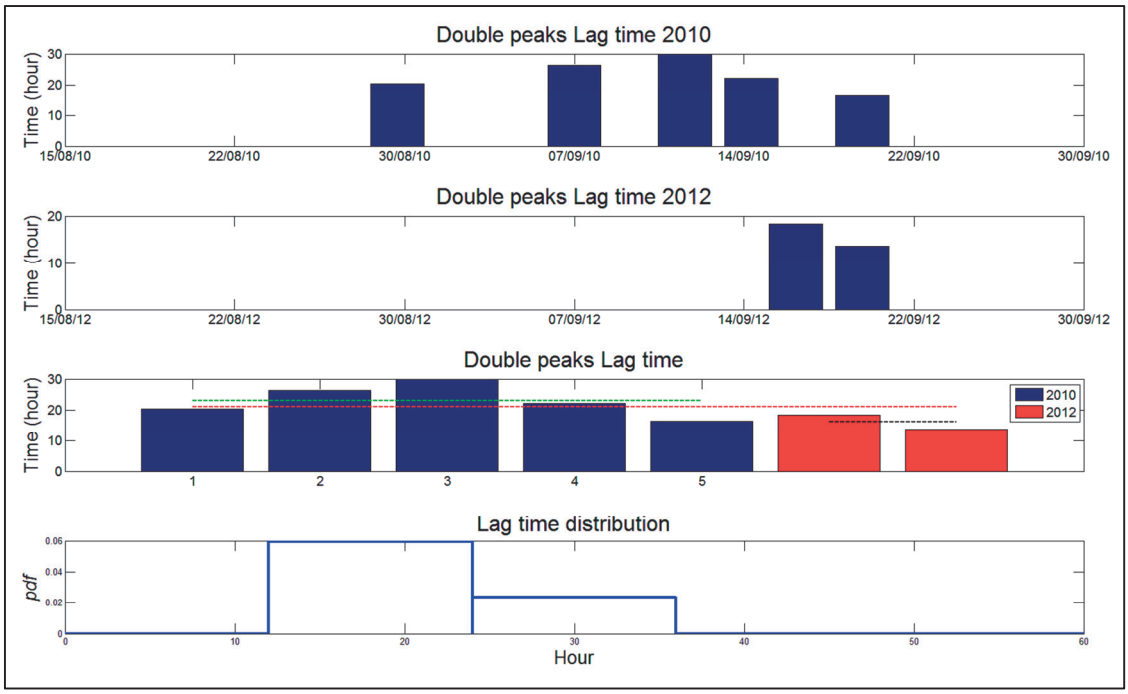

Figure 2.8: Lag time of the double hydrograph peak for the lower basin in 2010 (a) and 2012 (b). Panel (c) shows the lag time pattern in 2010 and 2012 and (d) presents the respective probability density function.

The lag time of the single peak hydrograph is less than one hour in 90% of the cases (Figure 2.7). However a slight increase of this lag time was observed in 2012, therefore the mean lag time of the single peak hydrograph shifted from (1/2 hours) in 2010 to (3/4 hours) in 2012 (Figure 2.7). This shift could be related to the 2011 drought observed in Tambarga between the two years of observations used in this study. Casenave (1978) found that a drought year significantly impacts the following year hydrological pattern with a decrease in base flow.

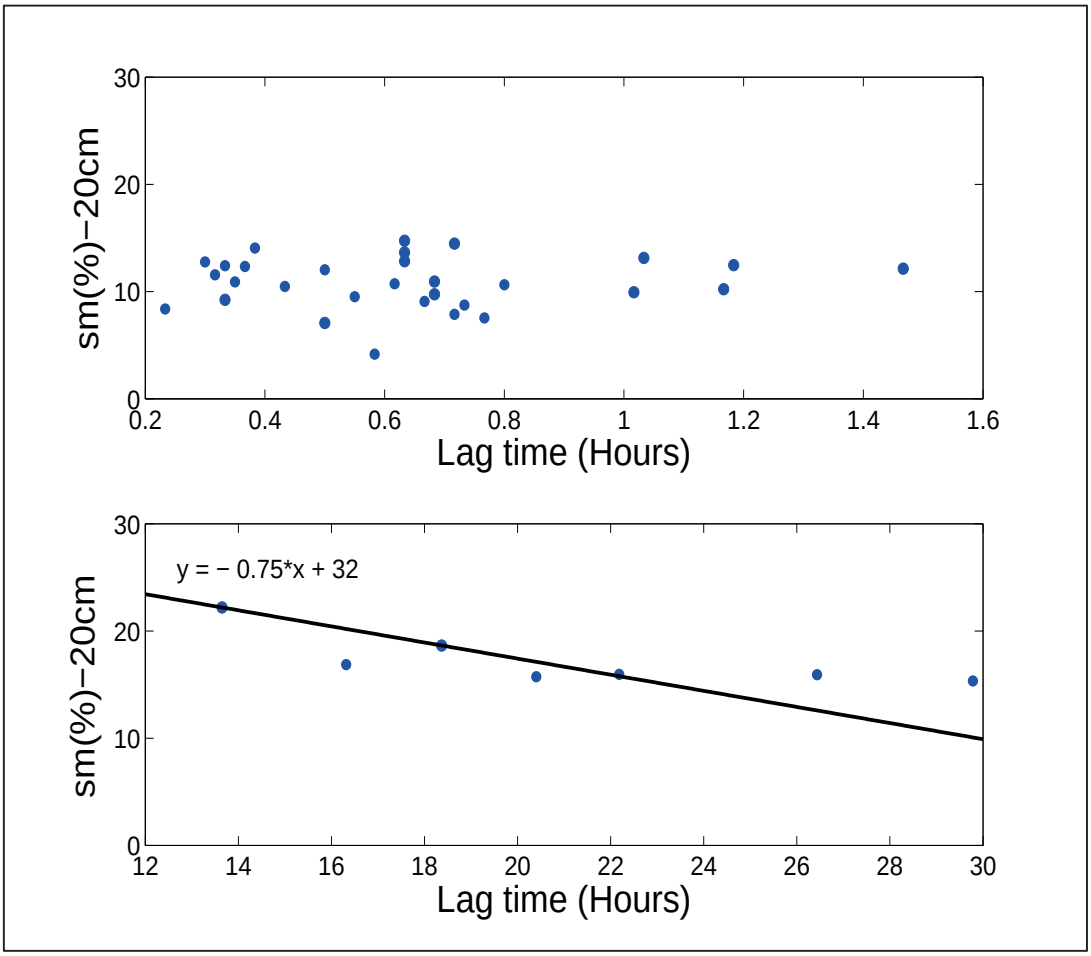

Figure 2.9: Correlation between riparian soil moisture and the corresponding lag time. Correlation with single peak lag time (a) and double peak lag time (b).

The second peak could be either caused by the bimodality of the rain event or by the delayed subsurface flow when the riparian soil is saturated. Here the second peak related to the rain event pattern and is easily modeled while the one driven by the delayed flow is difficult to assess. The delayed peak occurs when the base flow is established under moist soil conditions. Its occurrence coincides with the rise of the groundwater level (Figures 2.2, 2.3), correlation reported by several studies (Anderson and Burt 1978; Chevallier and Planchon 1993; Masiyandima et al. 2003) .

The time to peak is largely determined by drainage characteristics such as drainage density, slope, channel roughness, and soil infiltration characteristics. The lag time of 1.3 days (Figure 2.8) found for the double peak cases is strongly correlated to water level stage (Figure 2.2, 2.3) and to the antecedent soil moisture state (Figure 2.9 (b)). Therefore the smaller is the antecedent soil moisture condition the longer is the time taking to reach the peak of the delayed peak (Figure 2.9 (b)). Rainfall distribution in space also affects the time to peak, then the occurrence of the delay double peak hydrograph result also from a long and less intense rain event (1.5mm/ hour). These types of events start mainly during night time and last several hours until morning. The intensity of rainfall causing delayed hydrograph is approximately 10 times less than the one causing single peak hydrograph. The combination of rainfall intensity, antecedent soil moisture condition and recharge stage allows explaining the occurrence of the delay double peak hydrograph.

2.4 Conclusion

This study is focused on changes in stream flow hydrographs during the rainy season in a small basin in West Africa (Tambarga, Burkina Faso). The factors controlling the stream hydrograph peaks were underscored by using groundwater recharge, lag times and soil properties. The hydrograph peaks in Tambarga are generated by direct runoff and delayed subsurface flow. About 90% of all rainfall events resulted in single peak hydrographs and 10% in double peak hydrographs. The riparian soil moisture and the recharge levels control the hydrograph double peak generation albeit the recharge is the preliminary cause. The delayed subsurface flow is more dependent on the antecedent soil moisture than the quick surface runoff, which seems more correlated to the rainfall intensity and temporal distribution. The lag time between the peaks in rainfall and the hydrograph is a function of the type of hydrograph itself, where a single peak hydrograph is linked to a short lag time of about 1/2 hour while the delayed double peak hydrograph takes place 1.3 days after the rain event. The lag time and the hydrograph shape are correlated with the rain intensity and the ground water recharge. In addition to recharge being the main control of the flow condition, the antecedent soil moisture as well as the rainfall intensity are essential to characterize the double peak hydrograph in combination with the lag time.

References:

Anderson, M. G, and T. P Burt. 1978. "The Role of Topography in Controlling Throughflow Generation." *Earth Surface Processes* 3 (4) (October 1): 331–344. doi:10.1002/esp.3290030402.

Bagayoko, F., S. Yonkeu, J. Elbers, and N. van de Giesen. 2007. "Energy Partitioning over the West African Savanna: Multi-year Evaporation and Surface Conductance Measurements in Eastern Burkina Faso." *Journal of Hydrology* 334 (3-4): 545–559.

Beven, K. J. 2004. *Rainfall-runoff Modelling: The Primer*. John Wiley and Sons.

Boeye, D, and RF Verheven. 1992. "The Hydrological Balance of the Groundwater Discharge Fen." *Journal of Hydrology* 137 (1-4) (August 15): 149–163. doi:10.1016/0022-1694(92)90053-X.

Brutsaert, W. 2005. *Hydrology: An Introduction*. Cambridge University Press.

Brutsaert, W., and J. L. Nieber. 1977. "Regionalized Drought Flow Hydrographs from a Mature Glaciated Plateau." *Water Resources Research* 13 (3): PP. 637–643. doi:197710.1029/WR013i003p00637.

Burt, T.P., and D.P. Butcher. 1985. "On the Generation of Delayed Peaks in Stream Discharge." *Journal of Hydrology* 78 (3–4) (June 20): 361–378. doi:10.1016/0022-1694(85)90113-1.

Casenave, A., and C. Valentin. 1992. "A Runoff Capability Classification-System Based on Surface-Features Criteria in Semiarid Areas of West Africa." *Journal of Hydrology* 130 (1-4) (January): 231–249. doi:10.1016/0022-1694(92)90112-9.

Casenave, A. 1978. "Etude hydrologique des bassins de Sanguéré." *Cahiers ORSTOM.Série Hydrologie* 15 (1-2): 3–209. IRD Bondy.

Ceperley, N., A. Repetti, and M. Parlange. 2012. "Application of Soil Moisture Model to Marula (Sclerocarya Birrea): Millet (Pennisetum Glaucum) Agroforestry System in Burkina Faso." In *Technologies and Innovations for Development*, edited by Jean-Claude Bolay, Magali Schmid, Gabriela Tejada, and Eileen Hazboun, 211–229. Paris: Springer Paris. http://www.springerlink.com/index/10.1007/978-2-8178-0268-8_15.

Chevallier, P., and Olivier Planchon. 1993. "Hydrological Processes in a Small Humid Savanna Basin (Ivory Coast)." *Journal of Hydrology* 151 (2–4) (November): 173–191. doi:10.1016/0022-1694(93)90235-2.

Dubreuil, P.L. 1985. "Review of Field Observations of Runoff Generation in the Tropics." *Journal of Hydrology* 80 (3–4) (October 15): 237–264. doi:10.1016/0022-1694(85)90119-2.

Dunne, Thomas, and Richard D. Black. 1970. "Partial Area Contributions to Storm Runoff in a Small New England Watershed." *Water Resources Research* 6 (5): PP. 1296–1311. doi:197010.1029/WR006i005p01296.

Finnerty, B. D., M. B. Smith, Dong-Jun Seo, V. Koren, and G. E. Moglen. 1997. "Space-time Scale Sensitivity of the Sacramento Model to Radar-gage Precipitation Inputs." *Journal of Hydrology* 203 (1–4) (December 31): 21–38. doi:10.1016/S0022-1694(97)00083-8.

Freeze, R. A.. 1972. "Role of Subsurface Flow in Generating Surface Runoff: 2. Upstream Source Areas." *Water Resources Research* 8 (5): 1272–1283. doi:10.1029/WR008i005p01272.

Haga, H., Y. Matsumoto, Jun Matsutani, Masafumi Fujita, Kei Nishida, and Yasushi Sakamoto. 2005. "Flow Paths, Rainfall Properties, and Antecedent Soil Moisture Controlling Lags to Peak Discharge in a Granitic Unchanneled Catchment." *Water Resources Research* 41 (12): n/a–n/a. doi:10.1029/2005WR004236.

Hihara, T, and K Susuki. 1988. "The Double Peak Hydrograph During Storm Events in a Small Watershed of the Tama Hills, West of Tokyo." *Geographical Review of Japan* 61A: 804–815.

Ingelrest, F., G. Barrenetxea, G. Schaefer, M.Vetterli, O.Couach, and M. Parlange. 2010. "SensorScope: Application-specific Sensor Network for Environmental Monitoring." *ACM Trans. Sen. Netw.* 6 (2) (March): 17:1–17:32. doi:10.1145/1689239.1689247.

Komatsu, Y., and Y. Onda. 1996. "Spatial Variation in Specific Discharge of Base Flow in a Small Catchments, Oe-yama Region, Western Japan." *Journal Japan Society Hydrology & Water Resources* 9: 489–497.

Mahé, G., J. Olivry, R. Dessouassi, D. Orange, F. Bamba, and E. Servat. 2000. "Relations Eaux de Surface–eaux Souterraines D'une Rivière Tropicale Au Mali." *Comptes Rendus de l'Académie Des Sciences - Series IIA - Earth and Planetary Science* 330 (10) (May 30): 689–692. doi:10.1016/S1251-8050(00)00188-9.

Malard, F., K. Tockner, and J. V. Ward. 1999. "Shifting Dominance of Subcatchment Water Sources and Flow Paths in a Glacial Floodplain, Val Roseg, Switzerland." *Arctic, Antarctic, and Alpine Research* 31 (2) (May 1): 135–150. doi:10.2307/1552602.

Mande, T., N. Ceperley, S. V. Weijs, A. Repetti, and M. B. Parlange. 2014. “Toward a New Approach for Hydrological Modeling: A Tool for Sustainable Development in a Savanna Agro-System.” In *Technologies for Sustainable Development*, edited by Jean-Claude Bolay, Silvia Hostettler, and Eileen Hazboun, 85–98. Springer International Publishing. http://link.springer.com/chapter/10.1007/978-3-319-00639-0_8.

Masiyandima, M. C, N.C. Van De Giesen, S.Diatta, P. N. Windmeijer, and T. S Steenhuis. 2003. “The Hydrology of Inland Valleys in the Sub-humid Zone of West Africa: Rainfall-runoff Processes in the M’bé Experimental Watershed.” *Hydrological Processes* 17 (6) (April 30): 1213–1225. doi:10.1002/hyp.1191.

Mathon, V., H. Laurent, and T. Lebel. 2002. “Mesoscale Convective System Rainfall in the Sahel.” *Journal of Applied Meteorology* 41 (11) (November): 1081–1092. doi:10.1175/1520-0450(2002)041<1081:MCSRIT>2.0.CO;2.

McDonnell, J. J. 2009. “Hewlett, J.D. and Hibbert, A.R. 1967: Factors Affecting the Response of Small Watersheds to Precipitation in Humid Areas. In Sopper, W.E. and Lull, H.W., Editors, Forest Hydrology, New York: Pergamon Press, 275--90.” *Progress in Physical Geography* 33 (2) (June 4): 288–293. doi:10.1177/0309133309338118.

McGlynn, B. L., J. J. McDonnell, J. Seibert, and C. Kendall. 2004. “Scale Effects on Headwater Catchment Runoff Timing, Flow Sources, and Groundwater-streamflow Relations.” *Water Resources Research* 40 (July 28): 14 PP. doi:200410.1029/2003WR002494.

Onda, Y. 1994. “Contrasting Hydrological Characteristics, Slope Processes and Topography Underlain by Paleozoic Sedimentary Rocks and Granite.” *Transactions, Japanese Geomorphological Union* 15: 49–65.

Onda, Y., Y. Komatsu, M. Tsujimura, and J. Fujihara. 2001. “The Role of Subsurface Runoff through Bedrock on Storm Flow Generation.” *Hydrological Processes* 15 (10): 1693–1706.

Onda, Y., M. Tsujimura, J. Fujihara, and J. Ito. 2006. “Runoff Generation Mechanisms in High-relief Mountainous Watersheds with Different Underlying Geology.” *Journal of Hydrology* 331 (3-4): 659–673.

Onda, Y., Y. Komatsu, M. Tsujimura, and J. Fujihara. 2001. “The Role of Subsurface Runoff through Bedrock on Storm Flow Generation.” *Hydrological Processes* 15 (10): 1693–1706. doi:10.1002/hyp.234.

Onda, Y., M.Tsujimura, and H. Tabuchi. 2004. “The Role of Subsurface Water Flow Paths on Hillslope Hydrological Processes, Landslides and Landform Development in Steep Mountains of Japan.” *Hydrological Processes* 18 (4): 637–650. doi:10.1002/hyp.1362.

Pearce, A. J., M. K. Stewart, and M. G. Sklash. 1986. “Storm Runoff Generation in Humid Headwater Catchments: 1. Where Does the Water Come From?” *Water Resources Research* 22 (8): 1263–1272. doi:10.1029/WR022i008p01263.

Richey, D.G, J.J Mcdonnel, M.W Erbe, and T.M Hurd. 1998. “Hydrochemical Separation Based on Chemical and Isotopic Concentrations: a Critical Appraisal of Published Studies from New Zealand, North America, and Europe.” *Journal of Hydrology, New Zealand* 37 (2): 95–111.

Sklash, M. G., and R. N. Farvolden. 1979. “The Role of Groundwater in Storm Runoff.” *Journal of Hydrology* 43 (1–4) (October): 45–65. doi:10.1016/0022-1694(79)90164-1.

Van De Giesen, N. C., T. J. Stomph, and N. de Ridder. 2000. “Scale Effects of Hortonian Overland Flow and Rainfall–runoff Dynamics in a West African Catena Landscape.” *Hydrological Processes* 14 (1): 165–175. doi:10.1002/(SICI)1099-1085(200001)14:1<165:AID-HYP920>3.0.CO;2-1.

Zillgens, B., B. Merz, R. Kirnbauer, and N. Tilch. 2007. “Analysis of the Runoff Response of an Alpine Catchment at Different Scales.” *Hydrol. Earth Syst. Sci.* 11 (4) (July 18): 1441–1454. doi:10.5194/hess-11-1441-2007.

Chapter 3 : Two drivers for diurnal streamflow cycles in an ephemeral stream in West Africa, Burkina Faso.

Abstract

Evaporation is a key hydrologic variable in a water limited area such as Tambarga, southeastern Burkina Faso. Quantifying the evaporation into the atmosphere and its influence on local hydrology is essential for sustainable water management. Streamflow in Tambarga is largely generated by groundwater contributions and controlled diurnally by the local evapotranspiration and infiltration into the riverbed.

In this paper we investigate the typical daily streamflow pattern which has a maximum discharge early morning or late afternoon then decreases progressively until sometime midday and then recovers as plants reduce their transpiration and the net radiation declines.

The diurnal streamflow pattern is dictated by either evaporation along the stream edge and/or infiltration in the river underneath. Two regimes characterize the flow diurnal pattern in the river. In the early season when the watertable is below the streambed, the daily stream temperature variation controls the decrease of streamflow, whereas in the late season, it is controlled by evaporation and transpiration.

A simple method based on the ratio between the decrease in the streamflow and the actual evaporation measured over half-hour period has allowed evaluating the area controlling the diurnals streamflow pattern when the watertable was at streambed height.

The contributing areas computed in 2010 and 2012 during the rainy season represent 0.6% to 1% of the total area. The riparian zone could reasonably represent this area and seems corresponding to the primary source of evaporation. The daily partitioning of evaporation over the basin was highlighted using a clockwise hysteresis relationship found between actual evaporation and water loss in the stream. This relation is shifted to counter clockwise with any other additional inflow in the river such as rain event.

The relations highlighted are suited to provide insight into basin functioning and should be integrated in the hydrologic model for savanna region. Data to address these issues were collected using Eddy correlation flux tower in conjunction with two weirs as part of a field campaign in the southeastern of Burkina Faso in a mixed agricultural savanna watershed.

3.1 Introduction

Every year, the arid and semi-arid regions in West Africa experience a drastic increase of temperature. At Tambarga, the mean annual temperature is about 30°C and reaches more than 50 °C during the dry season. The high temperature is known to induce changes in hydrological variables. Previous research has shown the flow in the river to be a complex process, composed by surface runoff and baseflow. The surface runoff originates from two main processes: saturation overland flow and infiltration excess runoff. Infiltration excess runoff also called overland flow or Hortonian flow occurs mainly in arid and semi-arid regions when either the rainfall intensity is greater than infiltration rate, or all faults storage are filled (Horton 1933). The saturation excess overland flow, also called saturated overland flow, occurs during rain events when the soil is saturated and leads to direct runoff as the water cannot infiltrated. These two processes are highly linked to the antecedent soil moisture that controls the time which the soil pores and microspores taken to be fill by water .The baseflow or drought flow is the flow resulting from the drainage from the shallow groundwater or aquifers in the basin (Wilfried Brutsaert 2005; Wilfried Brutsaert and Nieber 1977). The baseflow is under the total control of the groundwater level; therefore it occurs only when the groundwater level is higher than the riverbed at some points in the basin. The amount of base flow in a stream depends highly to the soil permeability in the basin.

Like most ephemeral rivers in the semi-arid region, the Tambarga's river flows only during the rainy season and becomes continuous over the entire stream length when the groundwater level is above the riverbed throughout the basin. The careful observations of streamflow patterns at sub daily time step allowed us to highlight a typical daily pattern of streamflow. The diurnal pattern is depicted by the flow decreasing during the daytime to achieve the minimum rate at around noon and then starts increasing between 1pm to the sunset.

The diurnal cycle of streamflow gives insight into the role of all the hydrological variables involved in this process and then provides relevant information to characterize each variable and therefore the eco-hydrological system. The streamflow diurnal pattern was used by several scientists to estimate the evapotranspiration. The pioneers that used groundwater, free water and streamflow daily patterns to investigate the evapotranspiration were (White 1932), (Wicht 1941), Reigner (1966), Federer (1973) and Parlange et al (1975). Their studies provide strong evidence that the daily evaporation pattern is strongly linked to the flow daily pattern and therefore under certain conditions allows to assess evapotranspiration through models.

On the other hand, Constantz et al (1994) emphasized that there is not necessarily a strong link between the streamflow daily cycle and the measured evaporation. He found that the diurnal pattern observed in the streams in New Mexico and Colorado are mainly (95%) driven by infiltration of water into the riverbed while the part of diurnal variation explained by evaporation was less than 5%.

The diurnal cycle of streamflow is influenced by numerous hydrological parameters such as rainfall, radiation, stream temperature, evaporation, riverbed conductivity, soil moisture and groundwater recharge (Turk 1975; Stagnitti, Parlange, and Rose 1989; Constantz, Thomas, and Zellweger 1994; Ronan et al. 1998; Szilágyi et al. 2008; Gribovszki, Szilágyi, and Kalicz 2010). Understanding processes linked to the diurnal pattern also allows exploring the effect of climate change at basin scale (Lundquist and Cayan 2002). (Gribovszki, Szilágyi, and Kalicz 2010), in their literature review on the causes of the streamflow diurnal pattern, have highlighted five main causes: water loss in stream, precipitation, melting and freezing–thawing processes, evapotranspiration, and other causes (anthropogenic activities, water extraction). Some of these causes could be easily identified in the current studying catchment such as : precipitation(>1000mm/year); evapotranspiration through plant and free water surface (river, wet lands) which is enhanced by the high availability in evaporative energy in this area; heavy anthropogenic pressure resulting from agriculture which is the main activity with more than 8 000 stakeholders; and the intensive water resource exploitation through water extraction for supplying people needs, knowing that the groundwater is the unique source of drinking water.

The diurnal cycle is linked to water losses in the river and the catchment. The combined analysis of the groundwater and streamflow daily pattern allowed us to identify the two different main drivers of the diurnal cycle of streamflow at Tambarga. In the early season the upstream discharge is greater than the downstream. The diurnal pattern observed during this situation is led mainly by infiltration in the riverbed. The significant daytime stream temperature increase (~=+10°C) in the early season induces the increase of the infiltration rate as a consequence of the water viscosity decrease (Constantz, Thomas, and Zellweger 1994). An upward trend of groundwater level is also observed during this period, which provides more evidence for the infiltration into the riverbed.

Late in the year when the rainy season is completely established, with frequent rain recharging the groundwater, the downstream discharge becomes higher than the upstream,

while the daily streamflow pattern continues. Furthermore the groundwater is higher than the riverbed during this period, and a downward trend of its level is observed during the daytime. This trend allows us to reject the previously described pattern and assume that the diurnal pattern latter in the rainy season is mainly driven by evaporation through river and riparian plants (Bond et al. 2002). This hypothesis has also been confirmed for field experiments in a small headwater and numerical modeling(Bren 1997). The diurnal streamflow pattern driver thus shifts during the season. During the early season, when the groundwater level is under the riverbed, the high range of streambed temperature induces significant variations of the infiltration rate. While later in the season, when the groundwater level is above the riverbed, the loss in the stream is caused by evaporation and transpiration by plants in the riparian area. A clear evaluation and delineation of the area which controls this pattern is important for a better modeling of the hydrological processes.

In hydrology, before performing any modeling of processes, a clear delineation of the area where they take place is crucial. Several concepts such as topographic bounds, hydrological unit, drainage area and evaporation footprint has been by the scientific community to delineate the area contributing to a define process. During a rain event only a fraction of the watershed area contributes to the runoff hydrograph (Ragan 1968; Ben-Asher and Humborg 1992; Dunne and Black 1970; Lane et al. 1978; Ben-Asher and Humborg 1992; Peugeot et al. 1997; Wu, Suzuoki, and Dissado 2004; Spence et al. 2010). Several scientists have investigated the concept of partial area contributions to storm hydrographs. They found that the area depends on the rainfall intensity, soil properties, topography, land cover, soil moisture and groundwater network. The topographic bounds of the basin correspond rarely at the real runoff production plot (Spence et al. 2010). The contributing area expands or contracts seasonally or during a storm (Dunne and Black 1970; Ben-Asher and Humborg 1992). Therefore a clear definition of the area which controls the diurnal pattern is still waiting.

Unlike the contributing area during storms, little interest was devoted to the area likely contributing to streamflow during the period without rainfall. The drainage area (topographic bounds) and the evaporation footprint are roughly used as area that control respectively stream flow and evaporation. (Parlange and Aylor 1975) were the first to address an analysis between evaporation and the diurnal cycle of water outflow on a small watershed during 4 summers in North Madison, Connecticut aiming to delineate its contributing area.

The overestimation or underestimation of this surface is source of errors in the hydrological models and therefore the forecast with potentially severe consequences for humans and animals mainly in the regions with limited water resources. This study aims to complete the previous work done by (Parlange and Aylor 1975) by estimating the area which controls the streamflow diurnal pattern during the rainy season.

3.2 Study area

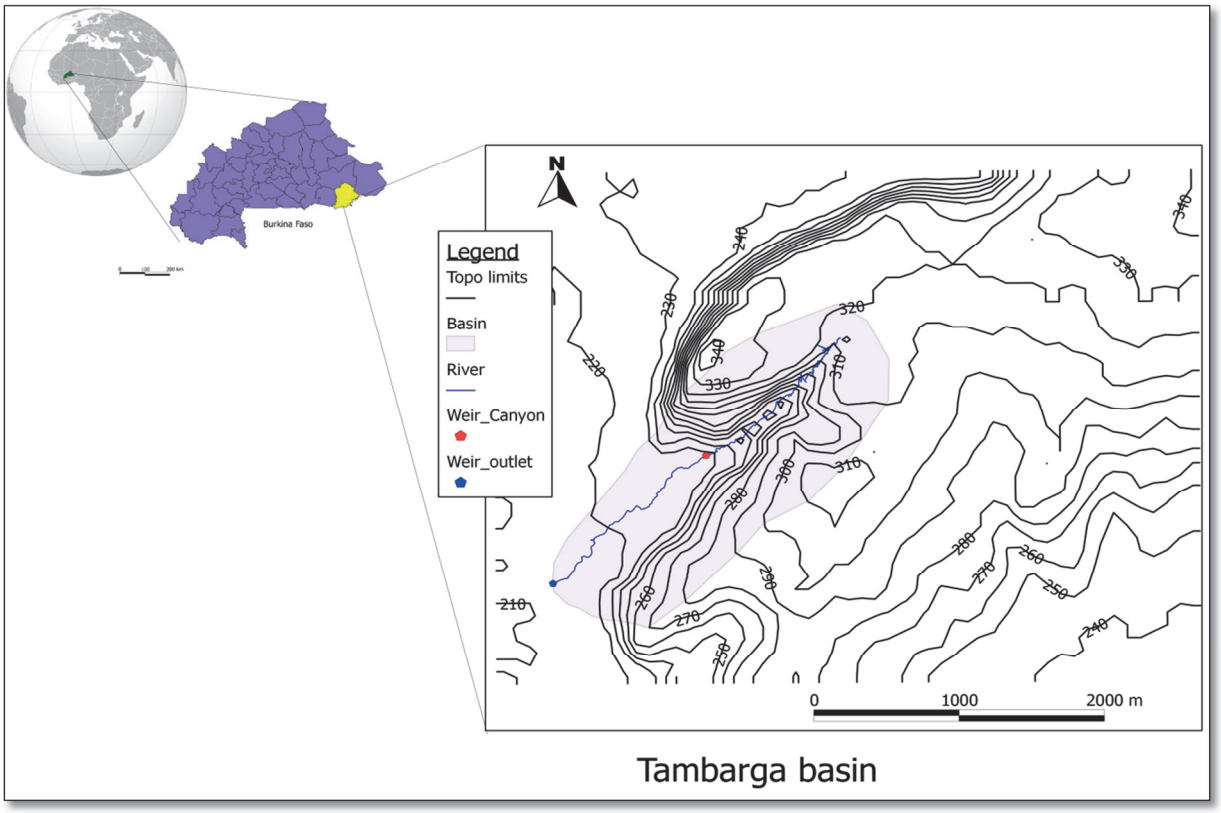

Figure 3.1: Location of Tambarga experimental basin, Burkina Faso

The study site is located in the southeast of Burkina Faso (11°26'42.79"N, 1°13'32.09"E) in the Soudano-sahelian climate zone (Figure 3.1). The basin is part of the Madjoari commune in the province of Kompienga. The trial basin is a sub-watershed of the Singou watershed which is part of the Volta basin.

The Singou basin is mostly covered with savanna forests, managed by private safari ranches. About one third of the basin is managed by the local communities, with villages, agricultural fields, and community owned savanna forests. Based on topography, landscape and land use the Tambarga basin could be subdivided in two parts (lower agricultural basin and upper open savanna forest).

Agriculture in Madjoari is very intensive and occupied more 90% of the population, however less than 11% of the surface is used for agriculture. Therefore the site encounters increasing anthropogenic pressure (over grazing land, expansion of farming zone…) and an appreciable decrease of rainfall since the seventies illustrated by the transition from the Soudanian to the Soudano-sahelian climatic zone between 1960 and 1980. The rainfall at Tambarga is monomodal with one rainy season (May to October) and one dry season (November to April) (Bagayoko et al. 2007). The rain events occur mainly early morning and early afternoon and are characterized by short and intensive events with an average annual rainfall of 1000 mm/year.

The field experiment is ongoing since April 2009 to provide a comprehensive dataset aiming at investigating the impact of evaporation on streamflow diurnal pattern. Data used in this paper were collected during 2010 and rainy seasons, with advanced research equipment such as three-dimensional sonic anemometers and open path infrared H2O/CO2 gas analyzers, two weirs and wells provided with automatic pressure sensor.

3.3 Material and Method

A wireless sensors network of meteorological stations (SensorScope) was distributed over the whole watershed aiming to capture the spatial and temporal distribution of the meteorological variables. SensorScope stations are autonomous and connected through a distributed multihop network which allows to route all data through the GSM network to a central data base accessible in real time in the web (Ingelrest et al. 2010; Simoni et al. 2011).

Twelve stations were deployed over the site with respectively three stations on the savanna open forest, seven stations in the agricultural field and two stations in the wetland at the basin outlet. This distribution of stations was chosen based on the land use, land cover and watertable partitioning over the entire watershed. Each station measures several environmental variables such as rainfall, air temperature and humidity, wind speed and direction, skin temperature, solar radiation, soil moisture and soil potential at different depths.

After two years of field campaigns and having regard to the data quality and the quantity (gaps in the time series, accuracy, locations of measurements etc.). We refined the study by upgrading six stations over the basin; two in each of the three different geomorphological units (upper basin open savanna forest, middle agricultural fields and bottom wetland).

These stations have been upgraded with: soil moisture sensors at four different depths (5, 10, 20, 40 cm) aiming to understand the process of moistening and drying of the soil; Two solar radiation sensors oriented up and down aiming to estimate the net radiation and complete the local energy budget; two rain gauges were set up in each station, aiming to improve the rainfall measurements by reducing the errors (false measures, communication issues, dust issues etc.).

3.3.1 Groundwater

The groundwater is one of the main components in hydrology mainly in the water limited areas (arid and semi-arid region). Understand the pattern of recharge is important and allows better forecasting of flood events (Szilagyi, Parlange, and Balint 2006; Szilágyi et al. 2008). The recharge process is strongly related to the rain type, the soil texture and structure, the streamflow and evaporation pattern. The groundwater at Tambarga is characterized roughly by two shallow perched water tables located upstream and downstream separated by a deeper water table in the middle part of the basin (Mande et al. 2014).

To understand the watertable pattern over the basin, we monitor since 2009 the water level of seven existing wells distributed in the lower agricultural basin along the cross section. These wells are the primary sources of drinking water for the local population, livestock. The local influence of water level due to the local uses did not allow capturing the real influence of the rain on recharge. Therefore to be able to understand the real recharge dynamic, not too much disturbed by human direct influence, the wells were monitored in the early morning (4 am to 5 am), just before the local population starts to use water from the wells. Additionally in 2011, two wells were dug directly in the riverbed at the basin upstream and downstream. These wells were provided with automatic pressure transducer to monitor at a finer time scale the groundwater level. The previous monitored wells sampling time were intensifying (every day against twice a week in the past).

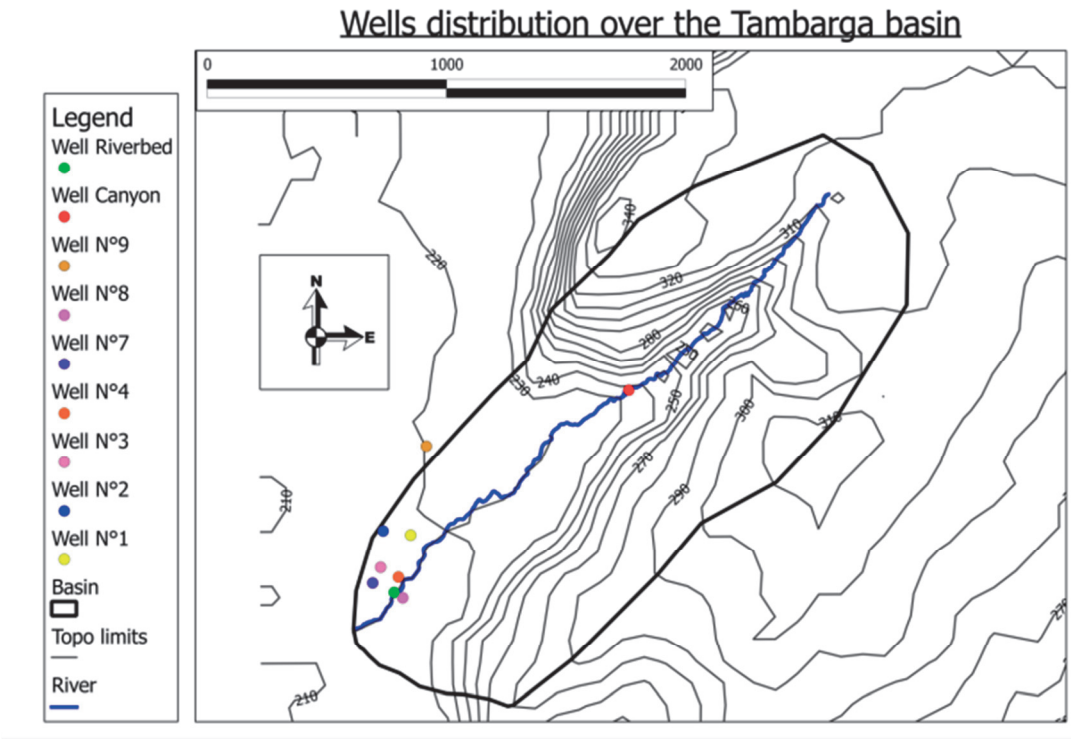

Figure 3.2: Groundwater monitoring locations

3.3.2 Streamflow

In hydrology one of the challenging parameters to predict remains the stream flow as far as it depends upon several variables like rainfall intensity, soil structure, land cover and geometry of river (slope, roughness etc.). Besides these natural factors, the stream flow pattern can be changed by badly planned human activities, such as groundwater over exploitation, drainage of wetlands, deforestation, soil erosion and compaction(Ghimire and M. Janga Reddy 2010).

The riverbed change over the season is a critical issue for flow measurement. To take into account this issue the riverbeds were stabilized at the two outlets using concrete channels (5X 2 X 1) [m]. The weirs were previously designed in Switzerland with aluminum plates and after calibrated in the hydraulic laboratory at EPFL. The calibration allowed establishing the first rating curve for each weir.

The real world flow conditions are influenced by rainfall intensity, particle settling and soil properties. Field observations allowed finding that the upstream basin didn't carry sediments into the river while the downstream basin carries a significant amount of sediment which could affect the rating curve. Additionally the river network upstream doesn't satisfy to the conditions for use the salt dilution method. Therefore we chose to recalibrate only the downstream weir and kept the laboratory rating curve for the upstream weir.

To reduce the impact of erosion and sedimentation on the rating curve a field calibration was done for the downstream weir. Daily discharge measurements were done by using salt dilution method. The data collected by this method and the water stage recorded in the downstream weir allowed to correct the previous rating curve obtained in the laboratory for local conditions. The rating curves were used to convert upstream and downstream stage to discharge. Stage at each weir was measured and recorded every minute by using automatic pressure sensors (manufactured by MADD TECHNOLOGIES, Switzerland) and converted to streamflow through stage-discharge curves (Figure 3.3 a,b).

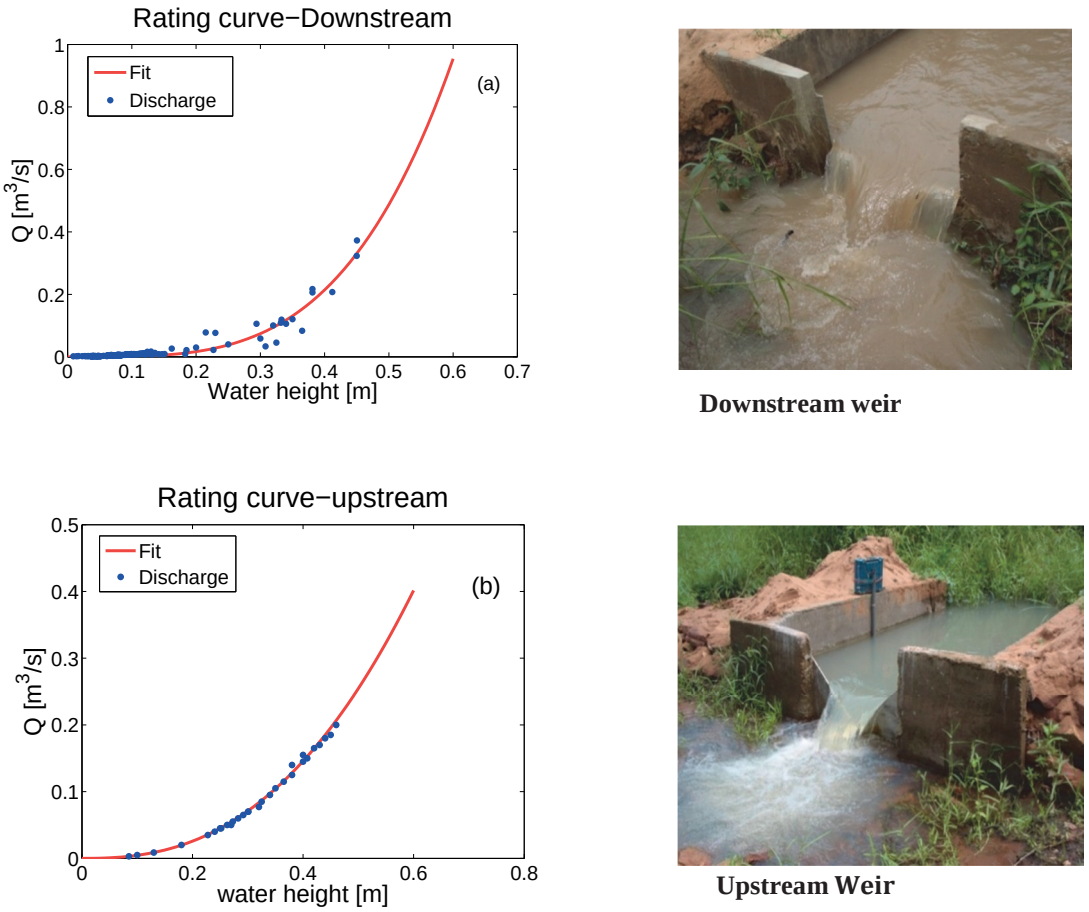

Figure 3.3: Rating curves (RC) of the two weirs at Tambarga. Downstream's weir RC (a) with picture of the weir at its right. The discharge data (blue dots) of (a) are field measurements (salt dilution method). Upstream's weir RC (b) with the picture of the weir on its right. The discharge data (blue dots) of (b) come from laboratory experiment at EPFL.

(1) $Q(h) = 1.44 * h^{5/2}$ $(m^3 S^{-1})$: Upstream weir with adjusted R-squared coefficient of 0.99.
(2) $Q(h) = 6.27 * h^{3.68}$ $(m^3 S^{-1})$: Downstream weir with adjusted R-squared coefficient of 0.93. Where Q is the discharge in (m^3 s^{-1}) and h is the water level in m.

3.3.3 Stream Temperature

The gaining or losing of water by the stream is detectable by its temperature pattern. Monitoring the stream temperature has been used previously for partitioning the water sources and completing water balance (Selker et al. 2006; Constantz, Thomas, and Zellweger 1994). Therefore to understand the influence of temperature on the water balance, we set up a fiber-optic cable for Distributed Temperature Sensing (DTS) in the riverbed from 2009 to 2010 aiming to investigate the spatial and temporal variation of stream temperature in the riverbed. Additionally a set of localized temperature sensors (tidbit, pressure transducers) were installed in the riverbed and at the outlets.

3.3.4 Sensible and Latent heat flux

Evapotranspiration occurs through a very complex process involving all the water losses due to direct evaporation from free water and bare soils, and transpiration from plants through water uptake (Stagnitti, J. Y Parlange, and C. W Rose 1989). Each of these components is also governed by complex processes which increase the complexity of measuring the evapotranspiration. Nowadays Energy balance or eddy correlation methods are proven approaches for estimating evapotranspiration (Swinbank 1951; Brutsaert and Parlange 1998; Vercauteren et al. 2009;Bagayoko et al. 2007; Zhu et al. 2011). Eddy covariance towers including three-dimensional sonic anemometers (Campbell Sci.) with fast response H2O/CO2 (Licor) were used to measure sensible and latent heat flux as well as ground heat flux, net radiation, the surface shear stress and other turbulence characteristics. The stations were set up in the agricultural field and the open savanna forest. In order to account for changing wind directions and long term operation, the agricultural section tower has been equipped with two sets of fast response turbulence instrumentation situated at 180° to avoid wind blockage of the tower in at least one direction at all times. Each tower also has a (Kipp and Zonen) net radiometer that measures separately short and long wave radiation upwards to avoid tower shadow effects. Soil heat fluxes are obtained using both heat flux plates, soil temperature and soil moisture at different depths in the agricultural field zone. Because of the field configuration, the hill section tower has been installed on the hill edge, with mono-directional equipment oriented toward the canyon. Each tower is located with sufficient upwind fetch to allow an integrated measure of the turbulent surface fluxes. Each tower records the turbulence data at 20 Hz in order to compute the heat fluxes. For this study the data of the tower on the

agricultural field were used, and the latent heat flux (LeE) was computed using the following equations then converted to evaporation (mm) through a simple mathematical relation.

$$R_n = H_s + L_eE + G + \varepsilon,$$

$$H = \hat{\rho}c_p\overline{w'T'} \ , \quad L_eE = \hat{\rho}c_p\overline{w'q'}$$

Rn = Net radiation, H = Sensible heat flux, LeE = Latent heat flux,
G = ground heat , ε = residual , ρ = density of air ,Cp = calorific capacity ,
w = vertical wind speed (z direction), T = temperature,
Le = Latent heat of evaporation, q = specific humidity ,

3.4 Results

3.4.1 Meteorological variables

3.4.1.1 Rainfall

The rainy season lasts 4 to 5 five months and occurs from May to October. The rainfall is generated by the combined effects of the West African Monsoon, migration of the inter-tropical convergence zone and the Sea surface Temperature. The rain is variable in space and time and characterized by short and intensive events. At Tambarga the rain events occurred mainly early morning or late afternoon. The variability of the rain in this region is more pronounced at the yearly and seasonal scale. The maximum rainfall measured per tipping obtained by comparing all the raingages has been used to characterize the rain overall Tambarga's basin. Therefore the annual variability was observed between 2010 and 2012. Indeed in 2011 less than 700 mm of total rain was collected in the basin against 1317 mm (2010) and 1243 mm (2012) (Figure 3.4). The rain in 2011 was almost 60 % less compared to average.

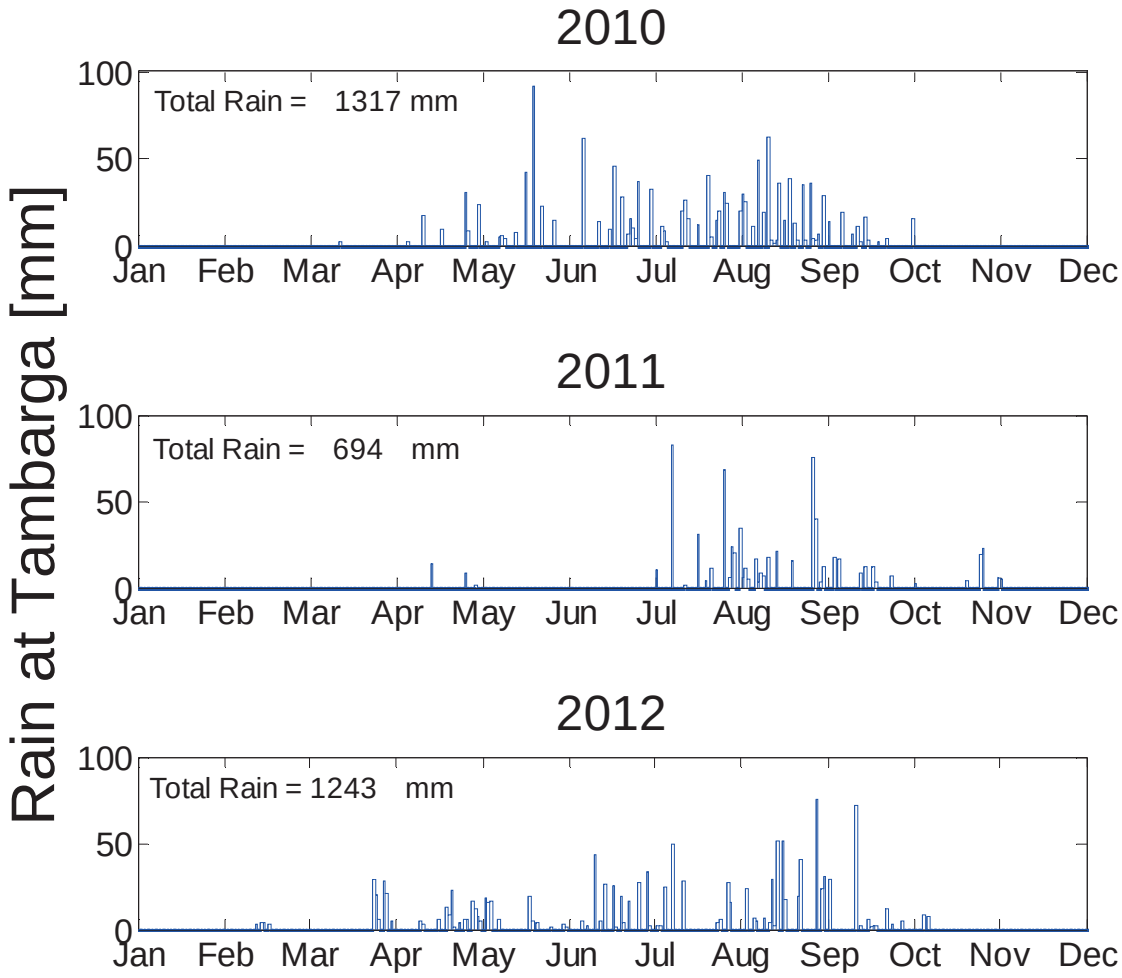

Figure 3.4: Rainfall yearly pattern at Tambarga (2010 to 2012)

3.4.1.2 Stream flow

The discharge is gauged at two locations in the upstream and downstream part of the basin. The river at Tambarga is seasonal and reacts fastest during rain events with hydrographs that last less than one hour due to quick overland flow. The maximum discharges observed in 2010 were (0.58 m^3/s and 0. 52 m^3/s) against (1 m^3/s, 1.25 m^3/s) in 2012 for respectively upstream and downstream weir. Unfortunately for technical reasons any discharge were collected in 2011.

In general the discharge downstream is higher than the discharge upstream; by contrast, at the beginning of the wet season the contribution of upstream is higher than the downstream; see Aug 2010 and September 2012 (Figure 3.5). The stream flow at Tambarga is ephemeral and starts flowing sometime after the season onset.

Three phases can be distinguished for the flows in the river during the rainy season. In the early season, only a section (300m from the outlet) at the downstream basin generates flow in the river when the downstream shallow groundwater is filled. In the middle season, when the upstream shallow groundwater is filled, the flows start at the upstream section of the river over 500m from the upper weir. This upstream flow is infiltrated between the two weirs during some days; thereafter the flow becomes continuous over the entire river (2.8 km) when the entire water tables network is interconnected.

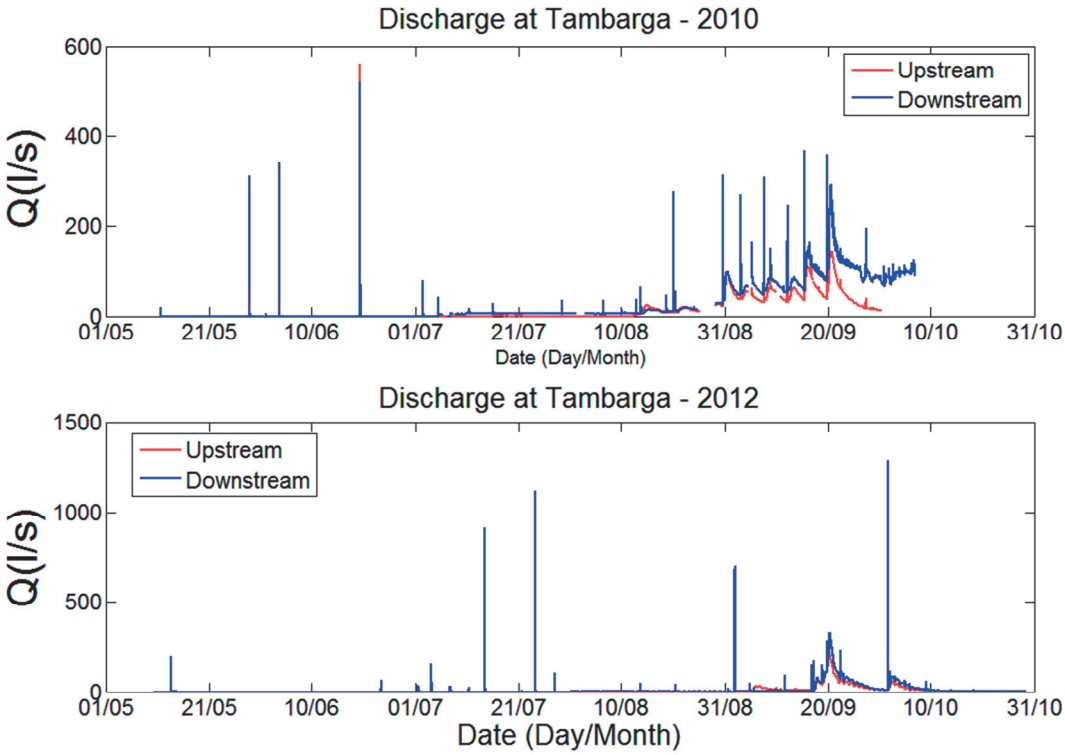

Figure 3.5: Discharge measured upstream and downstream

3.4.1.3 Groundwater

From 2009 to 2012 the groundwater data were recorded by hand twice a week. This monitoring time step gives good information at seasonal time scale but is not relevant for daily time scale (Figure 3.6, year 2009). Therefore in 2011, the measurements were refined, and two additional wells were dug in the riverbed and provided with automatic pressure sensors for monitoring the groundwater level. The water level data were collected at fine time resolution (5-min), the choice was made knowing that the time that the water takes to reach the groundwater is greater than 5 minutes.

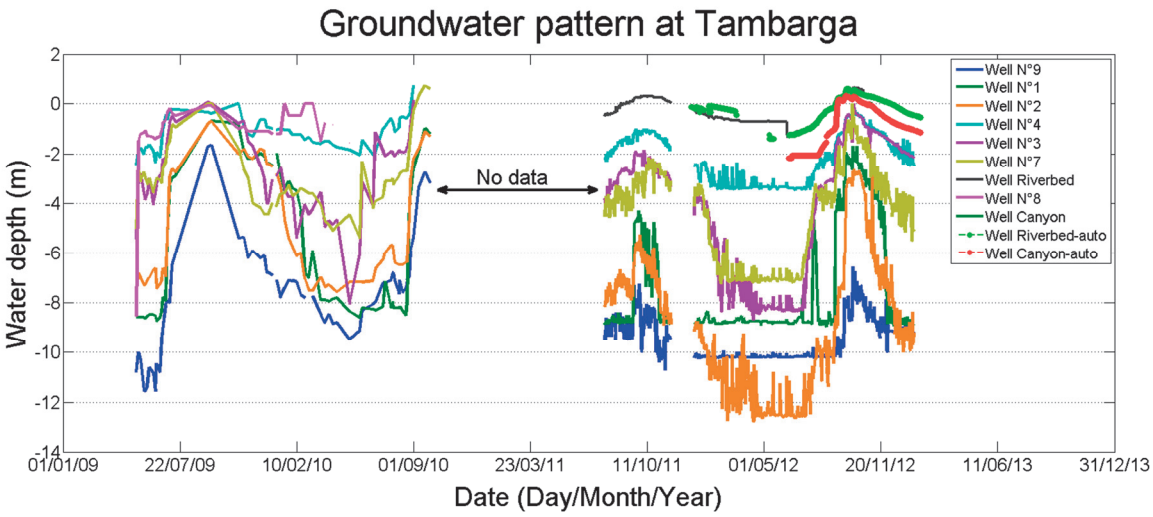

Figure 3.6: Groundwater pattern (2009-2012)

The groundwater patterns change according to the timescale. The change at Tambarga is more obvious at daily and seasonal scale. The groundwater follows a seasonal pattern with recharge and depletion respectively during the rainy season and dry season. The year 2011 was dry with minimal recharge and deeper decrease of the groundwater level over the basin (-12m for Well N°2). The recharge of the middle watertable takes less than two weeks, when the rain events are more frequent.

The rainfall is the unique source for groundwater recharge. The peaks of recharges are enhanced by the high frequency and intensity of the rainfall events. Looking in detail at the groundwater level (well N° 1, 2, 3, 4, 7, 8 and 9, Figure 3.6), some short term fluctuations appear. These fluctuations dependent mainly on two factors, short rainfall event and water extraction for human needs .Their amplitudes are function of the rainfall characteristics and the amount of water extracted.

3.4.1.4 Diurnal Patterns

a Streamflow

By carefully scrutinizing the daily streamflow and evaporation, a typical diurnal pattern could be highlighted. The time scale of the measurements is crucial for being able to capture the diurnal pattern, meaning that the scale should be much finer than one day. According to (Cuevas et al. 2010), studying diurnally the streamflow has been possible since the advent of advanced monitoring sensors. Regarding the number and the type of sensors available in the market, the choice of the sensor and/or the type of correction used could generate errors mainly for low discharge(Cuevas et al. 2010).

At Tambarga, the observation of the streamflow during two years allowed us to find some daily cycle of streamflow during the dry period inside the rainy season. The streamflow time series in Figure 3.7 highlight the daily pattern of the flow measured at upstream and downstream weirs, 1.6 km away. The streamflow diurnal pattern is characterized by a maximum flow rate early morning followed by a decreasing of the flow during the daytime to achieve the minimum rate at around noon. A phase of recovering starts when the minimum flow is reached; therefore between noon and the sunset the discharge increases to achieve a maximum in the early morning the next day (Figure 3.7). The lowering of streamflow takes place together with the increase of some variables such as temperature, evaporation and the strength of the radiation while the upward trend of the flow occurs in parallel with the downward trend of these variables.

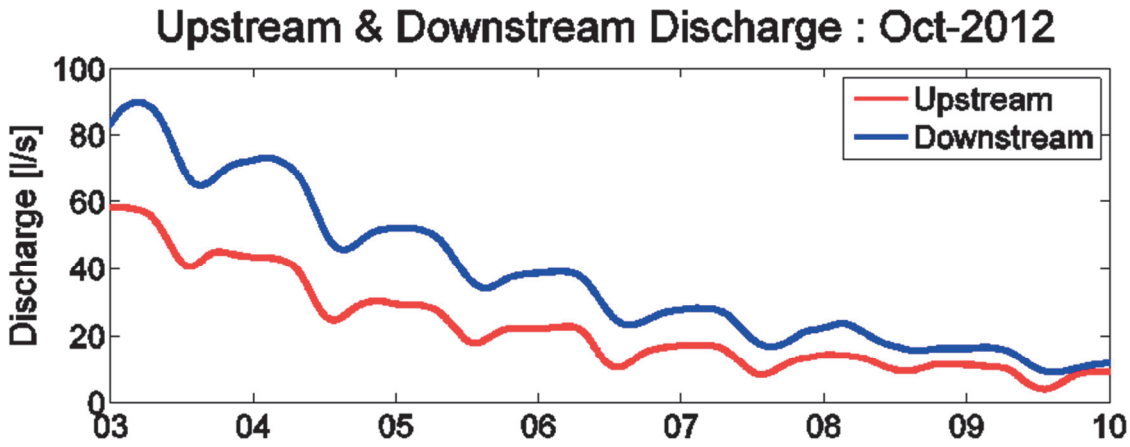

Figure 3.7: Streamflow time series, the blue line represents the discharge measured downstream and the red line the upstream discharge

b Diurnal evaporation

The evaporation is computed at half-hour time scale which allows highlighting its daily cycle. The evaporation is almost null or even negative during the night while the positive evaporation sometimes observed is caused by the night time winds. The diurnal cycle of the evaporation trend is opposite to that of the streamflow. Thus the evaporation almost null during the night and starts increasing with the sunrise and achieves the maximum around noon (maximum radiation) and then decrease to the sunset while also the net radiation strength declines (Figure 3.8).

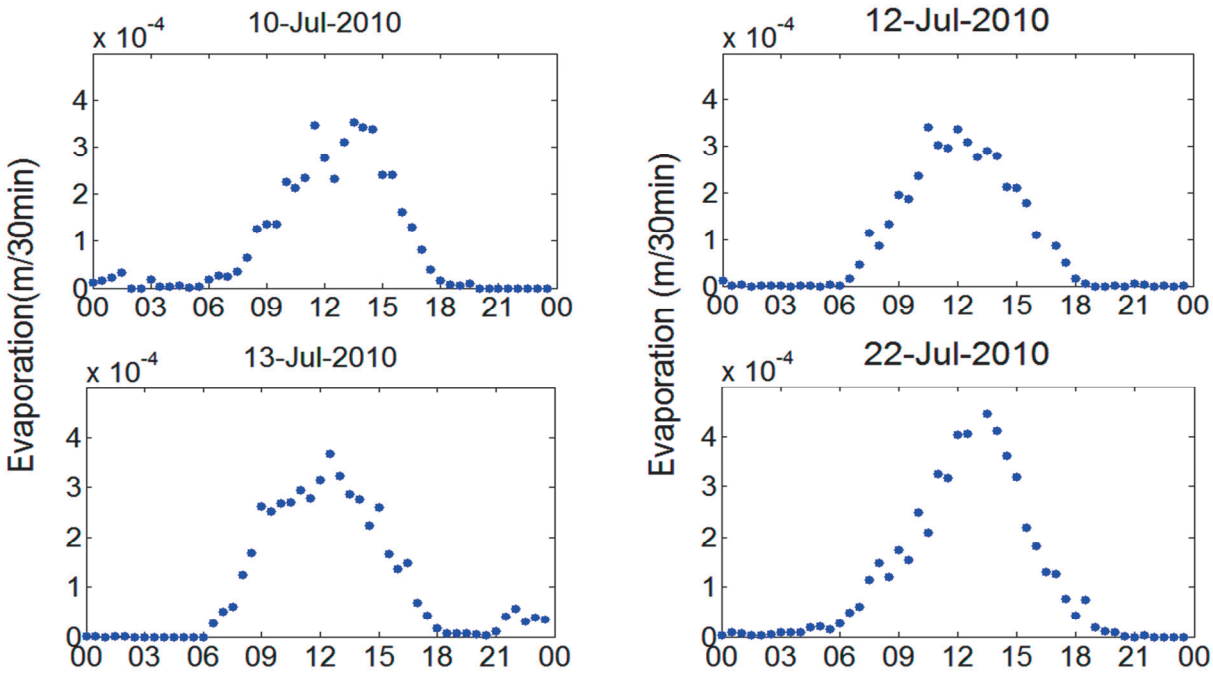

Figure 3.8: Evaporation diurnal pattern: four subplots of daily evaporation measured with eddy covariance technic in the agricultural basin

3.4.2 Two regimes of flow

The continuous flow in the river at Tambarga is completely under groundwater outflow control. The correlation between the trend of the water level in a river and in the groundwater below is strong. The streamflow becomes more pronounced with the increase of the groundwater level while the groundwater level decrease leads to lower the flows in the river (Szilágyi et al. 2008; Gribovszki et al. 2008; Cuevas et al. 2010).

Two regimes could be identified according to the amounts of discharge upstream and downstream. The first regime occurs in the early season when the soil is dry, the rain events sparse and important temperature range occurs at daytime. During this period the upstream flow is greater than the downstream flow (Figure 3.9). The second regime takes place with the connection of all the network of water tables and the downstream discharge greater than the upstream (Figure 3.10).

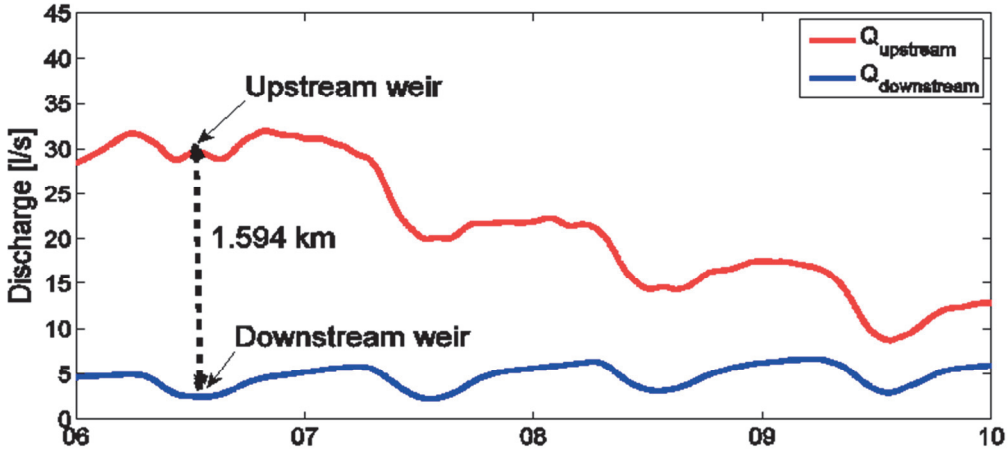

Figure 3.9: Upstream flow greater than downstream-September 2012: 1st regime of flow

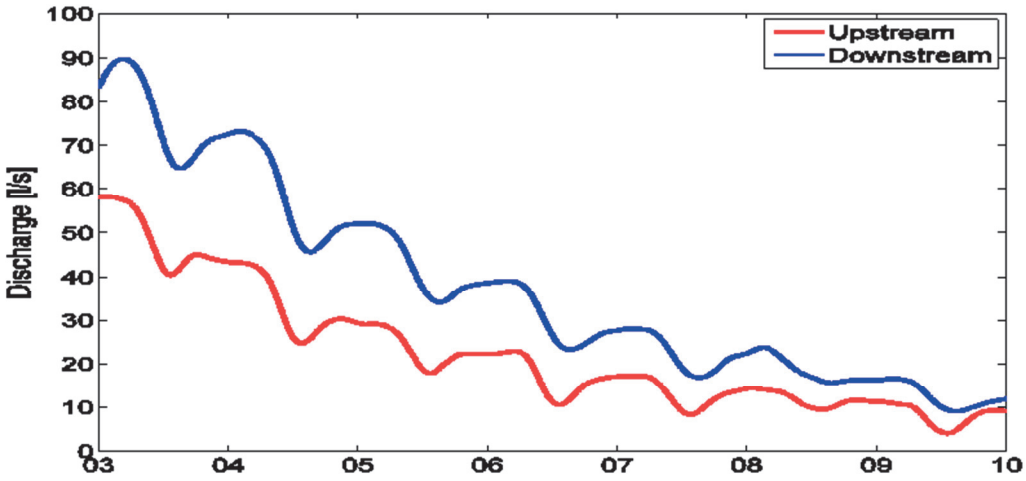

Figure 3.10: Downstream flow greater than upstream-Oct 2012: 2nd regime of flow

The diurnal streamflow pattern is dictated by either evaporation along the stream edge and/or infiltration in the river underneath. Two regimes characterize the flow diurnal pattern in the river. In the early season when the watertable is below the streambed, the daily stream temperature variation controls the decrease of streamflow, whereas in the late season, it is controlled by evaporation and transpiration.

3.4.2.1 Infiltration induced by viscosity change

Infiltration is the process by which any fluids go through a given medium (soil). The Infiltration is an important process for vegetation, human and animals, because it constitutes the only way by which the water could be supplied to the soil and therefore groundwater. The amount of water stored in soil is represented by the soil moisture in which several micro-organisms and vegetation live. The groundwater meanwhile is fundamental for water supply mainly in arid and semi-arid regions. The recharge of the groundwater depends upon the soil hydraulic conductivity which represents the speed of the water to infiltrate the soil. Several methods were developed in the literature to compute the hydraulic conductivity in which two main categories could be identified: hydraulic methods and the correlation methods. These methods can be laboratory methods or in-situ (or field) methods. Correlation methods are established according to the relationships between soil properties and the hydraulic conductivity value. The hydraulic methods used Darcy laws with imposed flow conditions in the soil. The hydraulic method can be done at overall scales but is more time consuming and relatively more accurate than correlation methods as they reduce the uncertainties induced by the complex soil properties.

Darcy was the first in 1856 to propose a way for quantify the amount of water that infiltrated during rain. Based on the established relationship between the rates of flow through (Q) a known cross-section area (A), the pressure head difference (Δh) and the length of the studying section (ΔL) (following equation)

$$Q = \frac{k * A * \Delta h}{\Delta L}$$

Darcy's law was developed for saturated flow in porous media, therefore (Richards,1931) has used partial differential equation to describe the water movement in unsaturated soil and derive to the following equation known commonly as Richards's equation:

$$\frac{\partial \theta}{\partial t} = \frac{\partial}{\partial x}\left[k(\theta) * \left(\frac{\partial \psi}{\partial z} + 1\right)\right]$$

Where : **k** is the hydraulic conductivity, **Ψ** is the pressure head, **z** is the elevation above a vertical datum, **θ** is the water content, and **t** is time.

However, reliable estimates of hydraulic conductivity remains an issue in the unsaturated zone (Van Genuchten 1980). The hydraulic conductivity varies highly in space and time and is also affected by the soil chemistry and geomorphology. Therefore to estimate the infiltration in the soil, it is crucial to have some knowledge on the soil, fluid properties and local conditions. The hydraulic conductivity is then function of the soil structure, texture, fluid properties and the moisture. Particularly, related to the soils and fluids properties, the hydraulic conductivity appears depending on the intrinsic permeability of the medium, the density and viscosity of the fluid. The density and viscosity of water are both temperature dependent, thus change of temperature leads to change of hydraulic conductivity. However the change on the water density is negligible comparatively to the water viscosity which is in the order of magnitude greater(Constantz, Thomas, and Zellweger 1994).

a Influence of temperature

Water temperature affects both physical and biological processes in stream (Gomi, Moore, and Dhakal 2006). Stream temperature was used in the past as tracer for partitioning old and new water therefore (Kobayashi, 1985) identified the subsurface water contributions to stream flow coming from groundwater based on the similarity of temperature between the groundwater and the river. According to (Alkhaier 2011), used temperature as tracer is ecological knowing that its signature is natural and doesn't affect the ecosystem as chemical tracers do.. Spatial anomalies of soil temperature were used by (Cartwright 1974) to investigate the riparian groundwater flow in Illinois. He found that the anomalies could be used to quantify groundwater and discharge.

Recently stream temperature was shown to play an important role on the streamflow diurnal pattern. Basically the groundwater inflow or outflow could be computed based on stream temperature measurements(Constantz, Thomas, and Zellweger 1994; Selker et al. 2006). Constantz, Thomas, and Zellweger (1994) found that the stream temperature change (increase) leads to the decrease of the viscosity and therefore an increase of the hydraulic conductivity, the increase is about 30% for a variation of temperature of 10 °C. The following Muskat equation(Muskat 1937) was used to validate this assumption. In this equation the hydraulic conductivity (K [m s^{-1}]) is function of intrinsic permeability (k [m^2]), the acceleration gravity (g [m s^{-2}]), the water density (ρ) and the dynamic viscosity (η [kg m^{-1} s^{-1}]).

$$\mathrm{K} = \kappa g \frac{\rho}{\eta} \quad (1.1)$$

This formula derived for the velocity potential (Φ) (Muskat 1937)

$$\Phi = \frac{\kappa}{\eta}(p \pm \rho g z) \quad (1.2)$$

± Signs correspond to the upward or downward direction of the flow.

Intrinsic permeability (κ); Gravity (g); Water density (ρ)

The equilibrium between free surface and atmosphere allows conclude that the pressure is uniform over the free surface and can be taken equal zero. Therefore equation (1.2) become (1.1) knowing that

$$\Phi = Kz;$$

Hydraulic conductivity (K)

The viscosity (also called dynamic viscosity and absolute viscosity) is a property of a fluid to resist to flow. This resistance is caused by the internal friction of the molecules in a moving fluid. The figure 3.11 highlights the relationship between the water temperature and viscosity. The increase of water temperature in the river leads to a decrease of the viscosity and therefore to increase of the hydraulic conductivity (Muskat 1937; Constantz, Thomas, and Zellweger 1994). However this trend is not valid for all the fluids such as gases, indeed the viscosity of the gases increases with the temperature.

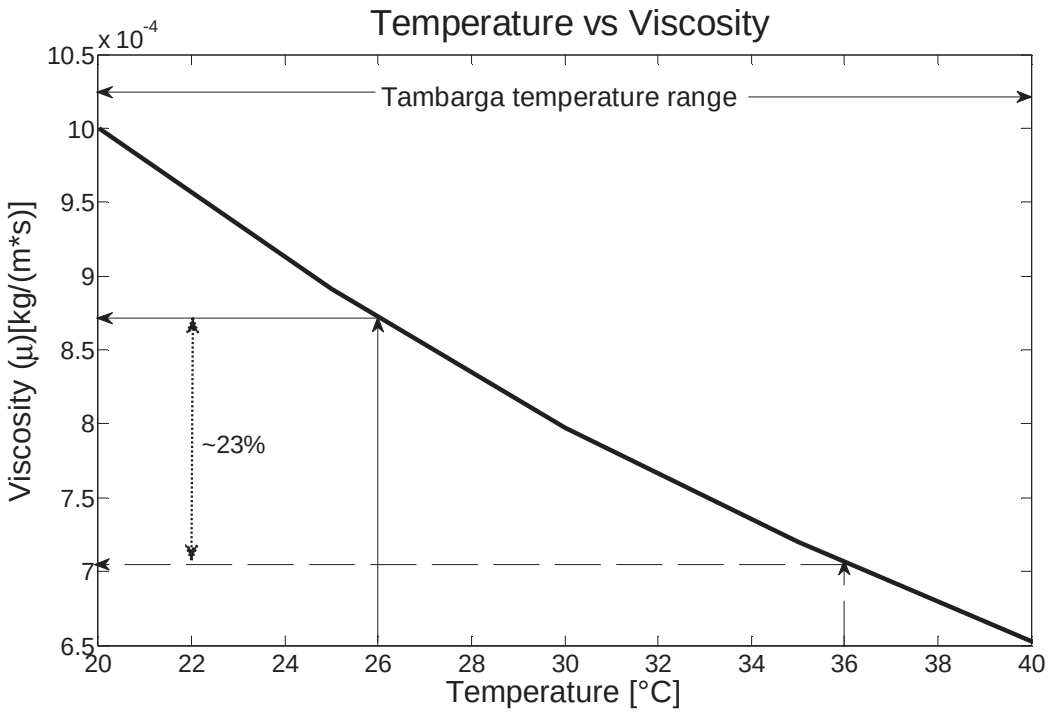

Figure 3.11: Relation between water temperature and viscosity

The stream temperature at Tambarga is range between 20°C and 40°C. The increase of 10°C (26 °C to 36 °C) of the stream temperature leads to 23% decrease of dynamic viscosity and therefore of 30% of increase of the hydraulic conductivity as demonstrated below. For simplify the water density was considered invariable, such as it varies in order of magnitude less than the viscosity .

$$\left.\begin{aligned} K_1 &= kg\frac{\rho}{\mu_1} \Rightarrow \text{Temperature (26°C)} \quad [1] \\ K_2 &= kg\frac{\rho}{\mu_2} \Rightarrow \text{Temperature (36°C)} \quad [2] \end{aligned}\right\} \Rightarrow \frac{[1]}{[2]} \Rightarrow K_2 = K_1 \times \frac{\mu_1}{\mu_2}; \Rightarrow K_2 = K_1 \frac{\mu_1}{(1-0.23)\times\mu_1} \Rightarrow K_2 = 1.29 \times K_1;$$

The diurnal cycle of flow is observed over all the dry days according to theirs behaviors. The losses deriving from this pattern could be explained by the important increase of infiltration rate in the riverbed due to the higher daily stream temperature. In the early season the flow occurs only over a section downstream and shows some discontinuities during the daytime. The streamflow decreases in the morning and then stops at noon for some hours before restarts to flow. The water loss in the river is total at the midday (Figure 3.12). The temperature observed in the stream during the same period demonstrates also a daily variation with almost 10°C daytime difference (Figure 3.12). This high variation in stream temperature combined with the no flow period at noon is probably caused by the infiltration of water.

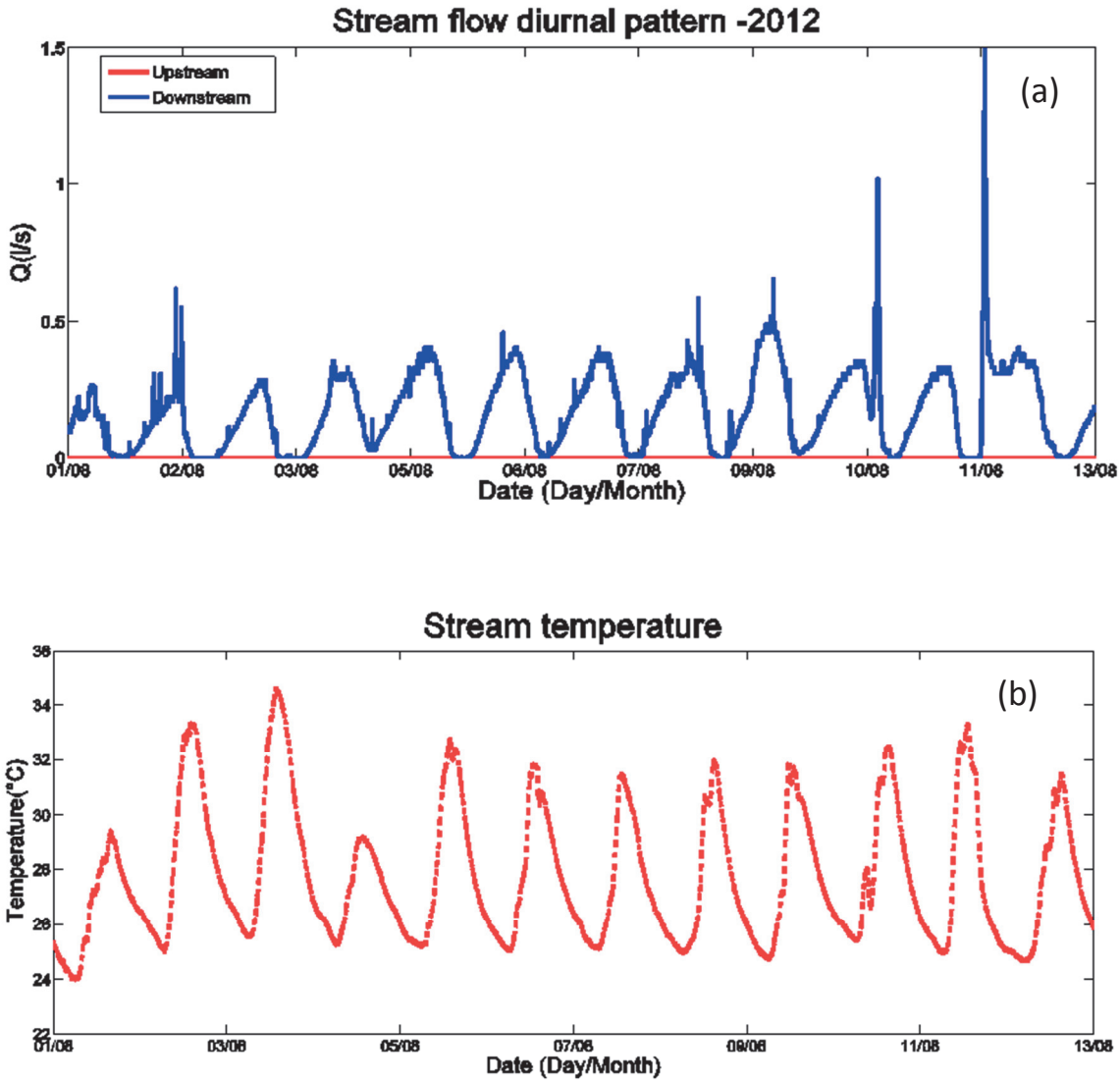

Figure 3.5: Stream flow (a) and stream temperature (b) time series-(01/08/12-13/08/12)

Additionally the groundwater trend allows validating reasonably this hypothesis of infiltration increasing. Indeed the groundwater level monitored on the streambed was observed to recharge during this period (Figure 3.13). The recharge observed is around 40cm over nine days with a mean of 4.5 cm per day. Without any rain which is the preliminary source of water on the area, the increase of the watertable level could be due to infiltration over the riverbed.

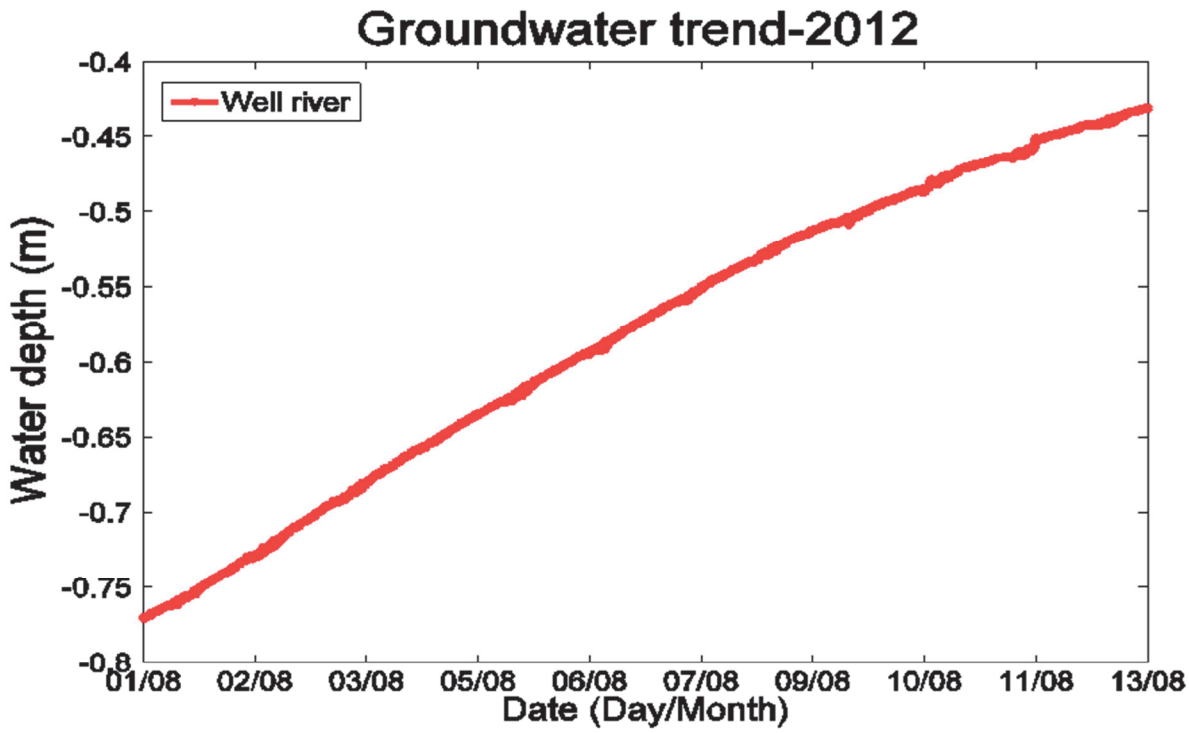

Figure 3.13: Recharge of groundwater-(01/08/12-13/08/12)

Figure 3.6 shows the discharge observed respectively upstream and downstream from 1st to August 13th. The upstream discharge is higher than the downstream discharge. The flow ranged between 10 to 35 (l/s) and 2 to 7 (l/s) respectively upstream and downstream (Figure 3.14). In this sense water is lost over the 1.6 km of river section (upstream weir and downstream weir). Indeed the flow downstream pattern is stable while the upstream flow decreases progressively toward the downstream flow level. The recharge of the groundwater (Figure 3.15) in addition to the recession curves slopes observed during the same time justifies the fact that the water could be supposed to infiltrate in the riverbed. The infiltration explains the groundwater table rise in no rain event case.

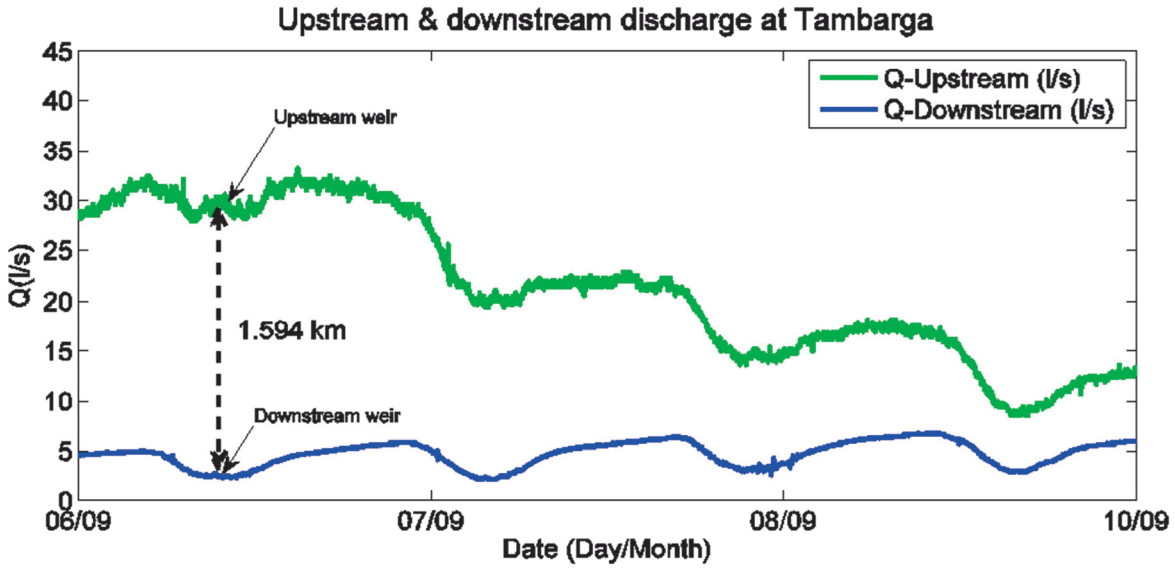

Figure 3.6: Stream flow time series: Upstream flow (green line), Downstream flow (blue line) - (06/09/12-10/09/12)

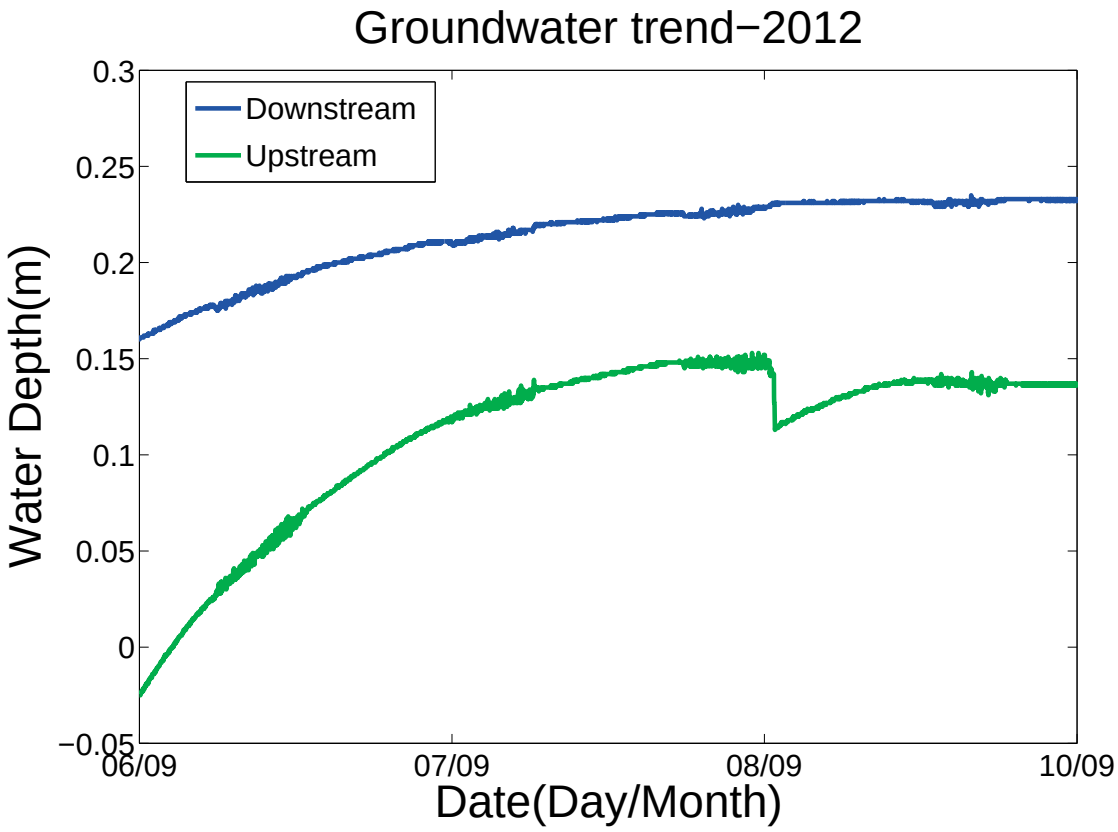

Figure 3.15: Groundwater recharge: (Blue line) corresponds to water level measured at the well located downstream while the (green line) is the water level measured upstream to the upper weir- (06/09/12-10/09/12).

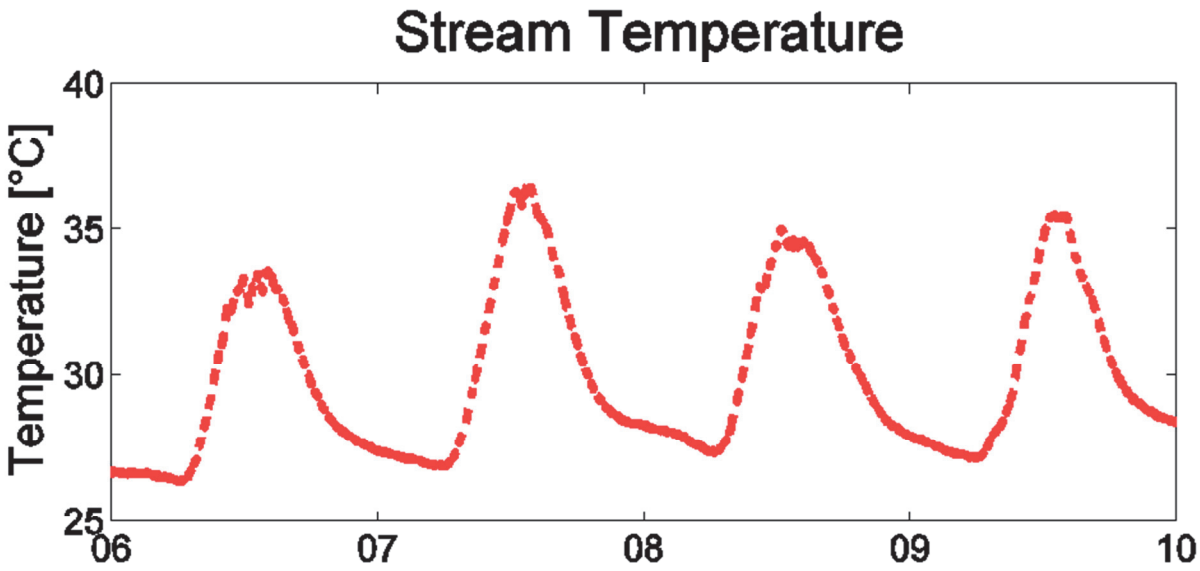

Figure 3.16: Stream temperature measured downstream (06/09/12-10/09/12)

The water loss is computed by subtracting the upstream flow to the downstream flow, thus the water loss is ranged between 5(l/s) to 25 (l/s). The way to compute the water loss didn't include the travel time of the drop form upper to lower basin (1.6 km). However the flow observed upstream and downstream show that the maximum streamflow occurs at same time. Therefore not considering the travel time in the river is realistic and didn't induce too much error.

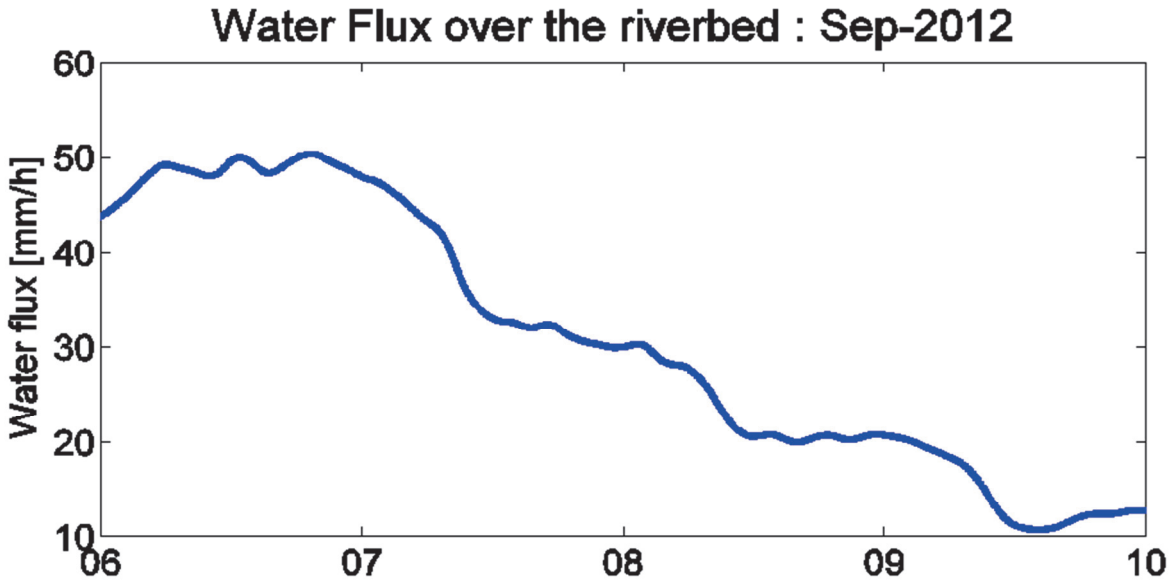

Figure 3.17: Water flux through the riverbed - (06/09/12-10/09/12)

The flux decreases matches with the decreasing slope of the groundwater level increase observed in figure 3.14. Considering the river section between upstream and downstream (1.594 km) and an average river width of 1m. The water flux in the river section varies between 10 to 50 mm/h (Figure 3.17).The figure 3.18 describes the sketch of the basin functioning during the second regime.

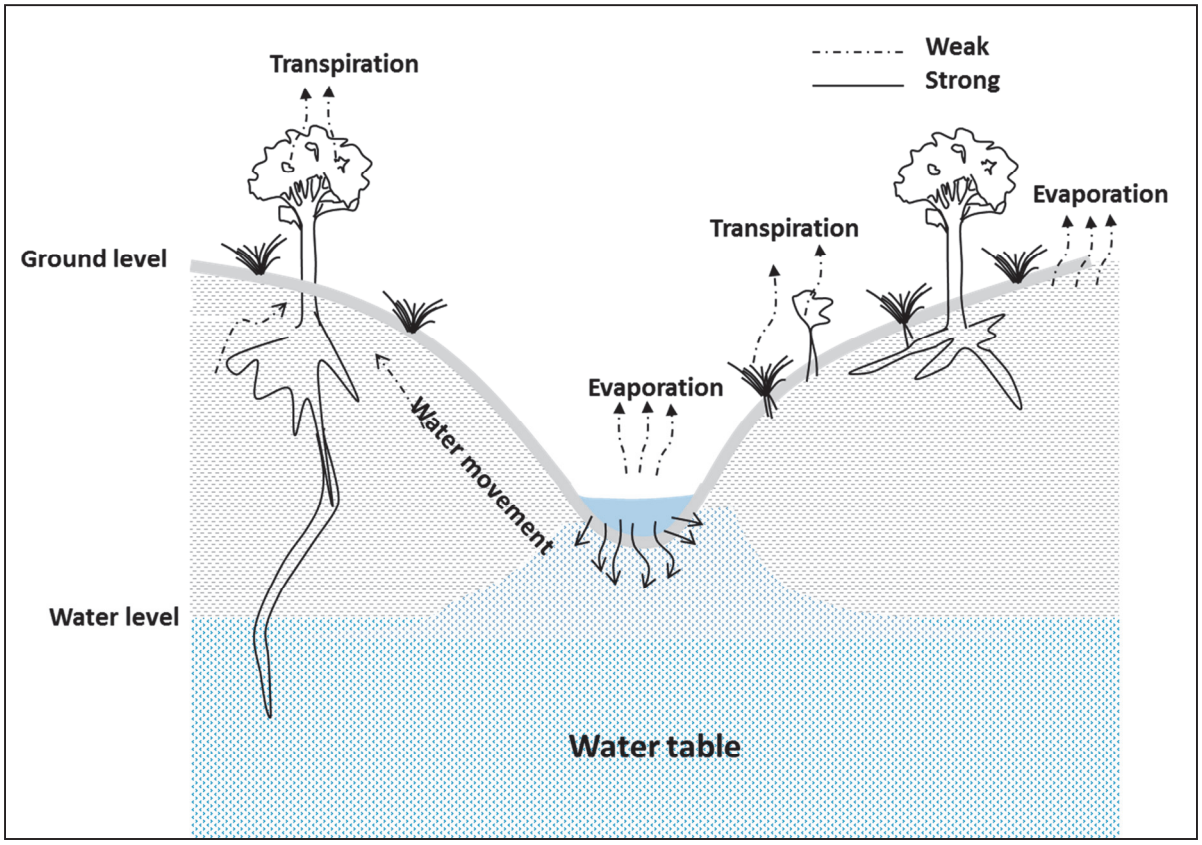

Figure 3.18: Schematic basin functioning in the early rainy season.

3.4.2.2 Evaporation Along the river edge

Evaporation is the process in which water returns into the atmosphere in vapor state, this evaporation occurs at several levels using different pathways. The evaporation takes place over open water surfaces (oceans, lakes, pond and rivers), groundwater, soil surface and vegetation. Direct evaporation from open water bodies or soil surface and transpiration are not easy to separate (Brutseart, 2005). The evaporation affects the groundwater and streamflow pattern mainly during the growing period, when the transpiration is enhanced by the crops and plants growing(Gribovszki, Kalicz, and Szilágyi 2013).

The streamflow follows a diurnal cycle driven either by infiltration in the riverbed and evaporation. During the first regime, when downstream flow is greater than the upstream flow, the groundwater network (Upstream shallow groundwater; deeper groundwater; downstream shallow groundwater) is interconnected and the global level higher than the streambed (Figure 3.19).

The riparian zone is occupied at the downstream outlet by evergreen mangoes trees in conjunction with a wetland over around one hectare and some ponds and springs. In general the trees are rare and sparse between the two weirs. During the dry season this section is occupied by dry grasses and progressively replace by green grasses and millet crops through the rainy season. This presence of evergreen trees, ponds, springs, rice field in the wet land and millet crop in the riparian zone contribute to enhance the evapotranspiration in the riparian zone through the soil and free water.

During the second regime the upper discharge is less than the lower streamflow which is different from the case studied by Constantz (1994) in Colorado and New Mexico. Therefore the evapotranspiration is the primary driver of the streamflow diurnal pattern as noticed by numerous researchers (White 1932; Troxell 1936; Wicht 1941; Croft 1948; Meyboom 1965; Reigner 1966; Parlange and Aylor 1975; Bren 1997; Lundquist and Cayan 2002; Bond et al. 2002; Hewlett 2003; Bauer et al. 2004; Gribovszki, Szilágyi, and Kalicz 2010).Additionally the groundwater level monitoring in the riverbed shows that its level is greater than the riverbed therefore no infiltration is possible (Figure 3.19, Figure 3.20).

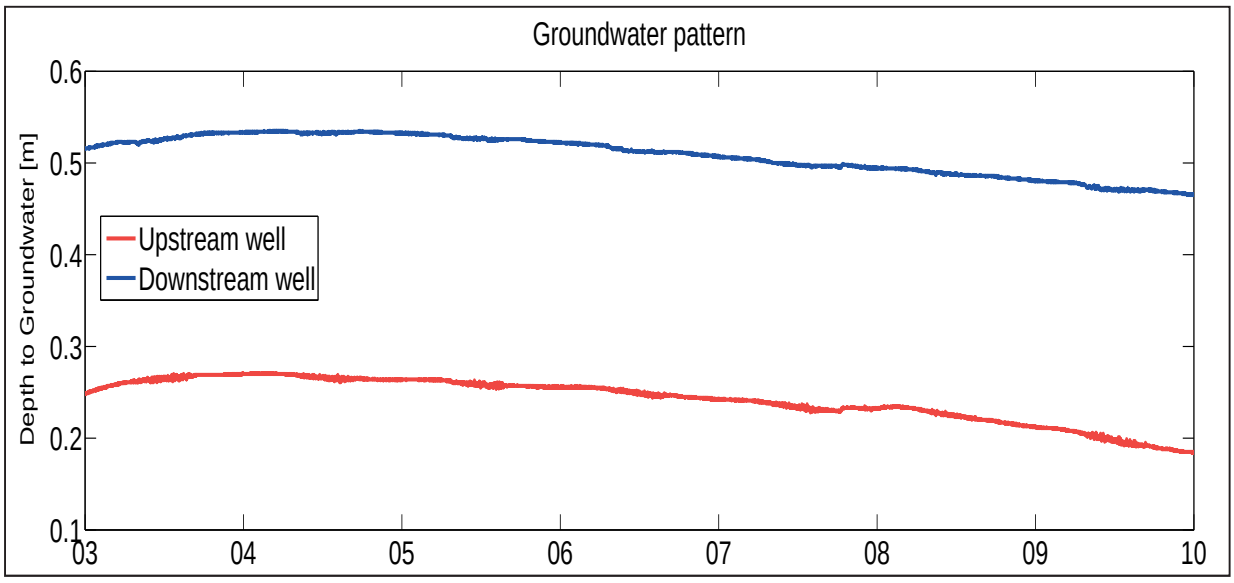

Figure 3.19: Groundwater trend (2nd regime) - (03/10/12-10/10/12)

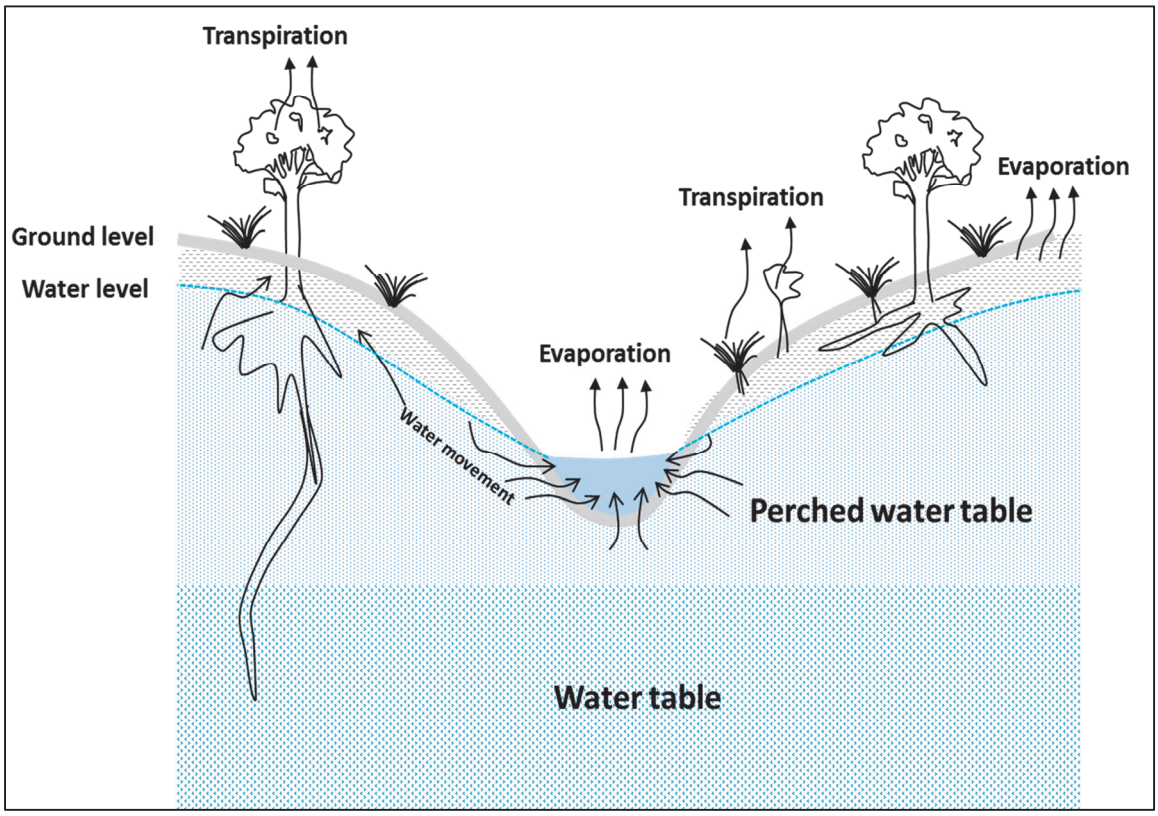

Figure 3.20: Sketch of the basin functioning during the second regime of flow.

The evaporation is then the main driver of the streamflow diurnal pattern during the second regime. Therefore aiming to integrate this regime in the Savannah hydrological models, a delineation of the area controlling this evaporation is crucial. For this purpose a simple method has been implemented, and the following paragraph will provide the method details.

a Evaporation control area (ECA)

The general assumption here is based on the strong relationship between water evaporated through plants, soil, surface water and the stream flow stages during a dry day. The streamflow daily pattern is caused by the evaporation from the stream surface and adjacent riparian areas (Reigner 1966; Bond et al. 2002; Gribovszki, Szilágyi, and Kalicz 2010). The area is defined as the ratio between the water lost from the stream (Qlost) and the evaporation in half hour period (Figure 3.21). In the hydrological point of view the discharge lost represents the additional amount of water that should flow if there were no uptake neither for plant, humans nor by Eco hydrological effects.

Method: contributing area

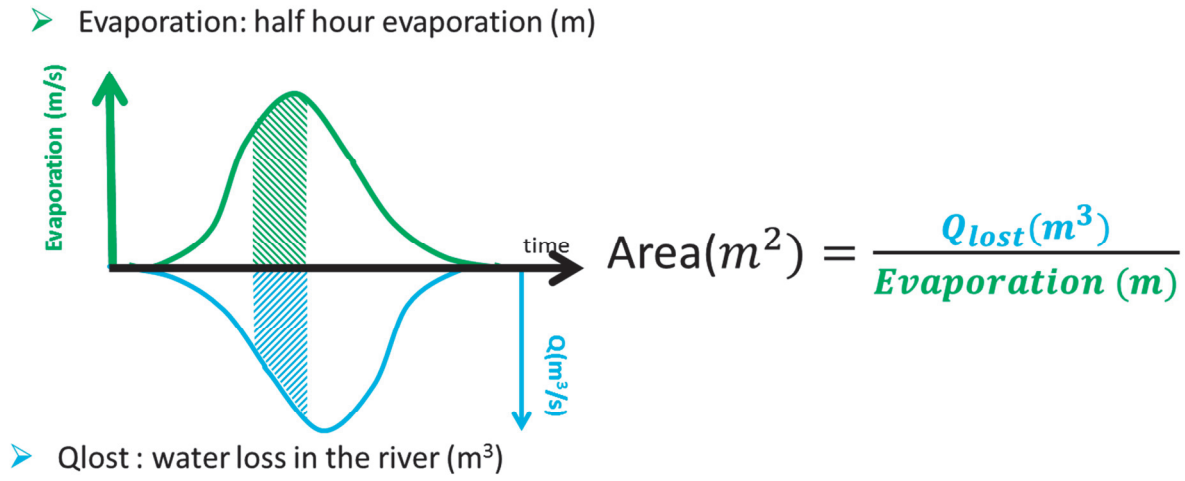

Figure 3.21 : Calculation method of the contributing area

The days used to compute the area were selected based on the following criteria:

3.1 No rain event between the sunrise (6 am) and the sunset (18 pm).
3.2 Availability of diurnal cycle of discharge and evaporation data.

Based on these criteria, 69 days collected respectively 21 days in 2010 and 48 in 2012. The year 2011 was not used for this study due to its drought (less than 300mm of total rain, almost 80 % less comparatively to 2010).

Several methods were tested to define the streamflow condition in absence of water loss by evaporation. Horizontal straight line passing by the maximum daily flow; the line linking the maximum discharge in the early morning and late afternoon; the line linking the flow rate at

respectively at sunrise (6 am) and sunset (6 pm); The line matching with the time of start and end of the evaporation at daily basis. Finally the hydrograph recession line was used as the potential upper limit of the streamflow (Figure 3.22) when the recession definition is possible; otherwise the line matching with the sunrise and the sunset is used. All the methods results are similar except the one using the daily maximum streamflow as potential upper limit. However the method proposed by (Reigner 1966) by linking the highest peaks of the time series by a straight line leads to important overestimation of the water loss.

The difference between the streamflow curve and the upper limit of the daily discharge represents Qlost. Thereafter with a simple integration the Qlost is computed (Figure 3.21).

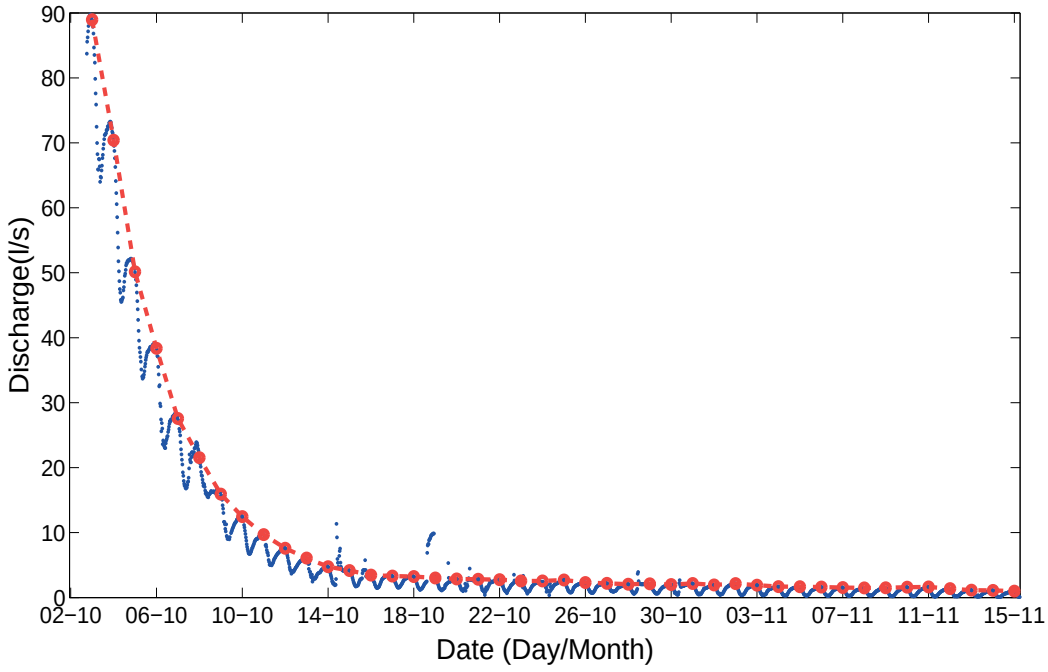

Figure 3.22: Upper limit of the streamflow definition

The data were first fitted by using the suitable fitting methods (Polynomial , smoothing spline, interpolant , exponential, quadratic etc.).The fits were done in order to remove the outliers, fill the gap and make the computation more robust.

The following graphs show a daily cycle of the latent heat flux computed each 30min using eddy flux station installed in the field. The water lost by evaporation is then computed by integrating the numerical function obtained.

The groundwater evaporation in the riparian area where the water table is close to ground surface influences the daily and seasonal pattern of streamflow(Brutsaert 2005).The evaporation increases during the daytime and achieves the maximum around noon then decreases towards the sunset (Figure 3.23) however the streamflow followed an inverse pattern i.e. it decreases until noon and starts to recover and achieve more or less the beginning level at the sunset (Figure 3.24). These figures showed that the evaporation pattern is comparable to the groundwater outflow during the dry day and seem correlated through an inverse function. The plants transpiration follows a diurnal pattern with maximum sap flow at around noon; this seems say that the plants reduce their transpiration rate during the afternoon (Oguntunde and van de Giesen 2005). Therefore the phase of recovering water could be explained by the reduction of the water uptake by the plants.

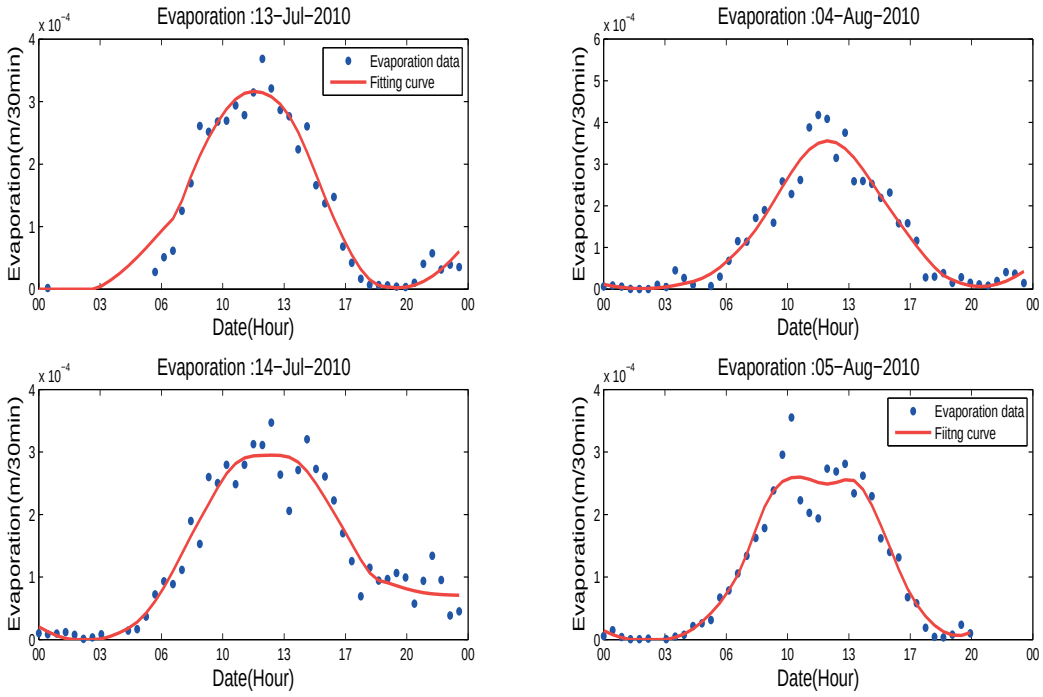

Figure 3.23: Evaporation pattern for four selected days. More examples and details can be found in the appendix.

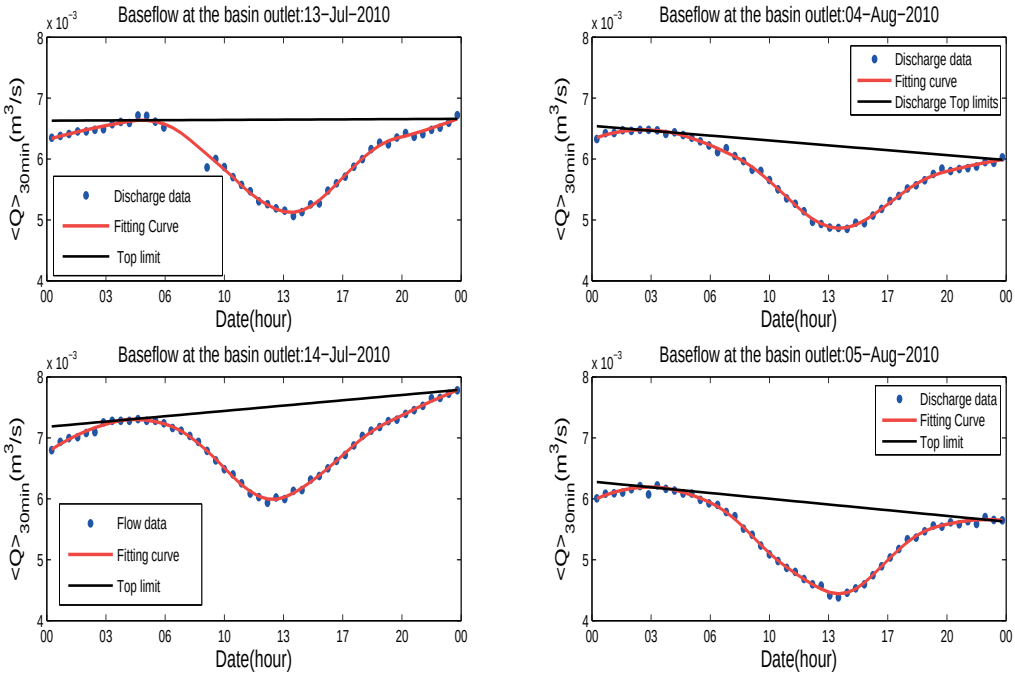

Figure 3.24: Diurnal streamflow pattern for four selected days. More examples and details can be found in the appendix.

The evapotranspiration controls the groundwater outflow daily pattern along the river mostly for the forested area (Szilágyi et al. 2008; Hewlett 2003; Gribovszki, Szilágyi, and Kalicz 2010). It is known by the scientific community, that only a portion of the watershed area contributes runoff to the storm hydrograph. Unlike the contributing area during storm a little interest was devoted to likely contributing area to streamflow during the period without rainfall. Parlange and Aylor, [1975] were the first to address an analysis to this area throughout exploring link between evapotranspiration and the diurnal cycle of water outflow on a small watershed during 4 summers in North Madison, Connecticut. Based on the straightforward link established between transpiration and groundwater outflow, they proposed a model for direct determination of transpirational water loss from forested area.

This part of study aims to complete the previous one done by (Parlange and Aylor 1975) by estimating the contributing area ‘‘Evaporation control area’’ during the dry period. The following graph presents a selected four days in 2010 for the contributing area computation. These results are also valid for the 69 other dry days selected in 2010 and 2012 (See appendix). The mean area compute is around 0.2 hectare and correspond almost to 6‰ of the total basin area (Figure 3.25). The area is very sensitive to rain events, baseflow rate and groundwater level.

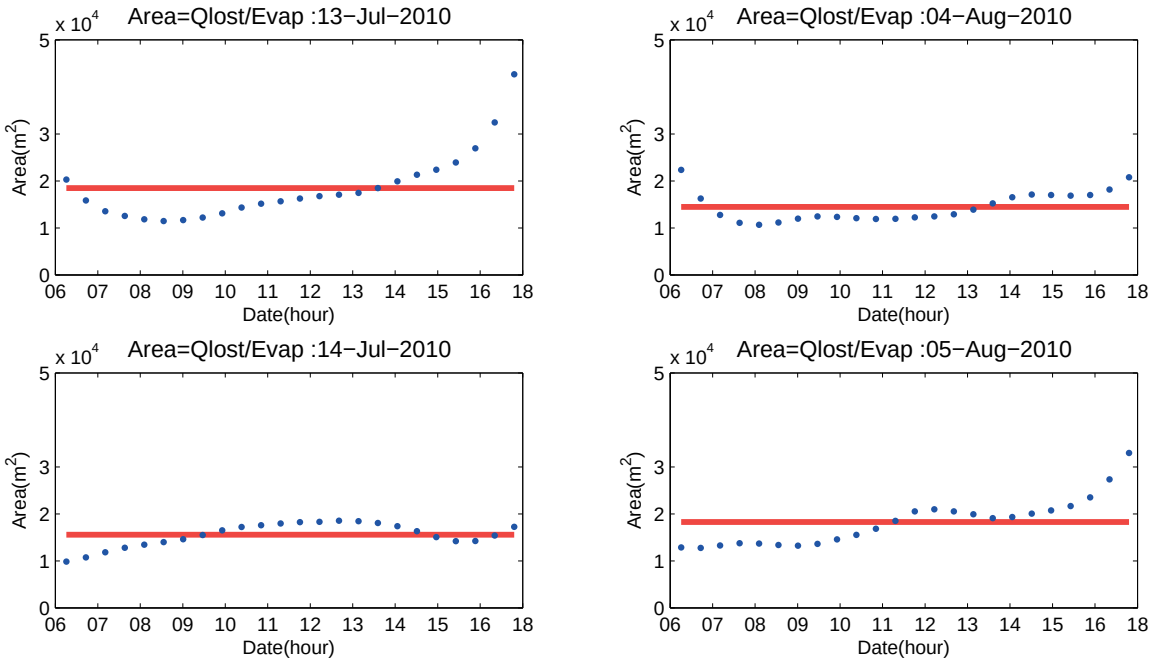

Figure 3.25: Control area for selected days. More details and examples can be found in the appendix of the chapter 3.

The area is dynamic and varies seasonally or throughout a storm and remained almost constant during dry days. During the dry period the wetting front in the soil is moving toward the riparian zone. The presence of holes filled by water and open springs at the basin outlet enhance the direct evaporation. The wet riparian area and the free water (river and springs) surfaces are able to produce the water vapor necessary to fill the pressure deficit in this not limited evaporative energy domain.

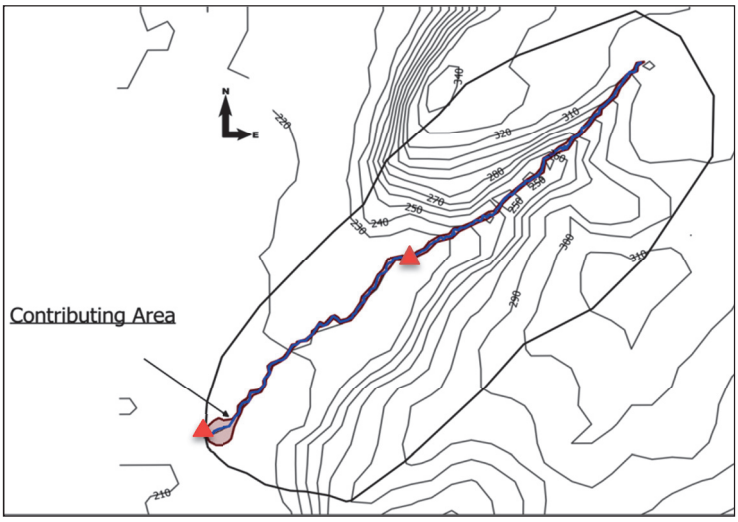

Figure 3.26: Schematic representation of the contributing area (grey hashed line). River (blue line) Red triangles are respectively the location of the weirs.

The area could be reasonably represented by the surface formed by the outlet rice field and the riparian riverbed (Figure 3.26). In detail this area could for example composed the wet land (0.1 ha) and the riparian zone over almost 3km of river length for 4m width.

b Hysteresis relationship

The correlation between the discharge lost and the evaporation was also computed at a daily basis. For this purpose the evaporation and Qlost data were normalized by their respective daily sum.

The daily distribution of water uptake was identified to follow a clockwise hysteretic relationship with Qlost (figure 3.27; 13 July, 4-Aug). This relationship is clearly not induces by the delayed response of one of these variables, which is proved by the non linearity trend of the relationship, whatever time shift tested. Several studies have documented the hysteresis relations mainly on the wetting and drying curve process into unsaturated porous media(Parlange 1976; Chow et al. 1988; Huang et al. 2005; Spence et al. 2010). However the hysteresis pattern at basin scale despite its prominent role into hydrology was recently documented by Spence et al., [2010]. The relationship found between the discharge lost shift to a counter-clockwise hysteresis (Figure 3.27; 21-July, 19-Aug) when a precipitation occurs during the daytime. During and after a rain event when the water is available, the plants shift the source of supply and use the water from surface layer. This change of source leads to reduce the effect of water uptake by roots on groundwater and therefore drives the counter clockwise hysteresis relationship between evaporation and streamflow. According to McGlynn et al., [2004], the lagged response of the local groundwater to runoff which occurs when the plants change the source of water uptake could be responsible for the counter-clockwise hysteresis relationship on the riparian floodplain.

The recognition and parameterization of an hysteresis provides insight into basin characteristics (Spence et al. 2010). The hysteric relationship highlighted between streamflow and the latent heat flux daily cycle is straightforward and provide a way to improve the modeling of watershed behavior and then better up scaling of the hydrological results on different landscape.

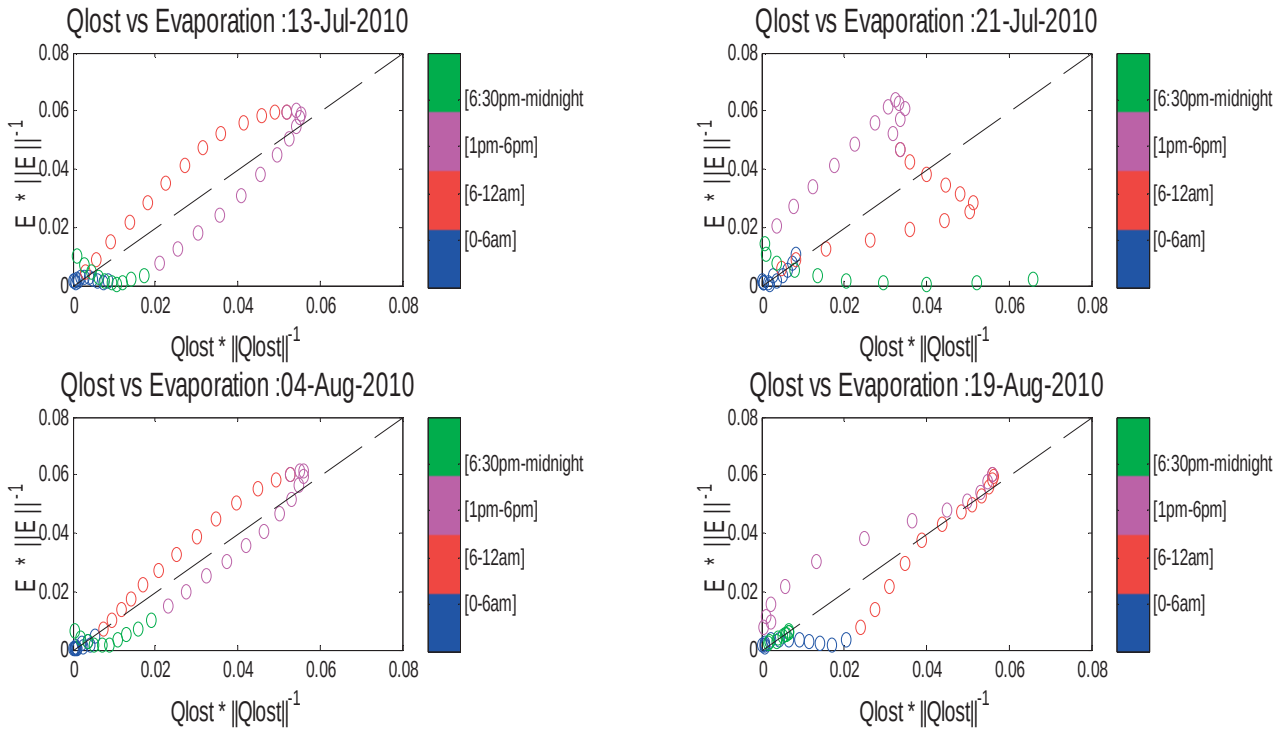

Figure 3.27: Hysteresis relationship between stream water loss and Evaporation

During the daytime the control of evaporation was shared between direct evaporation in the open surfaces and transpiration through water movement from soil to plant to atmosphere along a continuum of increasingly negative water potential. Between 6 am-2 pm (when the sunlight is max) the evaporation is prior to the streamflow decrease therefore the red scatters are located over the one to one curve. The Qlost decreasing is explained by the increasing of evaporation consequently to the combined activities of trees (physiological mechanisms) and the enhancement of the direct evaporation due to the availability in energy with sunrise. The purple scatters are under the one to one curve between (2pm to 6pm) when the evaporation trend to decrease and the water remove from plant start replenished. The Qlost starts recovering it level together with the reduction of plants transpiration and the lowering of the water pressure deficit which drove to a decreasing evaporation rate. In general there is no influence or uptake of discharge lost nor evaporation during nighttime. Therefore Qlost is constant almost zero during nighttime when the plant stop transpired and radiation is close to zero. Any water supply from rain or other input conducted to the inversion of control period. The delay flow in the river due to early morning rainfall event induced the reduction of the Qlost at least for the first hours of the day that explained the inversion control period.

3.5 Conclusion and remarks

The ephemeral stream flow diurnal pattern causes are still debated in the literature. Our study at Tambarga shows that the cause is highly linked to the domain characteristics, the local climate and how the hydrological processes are generated and controlled in the concerning basin. At Tambarga the flow over the entire river is under complete groundwater control. The baseflow occurred only when the groundwater is filled and all aquifer components interconnected. The groundwater outflow in the stream followed a diurnal cycle, the flow goes down slightly during the day, and water is replenished after sunset.

Two regimes of flow were highlighted with respectively higher flow upstream than downstream in the early season and the reverse in the late season when the baseflow is established. The diurnal stream flow is mainly caused by infiltration over the riverbed and evaporation along the stream edges. For the latter case the water loss in the stream was compared with evaporation at half-hour period. A straightforward relationship was established between evaporation and water loss diurnally in the stream which allowed defining a control area. Corresponding to 0.6% of the total basin area, this area is sensitive to early morning or late afternoon rain event, but stays almost stable during the complete dry day. The riparian zone could reasonably represent this area and seems corresponding to the primary source of evaporation. The daily partitioning of evaporation over the basin was highlighted using the clockwise hysteresis relationship found between actual evaporation and water lost in the stream.

The method proposed in this paper is robust, easy to implement and allows evaluating the area impacted by evapotranspiration. This area could be used for base flow characterization for hydrological modeling. The hysteretic relationship could be used to provide a daytime partitioning of evaporation over the watershed. A future research line should address the link between this control area and evaporation footprint.

References

Alkhaier, Fouad. 2011. “Shallow Groundwater Effect on Land Surface Temperature and Surface Energy Balance : Description Modeling and Remote Sensing Application”. Dissertation, University of Twente. http://www.itc.nl/library/papers_2011/phd/alkhaier.pdf.

Bagayoko, Fafre, Samuel Yonkeu, Jan Elbers, and Nick van de Giesen. 2007. “Energy Partitioning over the West African Savanna: Multi-Year Evaporation and Surface Conductance Measurements in Eastern Burkina Faso.” *Journal of Hydrology* 334 (3-4): 545–559.

Bauer, Peter, George Thabeng, Fritz Stauffer, and Wolfgang Kinzelbach. 2004. “Estimation of the Evapotranspiration Rate from Diurnal Groundwater Level Fluctuations in the Okavango Delta, Botswana.” *Journal of Hydrology* 288 (3–4) (March 30): 344–355. doi:10.1016/j.jhydrol.2003.10.011.

Ben-Asher, J., and G. Humborg. 1992. “A Partial Contributing Area Model for Linking Rainfall Simulation Data with Hydrographs of a Small Arid Watershed.” *Water Resources Research* 28 (8): PP. 2041–2047. doi:199210.1029/92WR00906.

Bond, Barbara J., Julia A. Jones, Georgianne Moore, Nathan Phillips, David Post, and Jeffrey J. McDonnell. 2002. “The Zone of Vegetation Influence on Baseflow Revealed by Diel Patterns of Streamflow and Vegetation Water Use in a Headwater Basin.” *Hydrological Processes* 16 (8): 1671–1677. doi:10.1002/hyp.5022.

Bren, Leon J. 1997. “Effects of Slope Vegetation Removal on the Diurnal Variations of a Small Mountain Stream.” *Water Resources Research* 33 (2): 321–331. doi:10.1029/96WR02648.

Brutsaert, Wilfried., and Marc. B. Parlange. 1998. “Hydrologic Cycle Explains the Evaporation Paradox.” *Nature* 396 (6706) (November 5): 30–30. doi:10.1038/23845.

Brutsaert, Wilfried. 2005. *Hydrology: An Introduction*. Cambridge University Press.

Brutsaert, Wilfried, and John L. Nieber. 1977. “Regionalized Drought Flow Hydrographs from a Mature Glaciated Plateau.” *Water Resources Research* 13 (3): PP. 637–643. doi:197710.1029/WR013i003p00637.

Cartwright, Keros. 1974. “Tracing Shallow Groundwater Systems by Soil Temperatures.” *Water Resources Research* 10 (4): 847–855. doi:10.1029/WR010i004p00847.

Chow, Ven. T, David. R Maidment, Larry. W Mays. 1988. “Applied Hydrology.” *McGraw-Hill Series in Water Resources and Environmental Engineering*.

Constantz, Jim, Carole L. Thomas, and Gary Zellweger. 1994. “Influence of Diurnal-Variations in Stream Temperature on Streamflow Loss and Groundwater Recharge.” *Water Resources Research* 30 (12) (December): 3253–3264. doi:10.1029/94WR01968.

Croft, A. R. 1948. “Water Loss by Stream Surface Evaporation and Transpiration by Riparian Vegetation.” *Transactions, American Geophysical Union* 29 (2): 235. doi:10.1029/TR029i002p00235.

Cuevas, Jaime G, Matìas Calvo, Christian Little, Mario Pino, and Paul Dassori. 2010. “ARE DIURNAL FLUCTUATIONS IN STREAMFLOW REAL?” *J. Hydrol. Hydromech.* 58 (3): 149–162. doi:10.2478/v10098-010-0014-0.

Dunne, Thomas, and Richard D. Black. 1970. “Partial Area Contributions to Storm Runoff in a Small New England Watershed.” *Water Resources Research* 6 (5): PP. 1296–1311. doi:197010.1029/WR006i005p01296.

Federer, C. Anthony. 1973. “Forest Transpiration Greatly Speeds Streamflow Recession.” *Water Resources Research* 9 (6): 1599–1604.

Ghimire, Bhola N.S., and M. Janga Reddy. 2010. “Development of stage-discharge rating curver in river using Genetic Algorithms and Model TREE” presented at the International Workshop ADVANCES IN STATISTICAL HYDROLOGY, May 23, Taormina, Italy.

Gomi, Takashi, R. Dan Moore, and Amod S. Dhakal. 2006. “Headwater Stream Temperature Response to Clear-Cut Harvesting with Different Riparian Treatments, Coastal British Columbia, Canada.” *Water Resources Research* 42 (8): n/a–n/a. doi:10.1029/2005WR004162.

Gribovszki, Zoltán, Péter Kalicz, and József Szilágyi. 2013. “Does the Accuracy of Fine-Scale Water Level Measurements by Vented Pressure Transducers Permit for Diurnal Evapotranspiration Estimation?” *Journal of Hydrology* 488 (April 30): 166–169. doi:10.1016/j.jhydrol.2013.03.001.

Gribovszki, Zoltán, Péter Kalicz, József Szilágyi, and Mihály Kucsara. 2008. “Riparian Zone Evapotranspiration Estimation from Diurnal Groundwater Level Fluctuations.” *Journal of Hydrology* 349 (1–2) (January 30): 6–17. doi:10.1016/j.jhydrol.2007.10.049.

Gribovszki, Zoltán, József Szilágyi, and Péter Kalicz. 2010. “Diurnal Fluctuations in Shallow Groundwater Levels and Streamflow Rates and Their Interpretation – A Review.” *Journal of Hydrology* 385 (1–4) (May 7): 371–383. doi:10.1016/j.jhydrol.2010.02.001.

Hewlett, John D. 2003. *Principles of Forest Hydrology*. University of Georgia Press.

Horton, Robert. E. 1933. “The Role of Infiltration in the Hydrologic Cycle.” *Transactions-American Geophysical Union* 14 (June): 446–460.

Huang, Han-Chen, Yih-Chi Tan, Chen-Wuing Liu, and Chu-Hui Chen. 2005. “A Novel Hysteresis Model in Unsaturated Soil.” *Hydrological Processes* 19 (8) (May 1): 1653–1665. doi:10.1002/hyp.5594.

Ingelrest, François, Guillermo Barrenetxea, Gunnar Schaefer, Martin Vetterli, Olivier Couach, and Marc Parlange. 2010. “SensorScope: Application-Specific Sensor Network for Environmental Monitoring.” *ACM Trans. Sen. Netw.* 6 (2) (March): 17:1–17:32. doi:10.1145/1689239.1689247.

Lundquist, Jessica D., and Daniel R. Cayan. 2002. “Seasonal and Spatial Patterns in Diurnal Cycles in Streamflow in the Western United States.” *Journal of Hydrometeorology* 3 (5) (October): 591–603. doi:10.1175/1525-7541(2002)003<0591:SASPID>2.0.CO;2.

Mande, Theophile, Natalie Ceperley, Steven V. Weijs, Alexandre Repetti, and Marc B. Parlange. 2014. “Toward a New Approach for Hydrological Modeling: A Tool for Sustainable Development in a Savanna Agro-System.” In *Technologies for Sustainable Development*, edited by Jean-Claude Bolay, Silvia Hostettler, and Eileen Hazboun, 85–98. Springer International Publishing. http://link.springer.com/chapter/10.1007/978-3-319-00639-0_8.

McGlynn, Brian L., Jeffrey J. McDonnell, Jan Seibert, and Carol Kendall. 2004. “Scale Effects on Headwater Catchment Runoff Timing, Flow Sources, and Groundwater-Streamflow Relations.” *Water Resources Research* 40 (July 28): 14 PP. doi:200410.1029/2003WR002494.

Meyboom, Peter. 1965. “Three Observations on Streamflow Depletion by Phreatophytes.” *Journal of Hydrology* 2 (3) (March): 248–261. doi:10.1016/0022-1694(65)90040-5.

Muskat, M. 1937. “The Flow of Homogeneous Fluids through Porous Media.”

Parlange, Jean-Yves. 1976. “Capillary Hysteresis and the Relationship between Drying and Wetting Curves.” *Water Resources Research* 12 (2): P. 224. doi:197610.1029/WR012i002p00224.

Parlange, Jean-Yves, and Donald E. Aylor. 1975. “Response of an Unsaturated Soil to Forest Transpiration.” *Water Resources Research* 11 (2): PP. 319–323. doi:197510.1029/WR011i002p00319.

Ragan, Robert M. 1968. “An Experimental Investigation of Partial Area Contributions.” *IAHS* 76: 241–249.

Reigner, Irvin C. 1966. “A Method of Estimating Steamflow Loss by Evapotranspiration from the Riparian Zone.” *Forest Science* 12 (2): 130–139.

Ronan, Anne Dudek, David. E. Prudic, Carl. E. Thodal, and Jim Constantz. 1998. “Field Study and Simulation of Diurnal Temperature Effects on Infiltration and Variably Saturated Flow beneath an Ephemeral Stream.” *Water Resources Research* 34 (9) (September): 2137–2153. doi:10.1029/98WR01572.

Selker, John, Nick van de Giesen, Martijn Westhoff, Wim Luxemburg, and Marc B. Parlange. 2006. “Fiber Optics Opens Window on Stream Dynamics.” *Geophysical Research Letters* 33 (24): n/a–n/a. doi:10.1029/2006GL027979.

Simoni, Silvia, Simone Padoan, Daniel. F. Nadeau, Marc Diebold, Amilcare Porporato, Guillermo Barrenetxea, François Ingelrest, Martin Vetterli, and Marc B. Parlange. 2011. “Hydrologic Response of an Alpine Watershed: Application of a Meteorological Wireless Sensor Network to Understand Streamflow Generation.” *Water Resources Research* 47 (October 22). doi:10.1029/2011WR010730.

Spence, C., X. J Guan, R. Phillips, N. Hedstrom, R. Granger, and B. Reid. 2010. “Storage Dynamics and Streamflow in a Catchment with a Variable Contributing Area.” *Hydrological Processes* 24 (16) (July 30): 2209–2221. doi:10.1002/hyp.7492.

Stagnitti, Frank, Jean-Yve Parlange, and C. W Rose. 1989. “Hydrology of a Small Wet Catchment.” *Hydrological Processes* 3 (2) (April 1): 137–150. doi:10.1002/hyp.3360030204.

Swinbank, W. C. 1951. “The Measurement of Vertical Transfer of Heat and Water Vapor by Eddies in the Lower Atmosphere.” *Journal of Meteorology* 8 (3) (June): 135–145. doi:10.1175/1520-0469(1951)008<0135:TMOVTO>2.0.CO;2.

Szilágyi, József, Zoltán Gribovszki, Péter Kalicz, and Mihály Kucsara. 2008. “On Diurnal Riparian Zone Groundwater-Level and Streamflow Fluctuations.” *Journal of Hydrology* 349 (1–2) (January 30): 1–5. doi:10.1016/j.jhydrol.2007.09.014.

Szilagyi, Jozsef, Marc B. Parlange, and Gabor Balint. 2006. “Assessing Stream–aquifer Interactions through Inverse Modeling of Flow Routing.” *Journal of Hydrology* 327 (1–2) (July 30): 208–218. doi:10.1016/j.jhydrol.2005.11.018.

Troxell, Harold C. 1936. “The Diurnal Fluctuation in the Ground-Water and Flow of the Santa Ana River and Its Meaning.” *Transactions, American Geophysical Union* 17 (2): 496. doi:10.1029/TR017i002p00496.

Turk, L.J. 1975. “Diurnal Fluctuations of Water Tables Induced by Atmospheric Pressure Changes.” *Journal of Hydrology* 26 (1–2) (July): 1–16. doi:10.1016/0022-1694(75)90121-3.

Van Genuchten, M.Th. 1980. “A Closed-Form Equation for Predicting the Hydraulic Conductivity of Unsaturated Soils.” *Soil Science Society of America Journal* 44 (5): 892–898. doi:10.2136/sssaj1980.03615995004400050002x.

Vercauteren, Nikki, Elie Bou-Zeid, Hendrik Huwald, Marc B. Parlange, and Wilfried Brutsaert. 2009. “Estimation of Wet Surface Evaporation from Sensible Heat Flux Measurements RID A-9796-2008.” *Water Resources Research* 45 (June 20). doi:10.1029/2008WR007544.

White, Walter Noy 1932. “A Method of Estimating Ground-Water Supplies Based on Discharge by Plants and Evaporation from Soil--Results of Investigations in Escalante Valley, Utah”. WSP - 659-A. Water Supply Paper. United States Geological Survey. http://pubs.er.usgs.gov/publication/wsp659A.

Wicht, C. L. 1941. “Diurnal Fluctuations in Jonkershoek Streams Due to Evaporation and Transpiration.” *Journal of the South African Forestry Association* 7 (1): 34–49. doi:10.1080/03759873.1941.9631119.

Zhu, Jianting, Michael Young, John Healey, Richard Jasoni, and John Osterberg. 2011. “Interference of River Level Changes on Riparian Zone Evapotranspiration Estimates from Diurnal Groundwater Level Fluctuations.” *Journal of Hydrology* 403 (3–4) (June 17): 381–389. doi:10.1016/j.jhydrol.2011.04.016.

Chapter 4 : Toward a New Approach for Hydrological Modeling: A Tool for Sustainable Development in a Savanna Agro-system.

Abstract

Agriculture in Tambarga, a small, remote village in the landlocked country of Burkina Faso, is dependent on the seasonally variable local hydrology. Extreme seasonal and spatial variability of rainfall significantly impacts the livelihood of farmers, who depend mainly on rainfed agriculture. This dependence on rainfed production makes them particularly vulnerable to meteorological conditions, and they continually experience food insecurity. The groundwater is promising as storage to mitigate effects of drought. However, because of its interaction with the various hydrological components, we need to better understand all the processes to fully assess the impacts of possible solutions. Hydrological and meteorological data were collected over a two-and-a-half-year period in the catchment adjacent to the village (area = 4 km²) to address these issues. The field studies show that the major portion of storm runoff was generated in the upper savanna basin, while baseflow appears to be mostly originating from the downstream agricultural field. The seasonal cycle of groundwater appears to control the stream flow and therefore, the continuous flow over the entire stream occurred when the water tables became interconnected and surfaced the ground level. Additionally, this chapter discusses water management scenarios (open dam, deeper wells and buried dam) for agricultural purposes using a simple and comprehensive hydrological model. Simulations based on reducing evaporation rate by keeping the water underground present a solution that could improve agricultural production, and therefore, reduce vulnerability of Tambarga's farmers to climate change.

4.1 Introduction and purpose

Groundwater storage is a promising strategy to mitigate the consequences of drought in West Africa. Thousands of open dams were built in the Volta basin with the aim to store water for livelihood in Burkina Faso since 1960. However, the flatness of the country, in addition to the high evaporation rate in this region, means water loss in open dams is significant. Additionally, the high rate of particle transport during the rainy season over this region leads to the sedimentation of the dam with the consequence of reducing the storage capacity.

Therefore, the open dams are not adapted for sustainable water management in the arid and semi-arid countries, as mentioned at the Earth Summit in Rio de Janeiro in 1992. Onder and Yilmaz (2005) noted that to tackle surface water scarcity, the groundwater represented the only sustainable resource for arid and semi-arid zones.

The sustainable management of groundwater resources requires a complete understanding of its interactions with the runoff, soil moisture, and evaporation (Gribovszki et al. 2010; Irvine et al. 2012). The processes that occur during groundwater recharge are complex because of the interactions between different variables such as rainfall, soil, runoff, evaporation, initial soil moisture, canopy cover, cloud cover, wind speed and solar radiation. These parameters vary in space and time and thus collecting accurate spatial and temporal data is elusive. Techniques that exist, such as radar, are very expensive, difficult to implement, weather-dependent, need frequent maintenance and therefore, are not feasible for poor countries.

Hydrological modeling is recognized as a powerful tool for the management of water resources at local, regional and continental scales (Beven 2004; Brutsaert 2005; Gnouma 2006; Ioslovich and Gutman 2001; Simoni et al. 2011). These models, which range from empirical lumped models to fully distributed models, are suitable for forecasting runoff, floods and droughts, and can be applied to evaluate water management strategies (Simoni et al. 2011). The accuracy of modeling is related to its ability to reproduce as close as possible the processes occurring in a delimited area. The accuracy is also related to the researchers' understanding of the processes and their abilities for calibration. The lack of available and accurate data is a limitation for most of the distributed and semi-distributed models in Africa. Several scientists have developed simple models using monthly aggregated data that are widely available (Ndomba et al. 2008). These models seem to give good results overall, but are not adapted to the intensive rainy season (four months) and rain events (less than one hour) that we find in Tambarga, and thus fail replicate the timing rainfall-runoff response.

Many authors have highlighted the sensitivity of modeling to several factors like landscape, land use, relief, soil, topography, plant characteristics, groundwater patterns and anthropogenic activities (Brutsaert 2005; Gnouma 2006; Simoni et al. 2011). The reliability of hydrological modeling for forecasting purposes is affected by the accuracy with which spatial and temporal distribution of forcing is known. To understand the processes that take place in a basin remains a crucial step for models. Therefore, highlighting and understanding

the hydrological processes appears to be a way to achieve successful modeling and subsequently, propose sustainable water management strategies. The objectives of this research are: 1) to explore the subsurface flow processes and explain the hydrograph patterns and their links with groundwater behavior and 2) highlight some possible results-based tools for improving food security for the local population through hydrological modeling.

4.2 Design and Methods

Tambarga is located in the commune of Madjoari, the province of Kompienga in the southeast part of Burkina Faso (11°26'42.79"N, 1°13'32.09"E) at the border with Benin in the Soudano-sahelian zone (Figure 4.1).

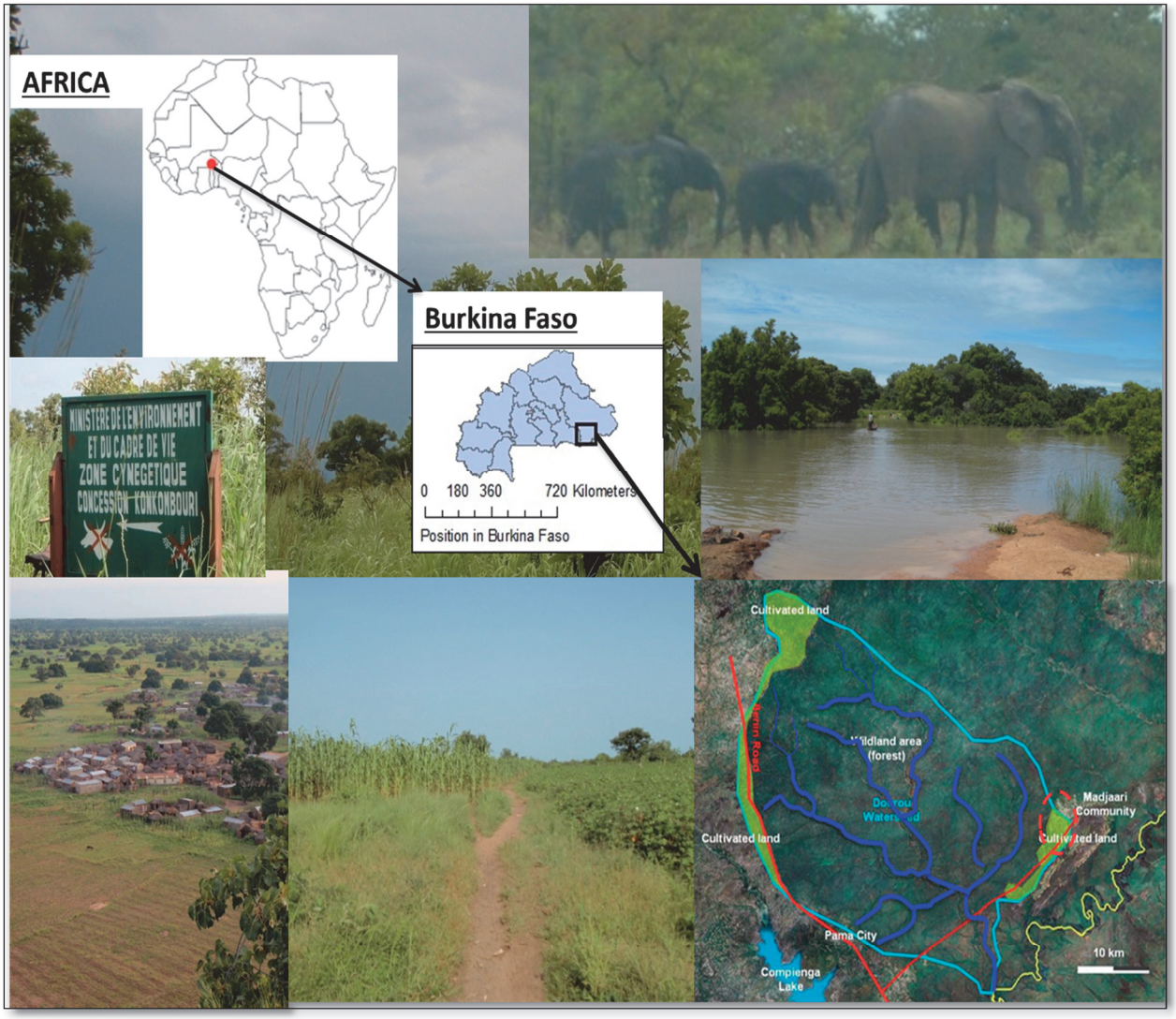

Figure 4.1: Trial site Madjoari in southeastern Burkina Faso.

Madjoari is composed of eight villages and more than twelve temporary houses (*hameaux de cultures*). The Gourmantche are the ethnic majority but there are also other ethnicities like Mossi (migrant framers), Peulh (breeders), Haoussas, Djerma and Yanas (traders). Agriculture is the main activity in Madjoari city and involves almost all of its population. The village is part of a protected hunting zone, rich in biodiversity: wildlife (lion, elephants, buffalo, hippopotamus, wild boar, etc.), and vegetation (*Sclerocarya birrea, Adansonia digitata, Annogeisus leiocarpus, Bombax constatum, Burkea africana, etc.*) (Ceperley et al. 2012; Commune Rurale de Madjoari 2009).

The annual average rainfall is between 900 and 1200 mm but can shift quickly to extreme values from one year to another (< 300 mm or > 1500 mm) (Ceperley et al. 2012). The rainfall pattern at Tambarga is monomodal with a rainy season from May to August, followed by the dry season from September to April. The rainfall distribution in time is variable according to the year. Two phases of rainfall have been identified in 2010: 1) May to mid-July was characterized by sparse rain and 2) from mid-July to August, the season with frequent rain (>1 rain event / 2 days) was completely established.

The Tambarga watershed has an area of 4 km^2 and is subdivided in three geomorphological units: 1) an upper basin (2 km^2) characterized by a grass open savanna forest, a "lithosol" soil with a rocky escarpment, and shallow perched groundwater, 2) a lower basin (2 km^2) characterized by a millet field with sandy soil, sparse trees and deeper watertable and 3) the bottom basin (0.1 km^2) a part of the field basin characterized by loamy clay soil, used as rice fields with a shallow perched groundwater. The altitude in the watershed ranges from 200 m to 400 m and the basin is about 700 m wide along most of its length.

A field experiment has been conducted since April 2009 to provide a comprehensive dataset aimed at investigating the hydrological processes and modeling the stream flow. Measurements were taken during three rainfall seasons in 2009 to 2012. The measurements were taken in both a "natural savanna" section and an adjacent "agricultural" section. This involved measuring hydrological, meteorological and soil data at high spatial and temporal resolution. Data were acquired with advanced research equipment such as SensorScope environmental monitoring stations, two weirs and eddy covariance fluxes stations.

4.2.1 Hydro-meteorological Variables: Sensible, Latent Heat Flux and Discharge

Tambarga, as is typical of villages in West Africa, experiences with high temperatures (>45°C in April) and therefore high evaporation rates. Additionally, the flatness of the country does not allow for capturing and storing water for users. Evaporation is therefore a crucial parameter to understand and estimate. Evapotranspiration, the combined effects of water loss through both evaporation from free water surfaces into atmosphere and transpiration from vegetation, is a complex process dependent not only on climatic variables (e.g., solar radiation, wind speed, rainfall), but also on geographical variables (e.g., local vegetation, slope, elevation, aspect, etc.), plant physiology (e.g., stomata1 resistance), and soil properties (e.g., soil moisture deficits, hydraulic conductivity, etc.) (Stagnitti et al. 1989). Eddy covariance techniques allow for accurate measurements of the sensible flux and latent heat flux (evaporation) (Brutsaert 2005). Two sets of Eddy covariance towers were installed respectively in the agricultural field to evaluate the influence of cultures on daily and seasonal patterns, and on the hill edge of the open savanna forest to capture the influence of trees on evaporation. Each tower records the wind velocity, air temperature and water vapor concentration data at 20 Hz in order to calculate the fluxes. For this study, the data from the tower on the agricultural field was used. The latent heat flux (LeE) was computed using the covariance of vertical wind fluctuations (w) and specific humidity (q) multiplied by the latent heat of vapor (Le) and air density (ρ) (Eq. 4.1). The evaporation (mm) is obtained simply by conversion of the latent heat flux (w/m^2).

$$L_e E = L_e \widehat{\rho}\, \overline{w'q'} \qquad (4.1)$$

Before performing any hydrological modeling or implementing any water management strategy it is crucial to be able estimate the amount of water flowing over the considered basin. For this purpose, we used weirs to measure the discharge. Discharge was measured at two levels in the basin: 1) using 90° V notch weir at the outlet of the upper basin and 2) a mix-triangular-rectangular weir in the agricultural flat basin. Stage at each weir was measured and recorded every minute by using automatic pressure sensors (manufactured by MADD Technologies, Switzerland) and converted to streamflow through a discharge rating curve (Eq. 4.2). The rating curve was obtained by combining measurements of water level over the weirs crest and in situ measurements of discharge by salt dilution method.

$$Q_{up}(h) = 1.414 * h^{1/2}\ (m^3 S^{-1}); \qquad Q_L(h) = 6.27 * h^{3.68}\ (m^3 S^{-1}); \qquad (4.2)$$

Where Q_L and Q_{up} are the discharges respectively at the lower and upper basins in $m^3\ s^{-1}$ and h is the water level on the crest in m.

4.3 Results

Figure 4.2 shows a relatively weak daily evaporation (average (μ) ~ 4 mm/day; standard deviation (σ) ~1mm). We found evaporation to increase during the rainy season. This trend is related to the increase of available water and the foliage of the numerous deciduous trees, crops and grasses growing (Bagayoko et al. 2007). Two peaks of evaporation rate were identified in June (high rainfall event, grass and crop growing) and September (frequent rainfall event). The latent heat flux, represented by the evaporation, is the most important term (71% during the rainy season) of the energy balance at Kompienga (Bagayoko et al. 2007). This important rate of evaporation is mainly a result of the high temperatures occurring in the region, which leads to increased plant transpiration. The mean daily air temperature in 2010 is 35°C within a range of 20°C to 45 °C in April.

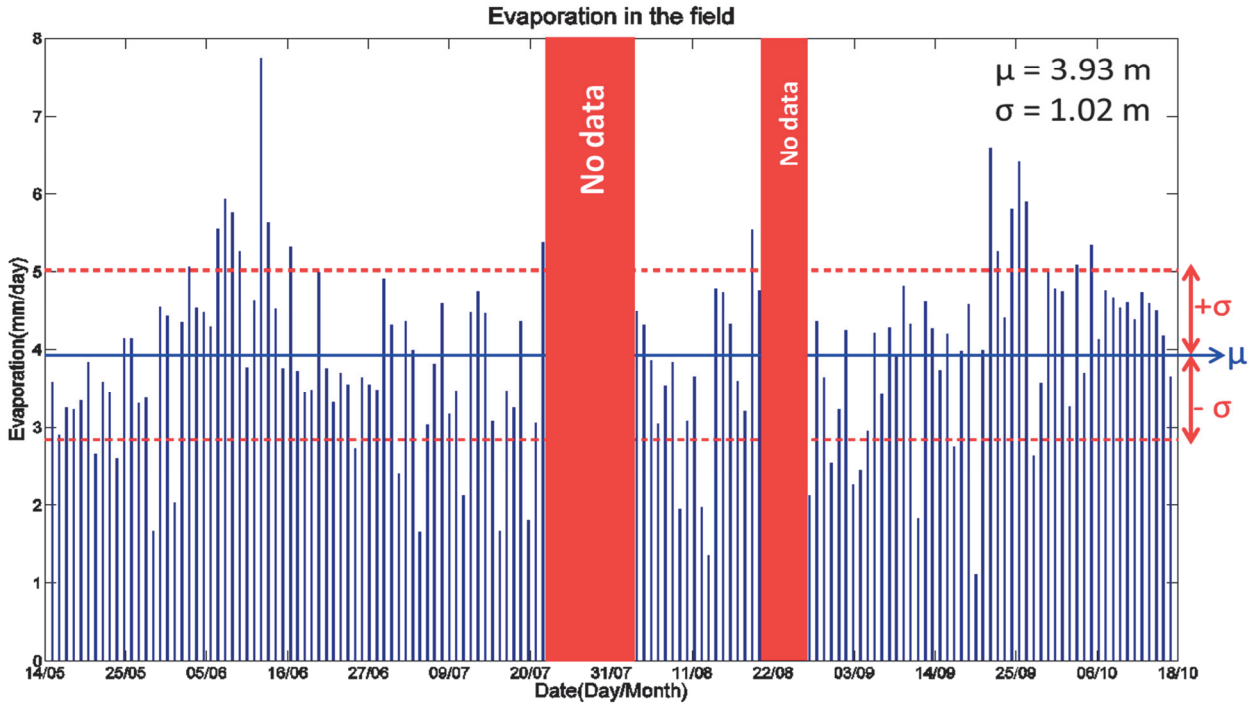

Figure 4.2: Daily evaporation measured in the agricultural field at Tambarga in 2010

The yearly (dry and wet season) pattern of evaporation is important for understanding the interrelationships between the variables that have effects on agriculture: net radiation, wind speed, antecedent soil moisture and root depth. Unfortunately, for technical reasons we do not have data for the dry season and some periods during the rainy season that would allow us to draw conclusions on the sensible and latent flux pattern for a complete year. Knowing that the net radiation is the primary source energy of evaporation (Bagayoko et al. 2007; Brutsaert 2005; Brutsaert 1982; Ojo 1983), the strong net radiation observed at the site allow us to assume that the evaporation could increase during the dry season. Therefore, it is clear that water storage will only be effective if high evaporation rates are counted as significant component in water management strategies.

The second relevant variable for water resources management is stream flow. The river studied is characterized by a length of 2.8 km, a width range between 2 and 7 meters, and a 1% slope (in the agricultural field) and a 7% slope (in the upper savanna forest). The river is ephemeral and started to flow with the rainy season onset but remained hortonian until groundwater was recharged. The discharge observed varied from 0 during the dry season to approximately 0.6 m^3s^{-1} (the maximum discharge observed during rainy season in 2010). Regarding the streamflow distribution between the two geomorphological units, the upper basin contributes to about 50% of the total surface runoff. The geology, mostly rocky on the edges, increases the surface runoff over this area. The topography of the upper basin, corresponding to a canyon (transversal slope >12%), is adaptable for storing water by constructing an open dam.

4.3.1 Groundwater and Streamflow

Groundwater storage is a promising strategy to mitigate effects of drought in West Africa. In Tambarga potable water is provided only by wells and therefore, understanding how the groundwater recharge occurs and how much water can be stored is crucial for the local population drinking water supply. Six wells were monitored in the agricultural basin with the aim to understand this process; the wells are distributed over a transverse cross-section on the left bank (from the basin boundary toward the river bed) over a 200 m distance. The groundwater is characterized by two shallow perched water tables in the bottom rice field and the upper savanna basin and one deeper water table in the intersection between these two (Figure 4.3) .

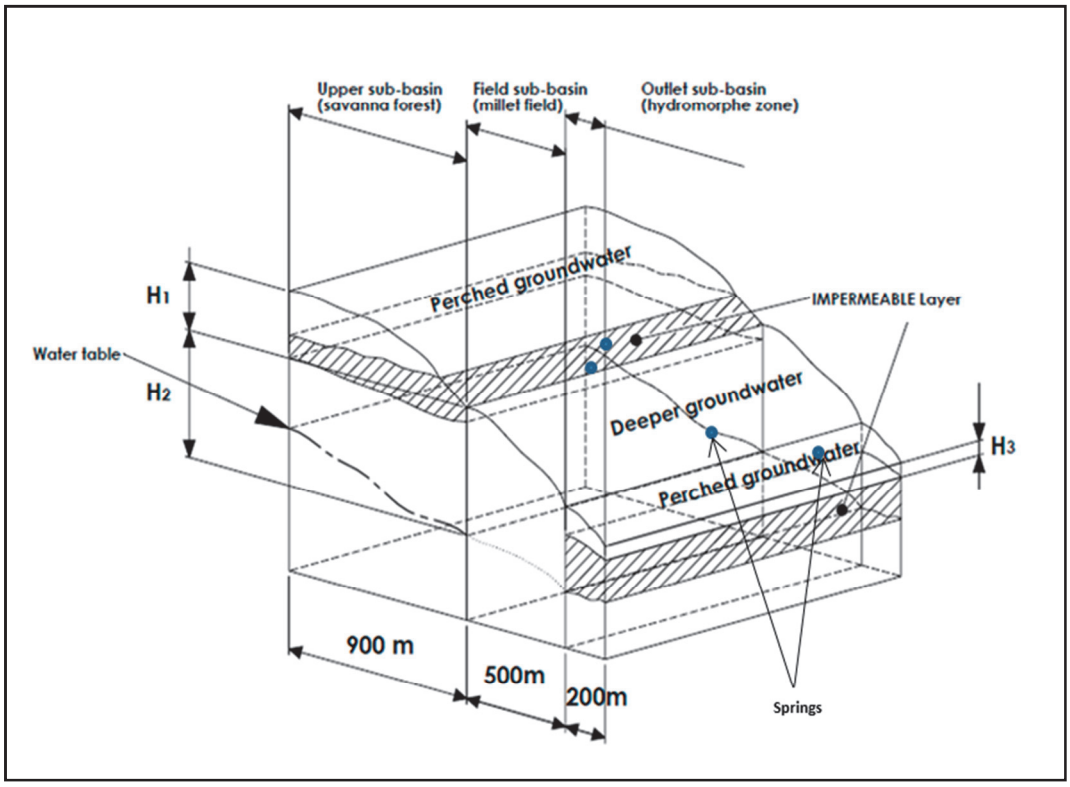

Figure 4.3: Groundwater network at Tambarga

The watertable recharge pattern is divided into two periods. During the first period, between the onset and mid-August, the groundwater was stable. The water requirements for humans, plants and evaporation were more or less equal to the recharge rate. A significant recharge moment was found during the second period, between mid-August and October, when the groundwater rose suddenly and reached the ground level, which resulted in an increasing streamflow. Three permanent and more than four seasonal springs were found throughout the basin. The seasonal springs appeared when the rainfall events became more frequent (>1 event per day), the soil moisture approached to saturation, and the overall watertable interconnected over the basin. The distribution of springs within basins during base flow is well known to be a good indicator of subsurface water flow paths (Komatsu and Onda 1996; Onda 1994; Onda et al. 2001).

The watershed runoff was generated by rainfall and controlled by the groundwater. Seasonal cycles of groundwater recharge appear to control the stream flow and are damped by storage and evapotranspiration on the agricultural basin. Brutsaert (1982) showed that the first saturated layers of shallow groundwater are influenced by the atmosphere and subject to evaporation.

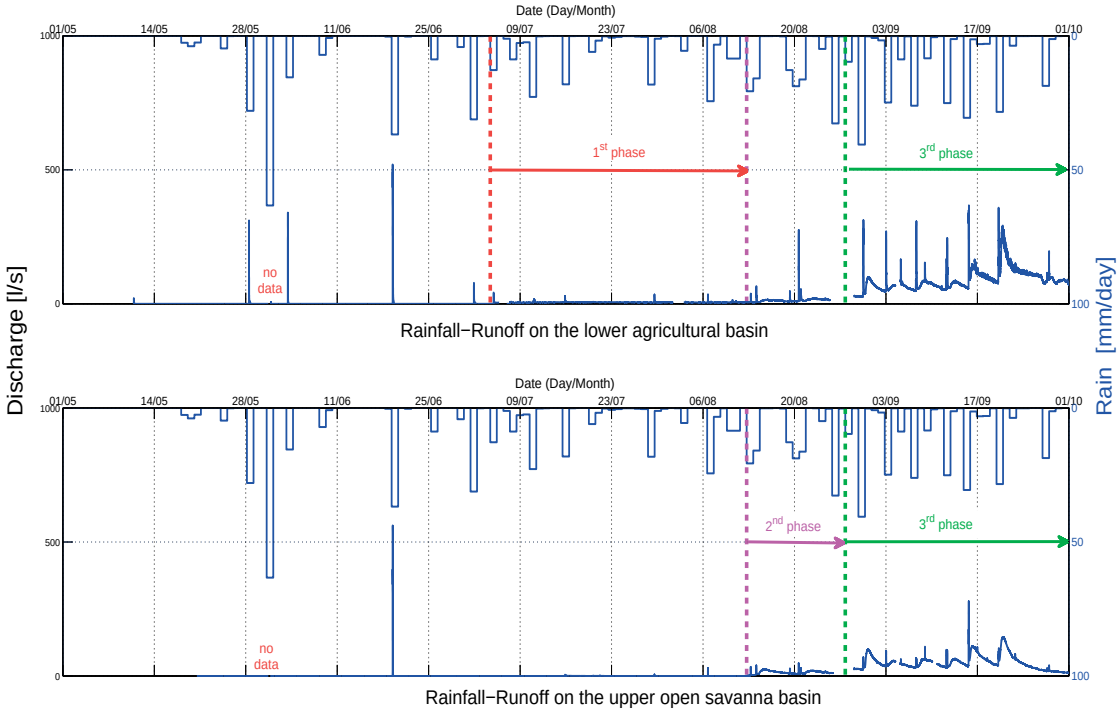

Figure 4.4: Streamflow phases over the rainy season

The analysis of the runoff dynamics highlighted the distribution of surface runoff and base flow according to the land use. Intermittent or truncated responses of streamflow were identified over the course of the season in 2010. Three phases were identified (Figure 4.4). First, after ten rain events with more than 210 mm in accumulation, the flow started to be continuous between springs 1 and the outlet of the basin (5-31 July) over nearly 200 m of the river. This flow is caused by the filling from the bottom by shallow groundwater. Second, from 12-15 August after twenty daily rain events were recorded with 360 mm of rainfall, the flow became continuous between springs 2 and 3 and the triangular weir in the upper basin (Figure 4.4). These flows seeped away into the ground directly downstream of the weir, where the soil acted like a deeper storage tank. Third, from 15 August to the end of October, when the intermediate storage tank became filled, the perched groundwater of springs 2, 3 and 1 became interconnected, which induced the continuous flow throughout the full 2.5 km of the river. The watertable distribution showed that the middle part of the basin represents an option for water storage underground. The cross-section between the deeper watertable and the lower perched groundwater could be the location to build a buried dam aiming to reduce the underground outflow, minimize the evaporation and stored water for crops and plants.

4.3.2 Implementation

Food insecurity affects a large portion of the population in sub-Saharan Africa and Tambarga. To meet future food requirements, current rainfed farming systems need to increase yield output. One way is to improve water and fertilizer management in crop production (Fox et al. 2005). Understanding the hydrological processes appears to be another way to improve water management at Tambarga and reduce the population's vulnerability to climate change because less than 10% of water resources are exploited in this region (Ceperley et al. 2012). To improve understanding of the hydrological processes at Tambarga's catchment, a simple lumped conceptual model with three sub-areas was developed. The catchment was subdivided based on dominant land use, soil type and peak flow observed in the field. The main components of the model are: rainfall, soil moisture, evaporation, groundwater depth and discharge (Figure 4.5). The model is used to simulate runoff, soil moisture, and groundwater to quantify the effects of irrigation on the local water balance. All the components are interconnected through linear processes. The interconnections are controlled by thresholds defined for soil infiltration capacity, rainfall intensity, hydraulic conductivity at saturation and groundwater depth. Reaching a particular threshold leads systematically to the generation of runoff, infiltration, or a recharge of the water table.

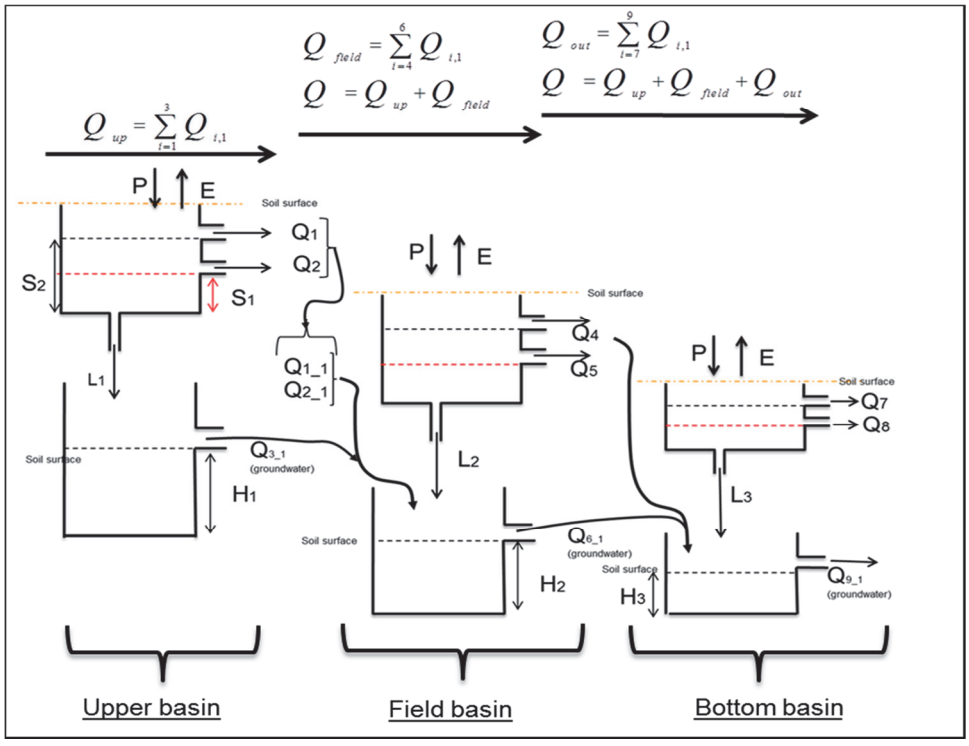

Figure 4.5 : Model diagram. Details of the model are in the appendix- chapter 4.

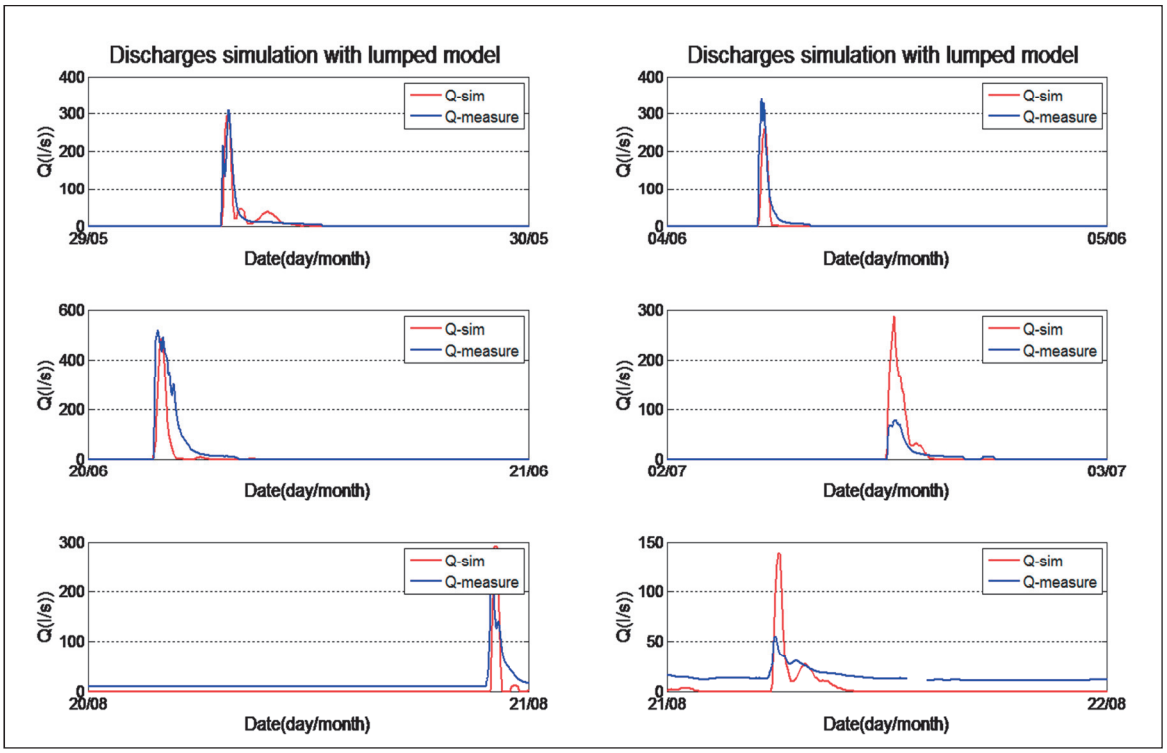

Figure 4.6: Rainfall-Runoff Simulation

Initial simulations of runoff produce satisfactory results for the beginning of the rainy season when the soil is dry, but runoff is overestimated when the rainy season is completely established with a permanent stream flow (Figure 4.6).

The model is able to account for the subsurface flow and reproduce the groundwater recharge pattern. The first results allowed us to conclude that the basin provides a significant amount of groundwater that could be used for irrigation to improve crop yield and consequently, reduce food insecurity. Three scenarios for storing this water are tested in this work: 1) Dams at the outlet of the open savanna forest (upper basin), 2) deeper wells for irrigation in the field and 3) dams buried to retain the water for the plants and crops in the field.

The first scenario, with a dam at the first outlet, could lead to capturing a significant amount of water for irrigation. The dam would be located in the river cross-section at the outlet of upper savanna sub-basin (290 m a.s.l.) (Figure 4.7). The proposed dam is 20 m in height, for a coverage area around 107,838 m^2 and around 2 million m^3 of water storage capacity. The water provided by this dam could be used for irrigation of 50 to 100 hectares of parcels, which would benefit more than 200 to 400 stakeholders by increased income for more than

200 households. These first estimations highlight the usefulness of the dam and how it could improve food security for local people. However, work is still needed to quantify exactly the amount of water that would be evaporated, and the overall impact on the local hydrology. Additionally, special attention should be devoted to the environmental impact with respect to the relative richness in trees in the upper basin and its social services.

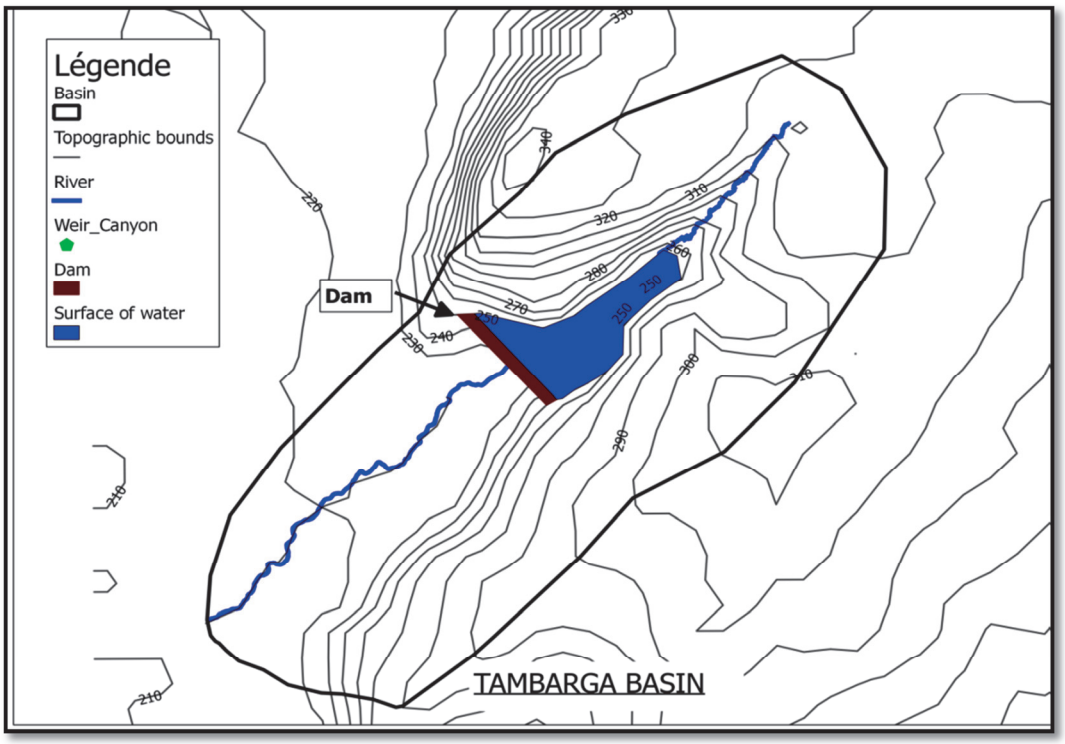

Figure 4.7: Open dam

The second scenario (Figure 4.8), of deepening wells, has already been tested by the local population. They found the shallow depth of the wells and the instability of the soil structure increased the difficulty of the project, which led to an abandonment of this irrigation strategy. Nonetheless, the deeper wells proposed in this chapter could be a solution to at least, minimize water unavailability and allow for better crop production. The proposed wells could range in between 20 to 40 meters and could be installed in the cross-section indicated in Figure 4.8. They could provide an average 48 m^3 per day of water, which can irrigate 20 to 30 hectares of crops and benefit 100 households. The wells must be stabilized by concrete and protected to avoid chemical contamination because farmers use fertilizers to improve crop yield. Attention should be paid to the long-term sustainability of this intervention, since the main source of drinking water is the groundwater.

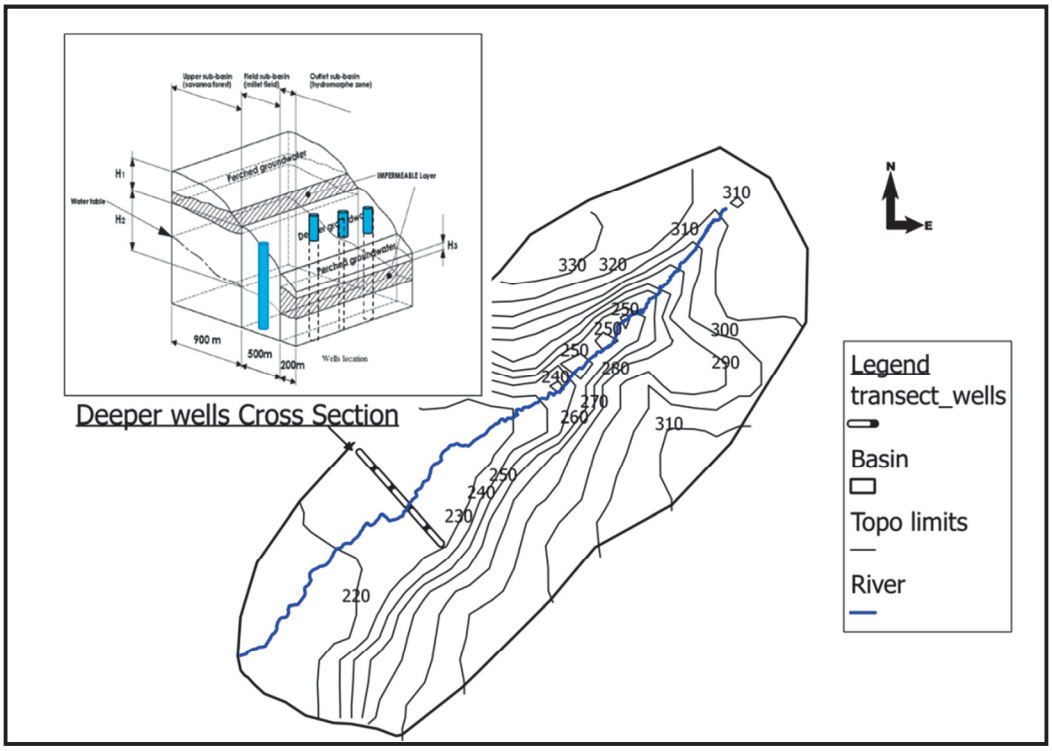

Figure 4.8: Deeper wells

The third scenario (Figure 4.9), with a buried dam, could be relatively cheap (~5,000 US$) or very expensive depending on the material used. Using local materials, such as clay, for waterproofing the dam section would be cheaper, while concrete would be very expensive (>50,000 US$). The buried dam principle consists of building an impermeable wall in a trench dug over a cross section in the basin whose bottom limit corresponds to the impermeable layer. Basically, the dam depth would range between 6 to 10 m over 100 m length. It would reduce the direct evaporation on the order of 99% compared to the open dam scenario. The buried dam would lead to an increase of the soil moisture in the field part of the basin and help to fight against dry spells by providing water to the plants and crops directly through the soil. Dry spells lead to a significant decline of rainfed production (Fox et al. 2005). However, this production reduction depends also on the crop development stage that is affected. Increasing the water level in the wells and consequently the soil moisture is a way to reduce the negative effects of dry spells. Storing water underground presents several other advantages such as: reducing cost of exploitation (no need to dig deep wells), reducing maintenance, reducing waterborne diseases, enhancing water quality, conserving the land above the dam and reducing desertification (Onder and Yilmaz 2005).

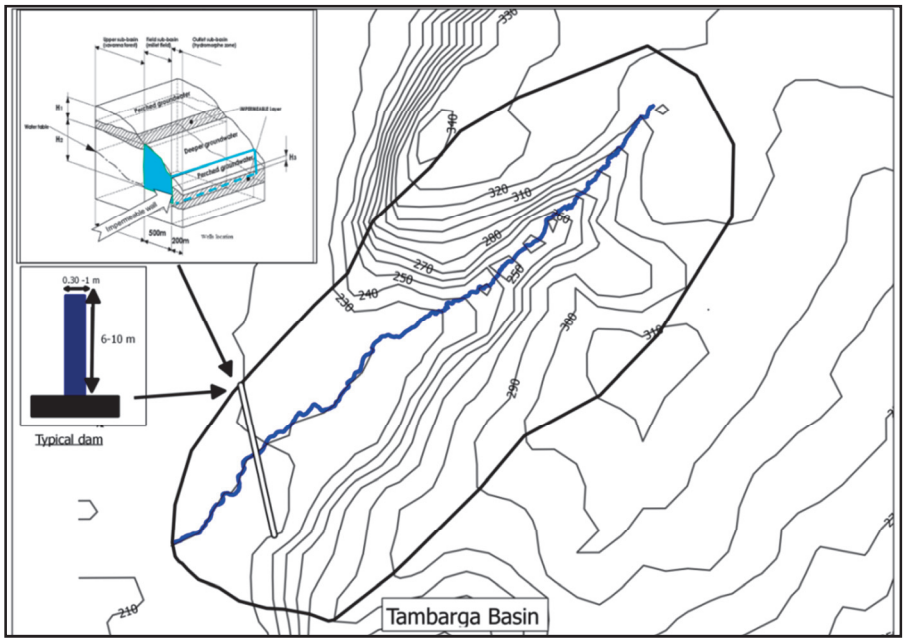

Figure 4.9: Buried dam location

Conclusion

In the basin of Tambarga the major portion of runoff is generated by direct precipitation. The groundwater is disconnected between three areas of the basin: two shallow perched water tables (upper and bottom basin) and one deeper groundwater in the agriculture. The complete river baseflow is controlled by groundwater. The seasonal pattern of evaporation allowed identification of two peaks of latent heat flux that correspond to the grass growing, tree foliage and crop heading.

The processes highlighted allowed us to implement a simple lumped hydrological model refined with understanding of land covers, watertable distribution, evaporation and streamflow patterns. The model is still in development, but the preliminary results are promising, as the model is able to simulate the complex runoff behavior.

The amount of water stored in the groundwater implies that irrigation is a way to sustainably insure the agricultural productivity for Tambarga's local people. Irrigation scenario tests show that using buried dams and deeper wells for irrigation are alternatives for better agricultural production. The groundwater storage management appears to be a sustainable way to store water for livelihood, crops and plants at Tambarga. Future research can explore the type and method of irrigation as well as the long-term sustainability.

References

Bagayoko, Fafre, Samuel. Yonkeu, Jan Elbers and Nick van de Giesen, N. (2007). Energy Partitioning over the West African Savanna: Multi-year Evaporation and Surface Conductance Measurements in Eastern Burkina Faso. *Journal of Hydrology*, *334*(3-4), 545-559.

Beven, Keith J. (2004). *Rainfall-runoff Modeling: The Primer*. Chichester, UK: John Wiley & Sons.

Brutsaert, Wilfried. (1982). *Evaporation into the Atmosphere: Theory, History and Applications*. Dordrecht, Netherlands: Kluwer Academic Publishers.

Brutsaert, Wilfried. (2005). *Hydrology: An Introduction*. Cambridge University Press.

Ceperley, Natalie, Repetti Alexandre and Parlange M.B. (2012). Application of Soil Moisture Model to Marula (Sclerocarya birrea): Millet (Pennisetum glaucum) Agroforestry System in Burkina Faso. In J.-C. Bolay, G. Tejada, M. Schmid, & E. Hazboun (Eds.), *Technologies and Innovations for Development: Scientific Cooperation for a Sustainable Future* (pp. 211-229). Paris: Springer.

Commune Rurale de Madjoari (2009). Plan communal de développement de Madjoari 2010-2014. Ministère de l'Administration Territoriale et de la Décentralisation Région de l'Est, Province de la Kompienga, Commune Rurale de Madjoari.

Fox, P., Rockstrom, J., & Barron, J. (2005). Risk Analysis and Economic Viability of Water Harvesting for Supplemental Irrigation in Semi-arid Burkina Faso and Kenya. *Agricultural Systems*, *83*(3), 231-250.

Gnouma, Raouf. (2006). Aide à la calibration d'un modèle hydrologique distribué au moyen d'une analyse des processus hydrologiques : application au bassin versant de l'Yzeron. L'institut national des sciences appliquées de Lyon: Cemagref Lyon.

Gribovszki, Zoltán, Szilágyi, József, & Kalicz, Péter. (2010). Diurnal Fluctuations in Shallow Groundwater Levels and Streamflow Rates and their Interpretation – A Review. *Journal of Hydrology*, *385*(1–4). 371-383. doi:10.1016/j.jhydrol.2010.02.001.

Ioslovich, Ilya and Gutman, P.-O. (2001). A Model for the Global Optimization of Water Prices and Usage for the Case of Spatially Distributed Sources and Consumers. *Mathematics and Computers in Simulation*, *56*(4–5). 347-356. doi:10.1016/S0378-4754(01)00306-8.

Irvine, Dylan J., Brunner, Philip, Hendricks Franssen, Harrie-Jan. and Simmons, Craig T. (2012). Heterogeneous or Homogeneous? Implications of Simplifying Heterogeneous Streambeds in Models of Losing Streams. *Journal of Hydrology*, *424-425*(0), 16-23.

Komatsu, Yokuse and Onda Yuichi. (1996). Spatial Variation in Specific Discharge of Base Flow in a Small Catchments, Oe-yama Region, Western Japan. *Journal Japan Society Hydrology & Water Resources*, *9*(6), 489–497.

Ndomba, Preksedis, Mtalo, Felix, & Killingtveit, Aanund (2008). SWAT Model Application in a Data Scarce Tropical Complex Catchment in Tanzania. *Physics and Chemistry of the Earth, Parts A/B/C*, *33*(8-13), 626–632. doi:10.1016/j.pce.2008.06.013.

Ojo, Oyediran. (1983). Water Balance Computation in West Africa: Problems and Prospects. Proceedings of the Hamburg Workshop, August. *IAHS Publication No. 148*.

Onda, Yuichi. 1994. Contrasting Hydrological Characteristics, Slope Processes and Topography Underlain by Paleozoic Sedimentary Rocks and Granite. *Transactions, Japanese Geomorphological Union*, *15A*, 49-65.

Onda, Yuichi, Komatsu, Yokuse, Tsujimura, Maki and Fujihara, Jun-ichi (2001). The Role of Subsurface Runoff Through Bedrock on Storm Flow Generation. *Hydrological Processes*, *15*(10), 1693-1706.

Onder, H., & Yilmaz, M. (2005). Underground Dams: A Tool of Sustainable Development and Management of Groundwater Resources. *European Water Publications*, 11/12, 35-45.

Simoni, Silvia, Padoan, Simone, Nadeau, Daniel F., Diebold, Marc, Porporato, Amilcare, Barrenetxea, Guillermo., Ingelrest, François., Vetterli, Marc, Parlange, Marc B. (2011). Hydrologic Response of an Alpine Watershed: Application of a Meteorological Wireless Sensor Network to Understand Streamflow Generation. *Water Resources Research*, *47*(October 22). doi:10.1029/2011WR010730.

Stagnitti, Frank, Parlange, Jean-Yve., & Rose, C.W. (1989). Hydrology of a Small Wet Catchment. *Hydrological Processes*, *3*(2), 137-150. doi:10.1002/hyp.3360030204.

Conclusion and future work

The present thesis investigated the rainfall-runoff processes over a semi-arid watershed characterized by two landscapes, an agricultural field (AF) and an open savannah forest (SF). An unprecedented field campaign was conducted since 2009 aiming to collect the hydro-meteorological data needed for this study. The water balance was explored through three components, rainfall, streamflow and evaporation, to understand their roles and interactions in the local hydrology. This understanding has provided four major findings:

Chapter 1 The rainfall events at Tambarga are convective and are impacted by land cover and land use differences. The events are short and intense and occur mainly daytime. The rainfall amount is 10-30% greater over the SF when compare to the AF. The enhancement of rainfall over SF is induced by the increased sensible heat flux.

Chapter 2 The flow in the river is correlated with the groundwater level, which produces either single-peak or double-peaked hydrographs. The shapes of the hydrographs are driven by the high rain intensity (single-peak) and the combination of the antecedent soil moisture and weak rain intensity (double-peak). However, one should pay special attention to avoid any confusion between a double-peak hydrograph caused by a bimodality of the precipitation and one caused by delayed subsurface flow, which is controlled by the groundwater level.

Chapter 3 The baseflow follows a diurnal pattern generated by two physical drivers, infiltration in the riverbed and evaporation along the riparian zone, over the course of the season. At the beginning of the season (September), the increased infiltration rate, caused by significant stream temperature difference, controls the diurnal pattern. While direct evaporation over the river, the wetland and riparian area controls the diurnal pattern later in the season (October-November). An evaporation control area, or footprint, was defined when the streamflow diurnal pattern is caused the evaporation. This area is about 0.6% of the basin surface and is confined by the wetland and riparian area. This area is relevant for hydrologists as it allows characterizing the evaporation and therefore, assesses its impact on the local hydrology.

Chapter 4 The last findings are some more insights into possible solutions for water management strategies. Underground water storage in combination with deeper wells seems to be a way to improve the agricultural production at Tambarga through irrigation.The local population at Tambarga is more familiarized with the concept of environmental conservation because conservation has real implications to their immediate well-being. Nevertheless, they still wait for concrete applications of the scientific results for their economic development. Therefore, future work will be focused on the validation of the evaporation contributing area by monitoring the wet surface over the basin. A set of soil sensors in the riparian area will be installed to investigate the correlation between the soil moisture conditions and the diurnal streamflow pattern.

The proposed water management strategies must be tested and validated by integrating the resilient effect on the groundwater, which is the unique source of drinking water. The hydrological model will be finalized by integrating all the findings. Recalibration and validation will, hopefully, provide answers to the local population's expectations: How to achieve food security in agriculture.

Appendix: Supplementary Material

The aim of this section is to provide some additional details for concepts that were not explicitly included in the thesis chapters because the chapters were formulated as manuscripts, soon to be submitted to scientific journals. This supplemental section describes methodologies and presents new graphs. Their interpretations may provide further understanding of some of my thesis conclusions.

Appendix-chapter 1

The mixed layer (ML), also called well-mixed layer, is driven both by mechanical shear and by buoyancy. The buoyancy driven ML, also called convective mixed layer, is more uniform than the mechanical one and is driven by the enhancement of vertical motions due to the anisotropy of the medium. The ML definition assumes a near constant potential temperature and humidity with height and constant wind speed and direction. The diurnal ML pattern is depicted by four phases which are: formation of a shallow ML; rapid growth; deep ML of the nearly constant thickness; decay of turbulence (Stull 1988).

For the ML modeling a thermodynamic encroachment hypothesis was done by neglecting advection and subsidence components. Based on this assumption, the ML at time t_{i+1} could be estimated by computing the amount of heat released during $[t_i\ t_{i+1}]$. This energy corresponds to the sum of the heat released between $[t_i\ t_{i+1}]$, which can be evaluate by integrating the area under the latent heat flux curve during this period.

The lifting condensation level (LCL) corresponds to the height at which the relative humidity over a vertical profile becomes saturated over a delimited air parcel. The LCL formation occurs through two simultaneous processes, which are increase of relative humidity and decrease of temperature of the air parcel. During this processes the specific humidity remains constant while the saturated vapor pressure decreases in magnitude. The LCL height corresponds to the cloud base height, at this level the clouds are saturated in droplets, which when combined with other mechanism such as ML growth, could trigger a rain event. The LCL depth also is dependent upon the antecedent moisture state and the land cover (vegetation) over the considered domain (Findell and Eltahir 2003; Juang et al. 2007).

The figures 1-4 are some examples daytime convective rainfall (CR) events. These graphs show the evolution of the ML (subplot a, dashed red line) together with the LCL (subplot a, black line). The intercept of ML and LCL is a necessary condition, but not sufficient for CR event identification. This condition in addition with occurrence of rain event within the 3 hours after the intercept occurs is sufficient for classifying a CR rain event. The subplot b shows the start time of the rainfall their intensities in half hour period.

The relative humidity (RH, subplot c, blue line) and the sensible heat (H, subplot d, black line), respective drivers of the LCL and ML, are also plotted. The start of the rain event coincides with an increase of relative humidity (almost saturation) and with a drop of the sensible heat flux (almost negative).

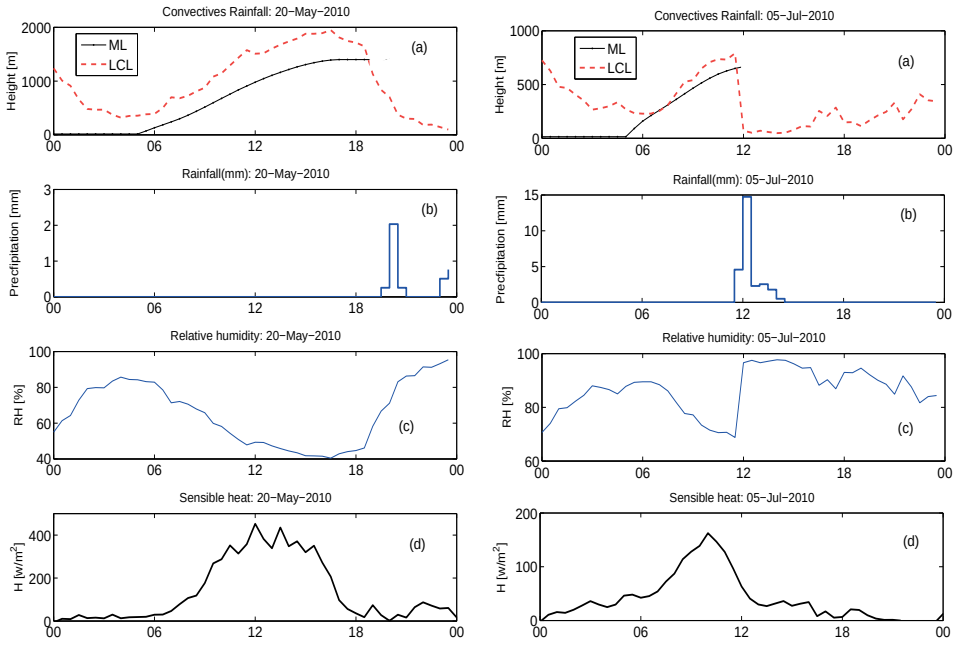

Figure 1: Tracking of CR rainfall. The x-axis represents the time (hours).

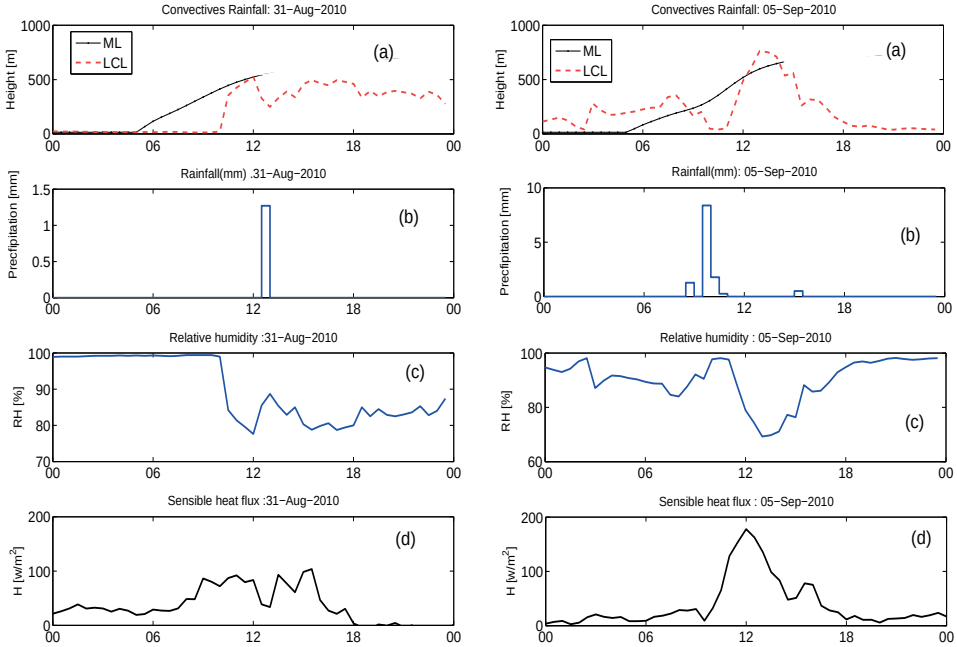

Figure 2: Tracking of CR rainfall. The x-axis represents the time (hours).

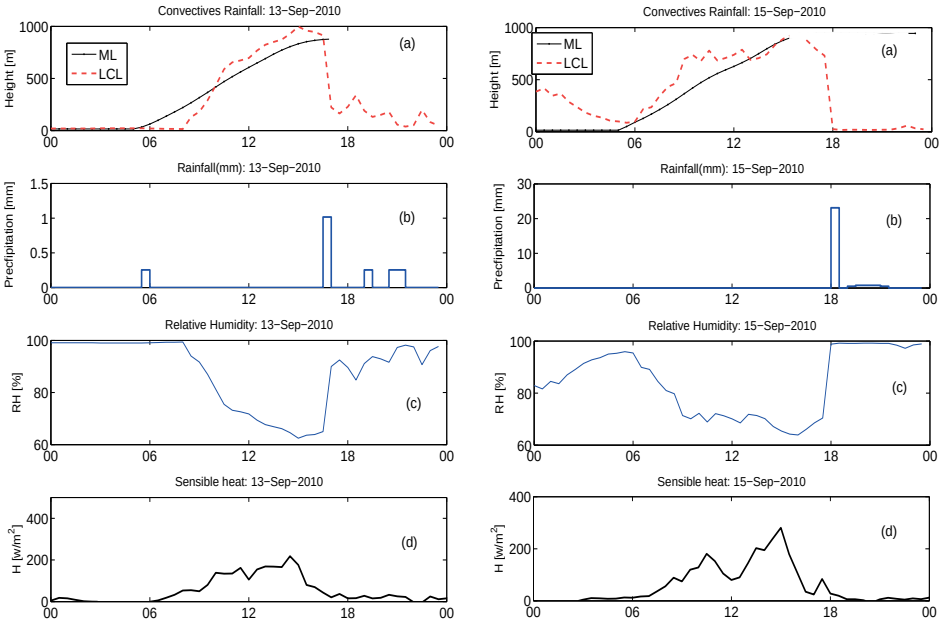

Figure 3: Tracking of CR rainfall. The x-axis represents the time (hours).

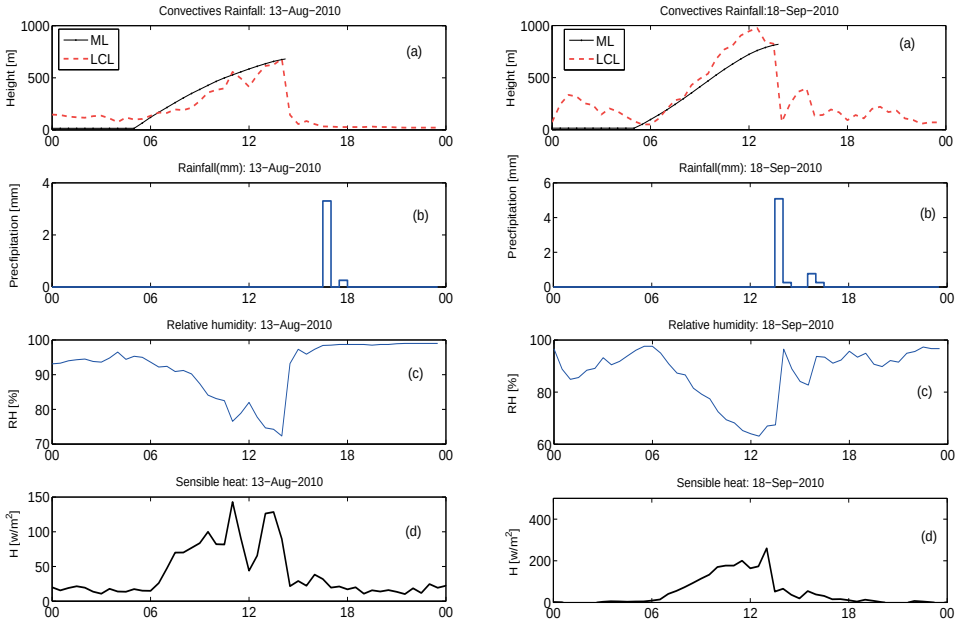

Figure 4: Tracking of CR rainfall. The x-axis represents the time (hours).

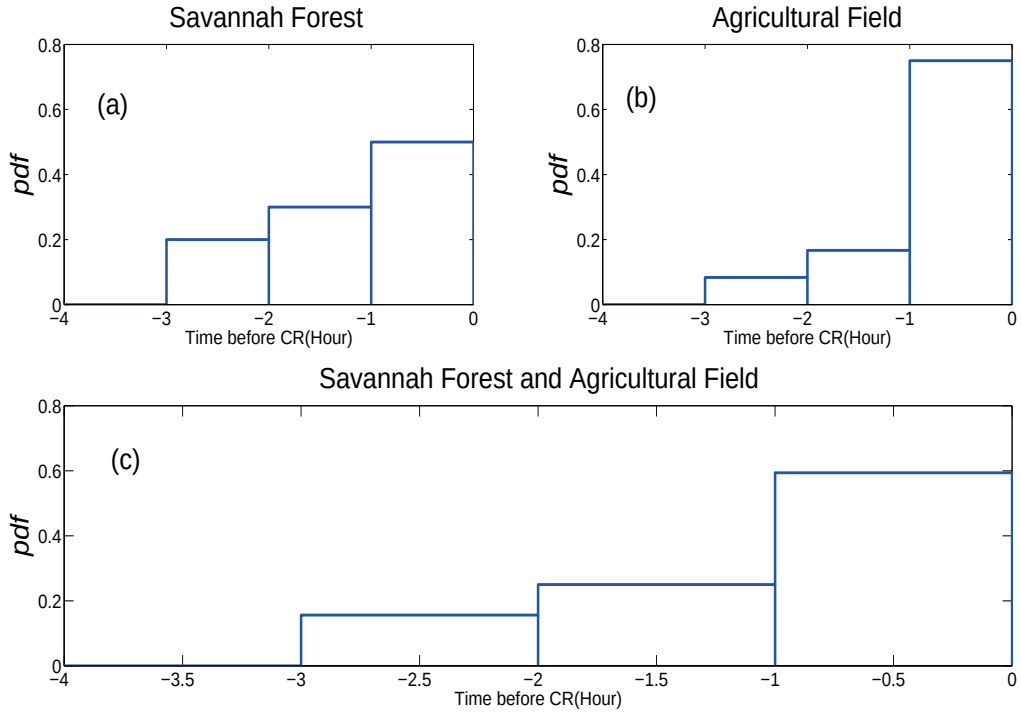

Figure 5: Probability distribution function of time lag before CR rainfall occurrence over AF and SF.

Figure 5 investigates the probability density function (*pdf*) of the time lag between the intercept of ML and LCL and the advent of rain event. The *pdf* all range within 3 hours, and the savannah forest (SF) *pdf* distribution seems more evenly distributed (Figure 5 a)while the agricultural field (AF) rain events occur mostly within the range of one hour (Figure 5 b). In general, more than 80% of the CR rain events occur in the range of 2 hour (figure 6 c).

Priestley Taylor

The Priestly Taylor method (eq. 1) was used to compute the evapotranspiration (ET) and subsequently, compare with the eddy covariance data over the two sites.

$$ET = 1.26 * \frac{\Delta}{\Delta + \gamma} R_n \qquad (1)$$

where R_n is the net radiation, Δ is a the slope of the saturation water vapor pressure curve and γ is the psychometric constant.

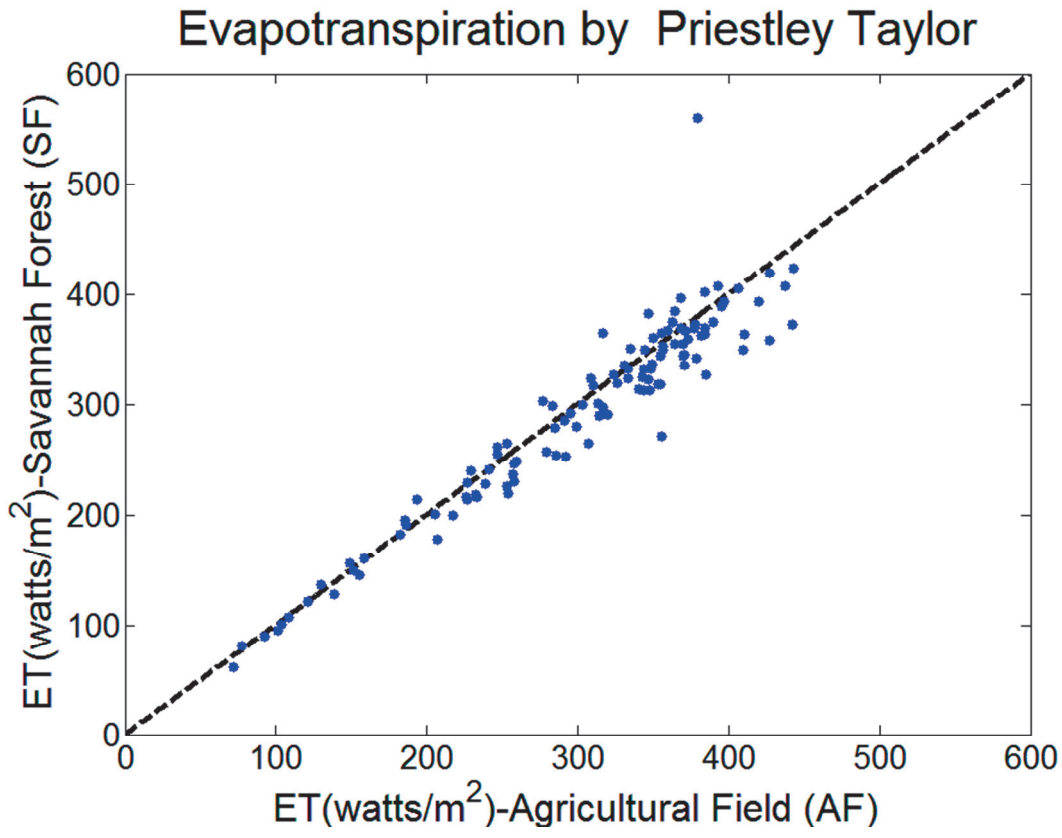

Figure 6: Evapotranspiration computing with Priestley Taylor method between AF and SF

The comparison between the two modeled ET obtained with Priestley Taylor method shows a good agreement between the ET over AF and SF (figure 6) while the sensible heat flux is greater over the SF. Therefore, the sensible heat flux plays a crucial role in the enhancement up to 30% of the convective rainfall over the savannah forest.

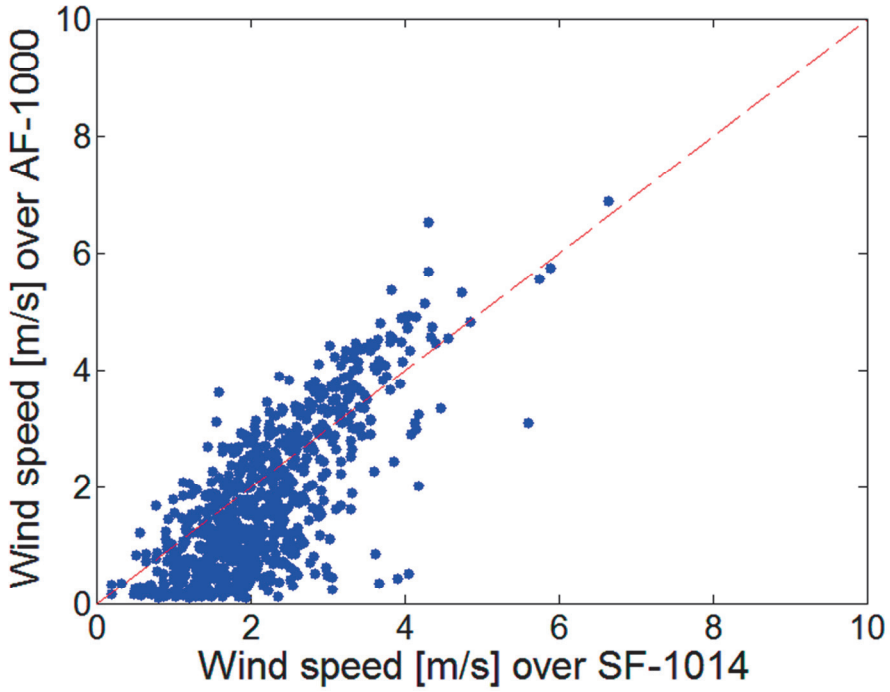

Figure 7: Comparison between horizontal wind speed between AF and SF over the rainy season. The station 1000 is located in the AF while the station 1014 is located on the hill above SF.

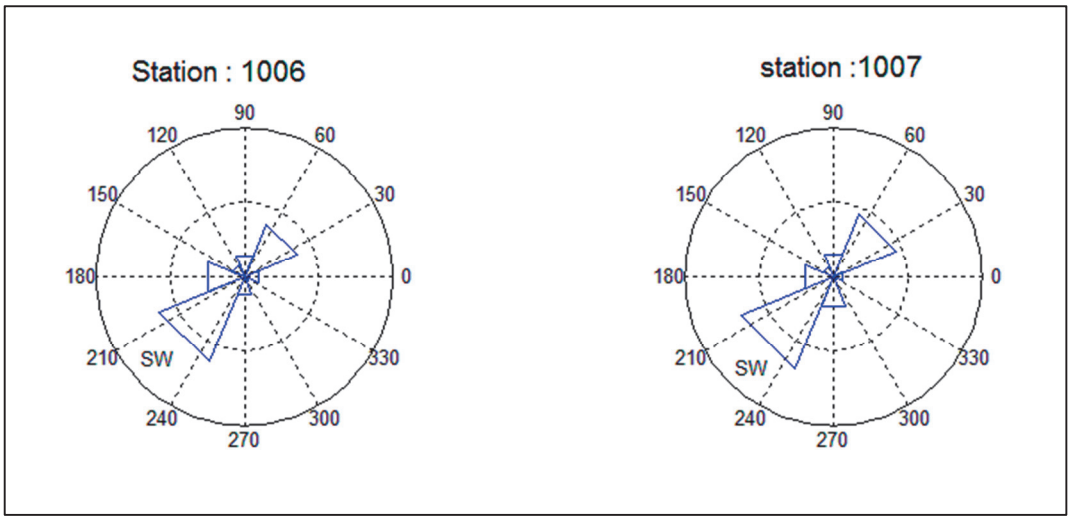

Figure 8: Wind direction over the entire basin for rainy days at two locations over the basin.

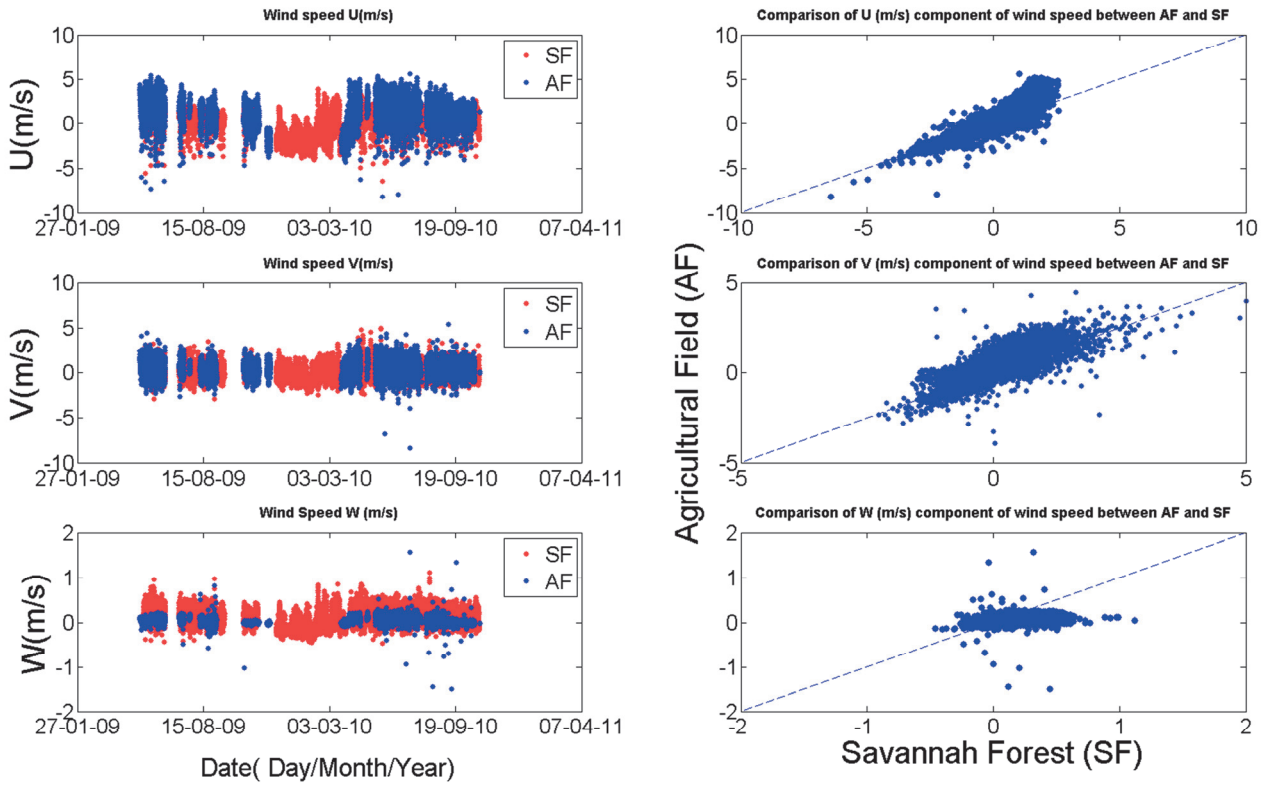

Figure 9: Three dimensional wind speeds (U,V,W) measured with eddy covariance stations over AF and SF (left panel). The right panel compares the components (U, V, W) between the two landscapes.

The wind speed and direction are critical variables to characterize a rain event. At Tambarga the rainy day daytime wind speed varies between almost zero to 7 m/s (Figures 7 and 9). The wind direction is variable, mostly southwest and parallel to the hill, which can exclude possible orographic effects to CR triggering (Figure 8). The components U and V seem consistent over the two sites while the W component is slightly more enhanced over SF (Figure 9).

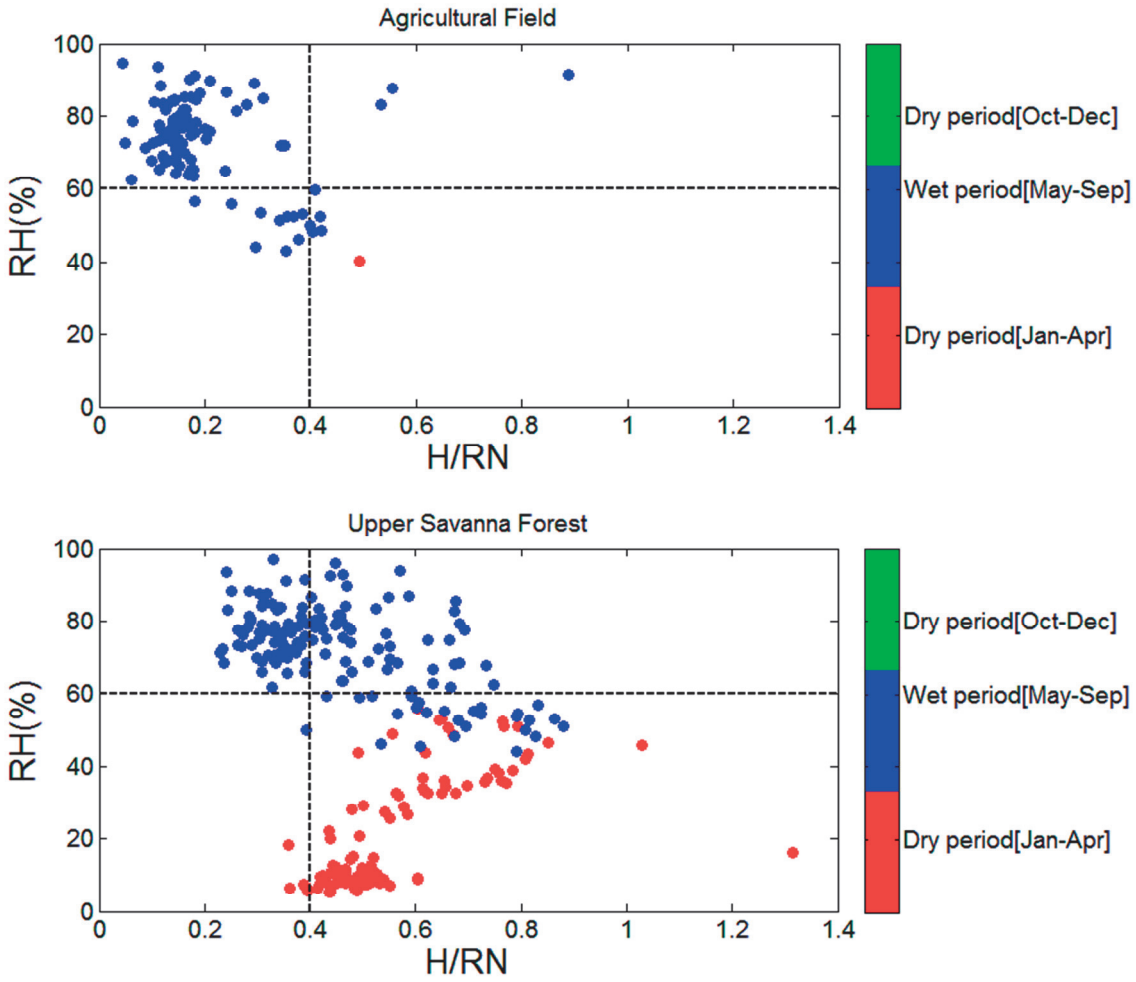

Figure 10: Relationship between RH and H/RN over the SF and AF.

The percentage of the sensible heat in the net radiation is compare over the SF and AF in comparison with the relative humidity in Figure 10. An larger proportion of energy is converted into sensible heat over the SF during the wet season compared to AF meaning that more than 50% of the flux measurements collected over the SF during the wet season consume more than 40% of the total energy produced, while less than 1% consumes more than 40 % of the energy on the field (Figure 10). This graph could explain the 30% enhancement of rain over the SF as more energy released induces more production of the convective rainfall.

Appendix-chapter 2

In chapter 2, I studied the hydrographs shapes over the rainy season which highlighted two types of hydrographs: single peak hydrograph and double peak hydrograph. The figure 11 shows a time series of soil moisture data at four depths over four different locations in the basin (one point on the savannah forest, two points on the millet agricultural field and the last point at the basin outlet. The double-peak hydrographs correlated with the antecedent soil moisture (thesis-chapter 2) also occurs when the moisture overall the agricultural field is in average greater than 20%, which mean that the soil need to be wet enough to drive a delay flow.

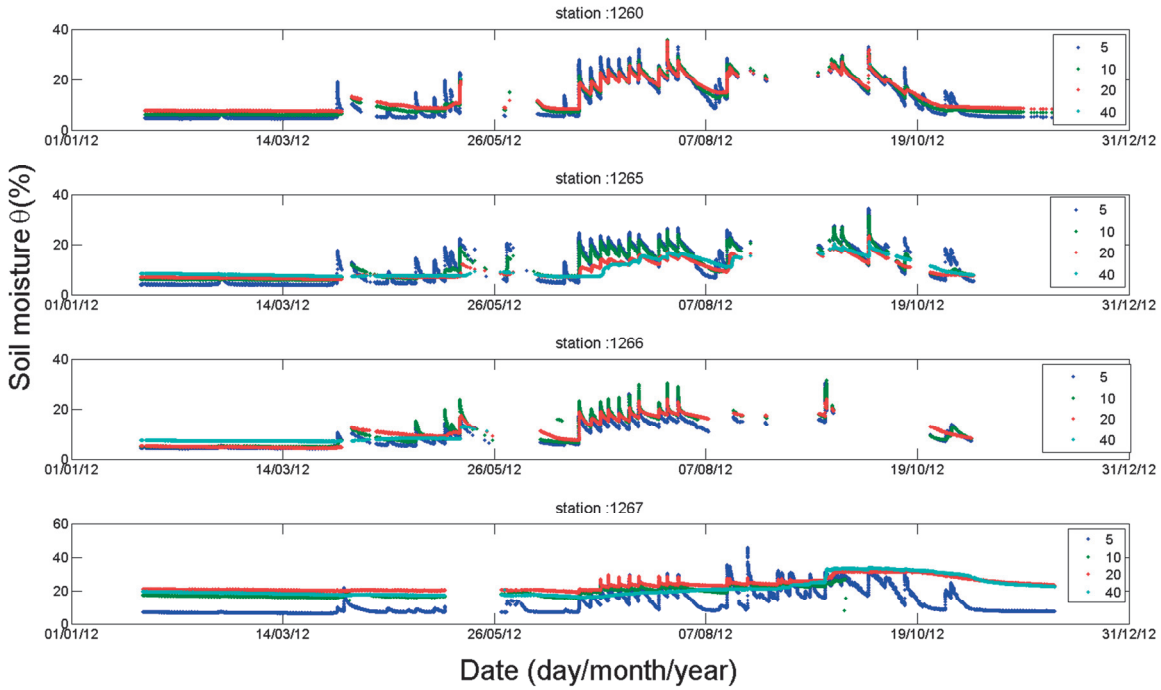

Figure 11: Soil moisture pattern at Tambarga in 2012. From the top to the bottom we have soil moisture measured at four depths (5, 10, 20, 40 cm) at different locations over the agricultural field (stations 1260, 1265 and 1266 in sandy soil, and station 1267 at the basin outlet with clay soil).

The rainy season is the period with the maximum soil moisture (~ 40%). During the dry season, the soil moisture is less than 5 % for all of the stations in the agricultural field, while at the outlet of the basin; it is almost 20% up to 10 cm depth. The first layer of soil (5cm) is in the same range as the other measurements in the AF. The moistening at station 1267 is explained by the presence of shallow groundwater at this location, which provides water to the soil.

The first 5 cm of soil over the basin outlet dries faster than the deeper locations because of the presence of fissure, which enhances infiltration for deeper soil. Since the soil in AF is better mixed, the drier soil moisture pattern is consistent over the four measurement depths.

The Figure 12 highlights the soil moisture four depths profile pattern at the station 1265 in the field. Seasonal relationship is found between the wet and dry front pattern during the rainy season. Therefore the soil becomes wet from May to end of September and starts to dry slowly from October to November concomitant with the reduction of rainfall frequencies and intensities. The soil is wetter at the surface from May to end of September and shifts to become wetter at a deeper level, which is consistent with the increase of net radiation (no clouds), and therefore evaporation and transpiration through plants. This suggests a hyteresis relationship (dashed arrows) even at seasonal scale for soil moisture.

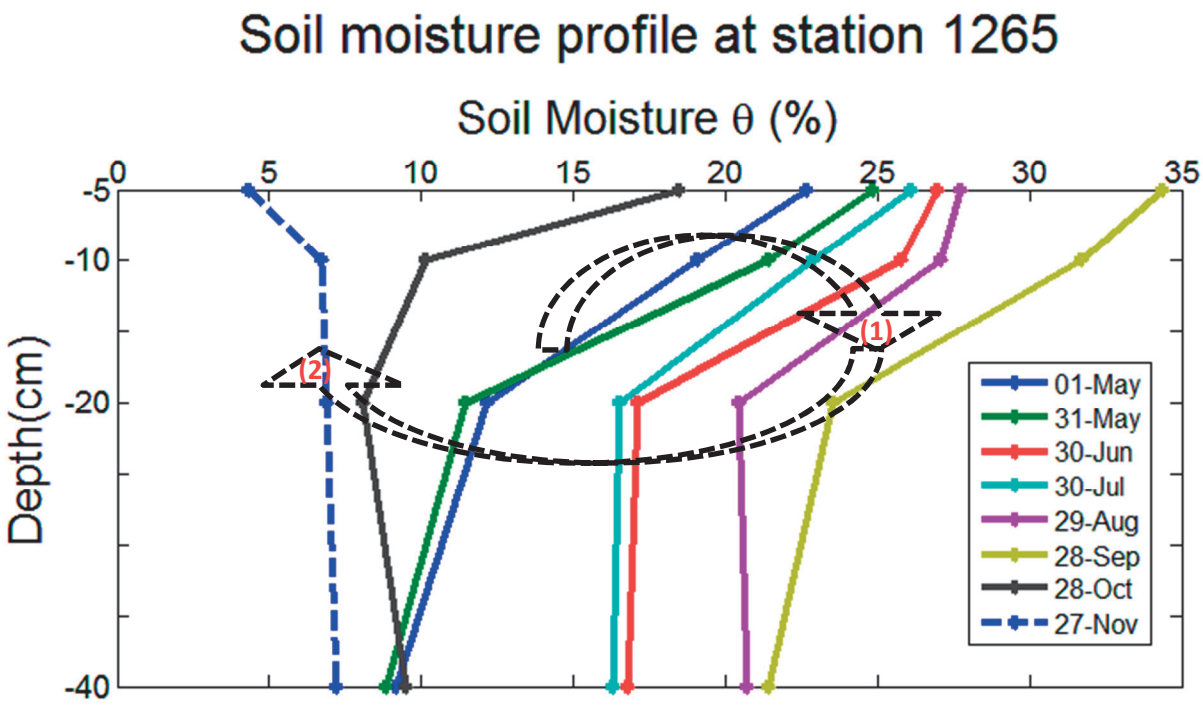

Figure 12: Soil moisture profile in the agricultural field in 2012. The profile is shown at 30 days' time step from May to November. The black dashed arrow (1) shows the increase of the wetting front from (May to September) while the black dashed arrow (2) shows the drying of soil (October to November).

Appendix-chapter 3

This section investigates others examples of the diurnal streamflow (Figure 13) and evaporation (Figure 14) pattern throughout nine selected days. The streamflow diurnal pattern highlights water lost in the stream and this loss was proven (chapter 3 in the thesis) to be caused by the evaporation. Therefore based on the simple ratio in half hour period between the water lost and the evaporation a contributing area computed (Figure 15).

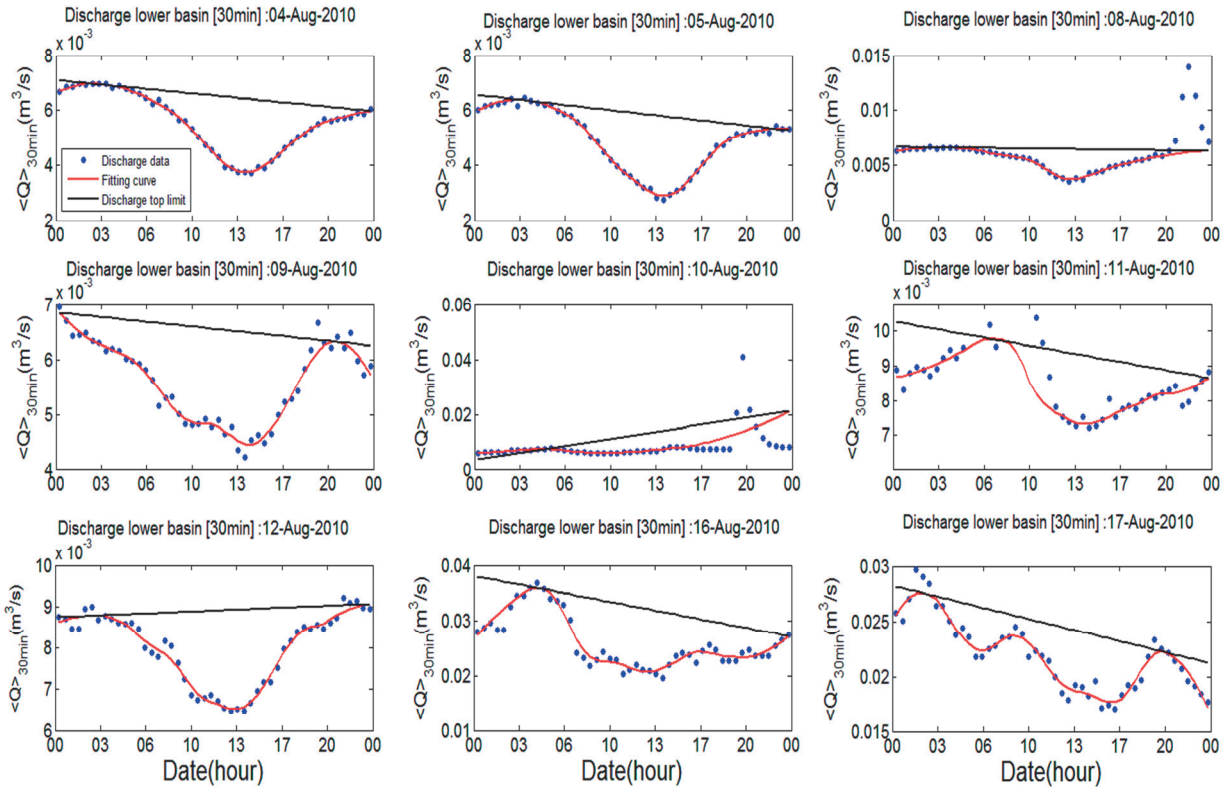

Figure 13: Daily streamflow pattern at the outlet of the basin. Each graph depicts a diurnal pattern with maximum flow in early morning (6 A.M.) followed by a decrease of the flow rate until sometime around 1 P.M. followed by an increase to achieve, more or less, its previous level. The black line represents the upper limit of the water level aiming to assess the amount of water loss.

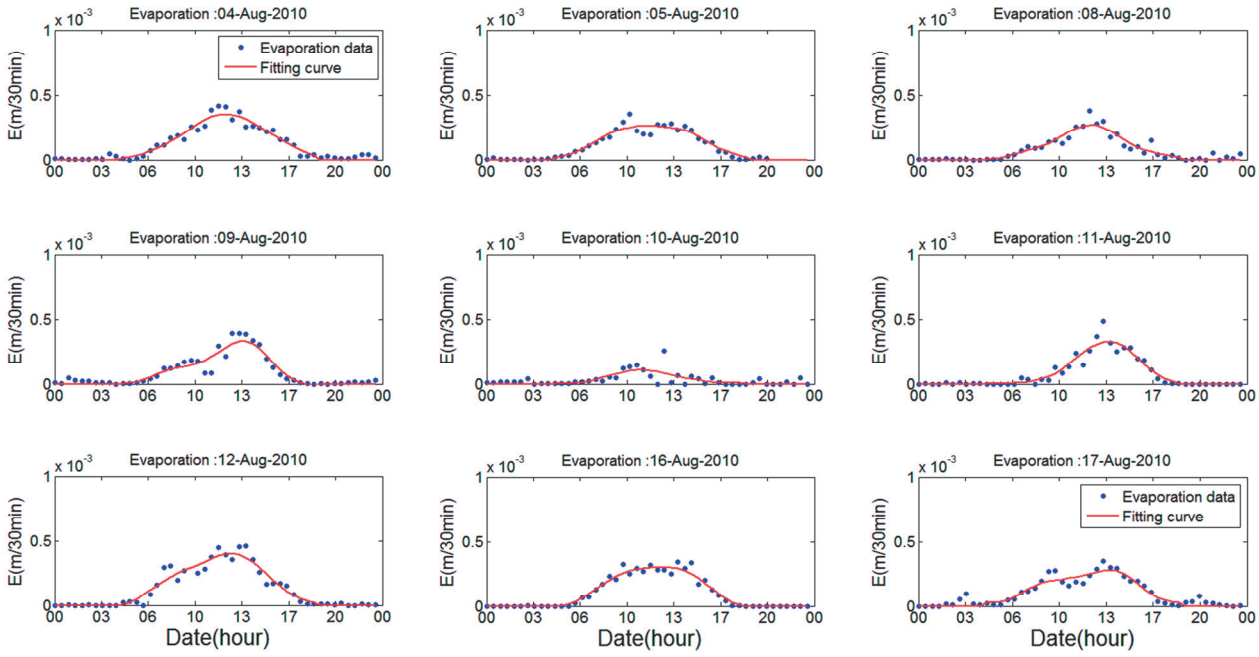

Figure 14: Daily evaporation pattern for nine selected days. Each graph is characterized by a diurnal pattern with a minimum latent heat flux early morning and night, and a maximum evaporation rate around 1 P.M.

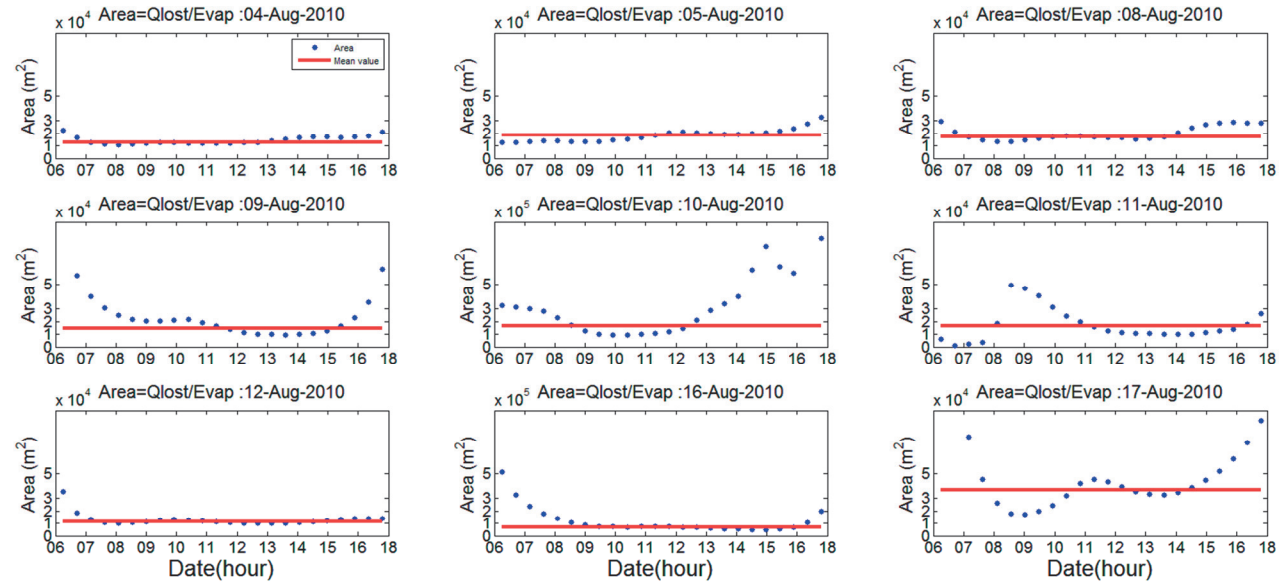

Figure 15: Evaporation control area (ECA) computed for each of the nine selected days through: $\boldsymbol{Area[m^2] = \frac{Q_{lost}[m^3]}{Evaporation[m]}}$

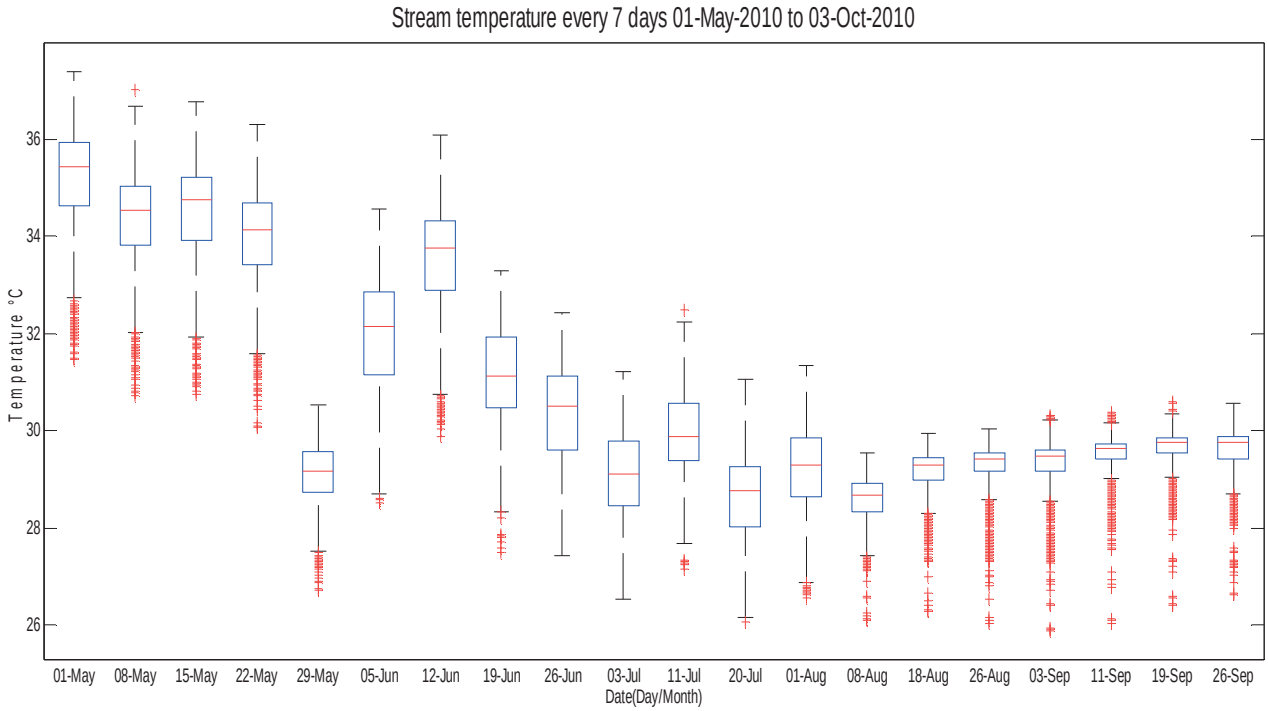

Figure 16: Stream temperature pattern measured with the Distributed Temperature Sensors (DTS).

Seasonal pattern of the stream temperature (measured at the center of the stream) highlights a higher stream temperature at the beginning of the rainy season that decreases progressively with the more frequent rain events and becomes more stable around 29°C from August to the end of September 2010. The daytime stream temperature difference at the beginning of the rainy season (May) is more pronounced than later when the rain becomes more frequent.

Figure 17 shows the straightforward link between the stream temperature high difference ΔT during the beginning of the rainy season and the concomitant infiltration ΔQ. The temperature difference is well correlated with the water lost, and the amount of water lost is greater when the daytime temperature difference increases. This occurs also when the groundwater level is still under the ground level. Therefore this allows validated the assumption of water infiltration over the riverbed during the first part of the rainy season, an assumption also proved through Muskat (1937) and Constantz, Thomas, and Zellweger (1994).

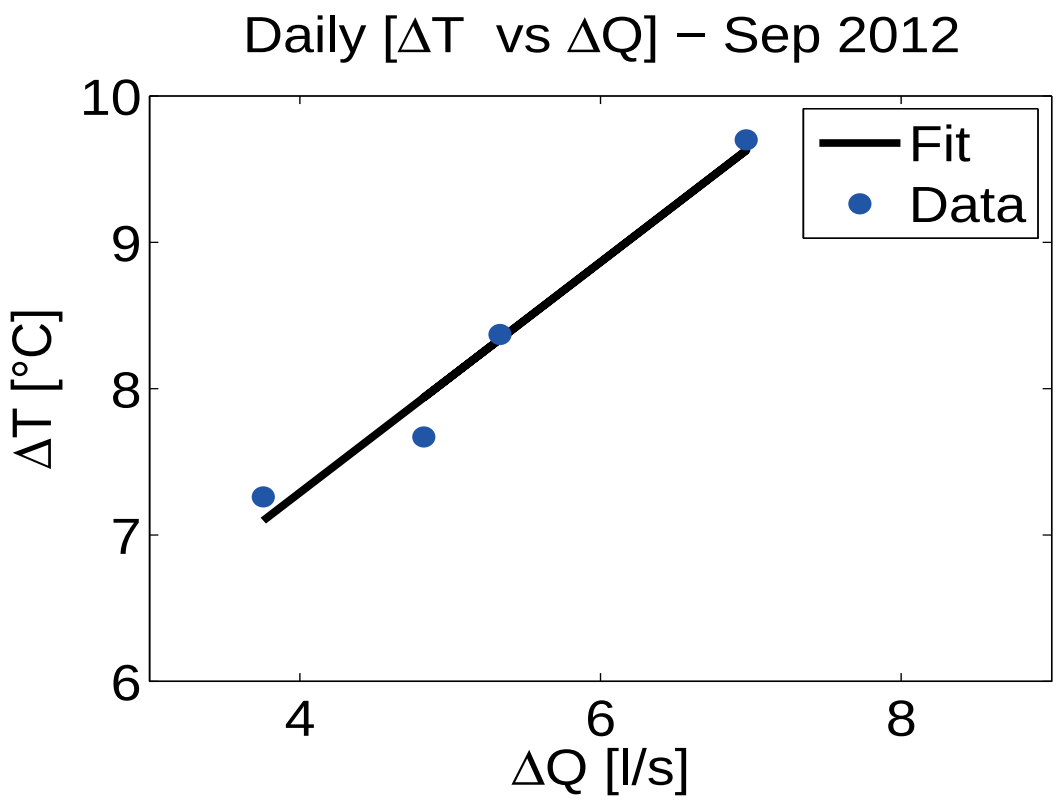

Figure 17: Comparison between stream temperature and stream discharge daytime variation.

Appendix-chapter 4

Model Description

A simple hydrological model was developed aiming to reproduce the streamflow response to rainfall events and the concomitant baseflow. The results obtained, in terms of process understanding, allowed for the division of the basin into three hydrological units (from the top-bottom): a transect with shallow groundwater [1-2 m], a transect with a deeper water table [up to 20m] and a transect with shallow groundwater [1 m].

For each hydrological unit three stages of runoff responses were assessed. The first stage concerns the direct runoff; the second stage is characterized by shallower runoff with deeper infiltration (leakage); the third stage represents the outflows from soil and groundwater.

For each of the sub-basins a vertical water balance is tested over each unit by computing the water storage (ds/dt) whether in the soil or the watertable.

$$\frac{ds(t)}{dt} = P(t) - I(t) - Q[s(t), t] - E[s(t)],$$

where P is precipitation, I interception and E evapotranspiration. Q denotes the overland flow composed of outflow water from this area over and under the ground.

$$i\{1,2,3\} = index\ of\ the\ sub\text{–}basin;$$
$$k\{1...n\} = index\ of\ event;$$

$$(1)\begin{cases} Q_{tot}(k,i) = Q_r(k,i) + Q_{sub}(k,i) + Q_g(k,i) \quad \left[m^3/s\right] \\ SM(k+1,i) = SM(k,i) + (PI_n(k) - Ev(k,i) \bullet A(i) \bullet dt - (Q_r(k,i) - R(k,i) + Q(k,i-1)) \bullet dt \quad [m^3]; \quad \begin{cases} Q(k,i-1) = 0 \ if \ (i=1) \\ Q(k,i-1) = 0 \ if \ (i \neq 1) \end{cases} \\ G(k+1,i) = G(k,i) + R(k,i) \bullet dt - Q_g(k,i) \bullet dt \quad [m^3]; \quad \{ \quad Q_g(k,i) = 0 \ if \ (H < riverbed) \end{cases}$$

Details of each basin functioning: The sub-basins are interconnected through the natural river and groundwater networks. The runoff is generated together by direct runoff consecutive to a rain event and the subsurface flow (controlled by the soil moisture state) and the groundwater outflow.

The total discharge is equal to the sum of the discharge over all three sub-basins. Each component of the discharge is a function of the rain intensity and the saturated hydraulic conductivity (eq. 2), soil moisture state (eq. 3) and the groundwater recharge level (eq. 4).

$$(2) \quad Q_r(k,i) = (PI_n(k) - K_s(i)) \bullet A(i) \quad if\ \left(PI_n(k,i) \geq K_s(i)\right) \quad \left[m^3/S\right]$$

Q_r = *quick runoff*; PI_n = *Rainfall intensity*; K_S = *Saturated hydraulic conductivity*; A = *sub-basin area*.

$$(3) \quad Q_{sub}(k,i) = \alpha \bullet (SM(k,i) - S_s(i)) \quad \left[m^3/S\right]$$

SM = *soil moisture*; S_S = *Soil saturation threshold*; α = *rate of infiltration* $\left[1/S\right]$;

$$(4) \quad Q_g(k,i) = \beta \bullet (H(k,i) - H(i)) \bullet A(i) \quad if\ \left(H(k,i) \geq H_S(i)\right) \quad \left[m^3/S\right]$$

SM_S = *Soil saturation threshold*; β = *constant rate of outflow* $\left[1/S\right]$;

Parameter

The saturated hydraulic conductivity as well as other variables were used as control thresholds in the model. The saturated hydraulic conductivity is the capacity of the soil to absorb water and before achieving saturation. This variable allows for assessing the water infiltration according to the rain intensity and the canopy pattern (for interception). Assessment of this parameter is important for modeling mainly for soil moisture state and the groundwater recharge. The saturated hydraulic conductivity was measured near stations throughout the basin several times between 2009 and 2012 with a mini disk infiltrometer (Decagon Devices, Inc.2365 NE Hopkins Court Pullman, WA 99163). At each station, the measurements were done at three locations around the station aiming to reduce the effect local spatial variability. The saturated hydraulic conductivity was compute by using the multiple head approach with Gardner's equation, which describes the relationship between the hydraulic conductivity and the pressure head, h (eq. 4.1).

$$K(s) = K_s \cdot e^{\gamma h} \qquad (4.1)$$

where K_s is the apparent field-saturated hydraulic conductivity, γ is a constant and is a measure of capillary forces and h is the pressure head.

For each sample two consecutives measurements were done exactly at the same location with two different suction strengths, 2 mbar and 4 mbar. Therefore, by solving the equation we are able to determine the saturated hydraulic conductivities, which are summarized in the table 1.

Location	Savannah Forest (hill)	Field (millet)	Outlet
Ks	37 mm/h	54 mm/h	11 mm/h

Table 1: Saturated hydraulic conductivity over the basin

These values are consistent with the porosity measurements over the basin at three locations, two at the AF and one at the SF. These locations were chosen over a top-bottom cross section that exhibits a significant difference in soil type (from top to bottom): sandy-loam soil with small stones (Hill), sandy soil (Field), and clay (Outlet).

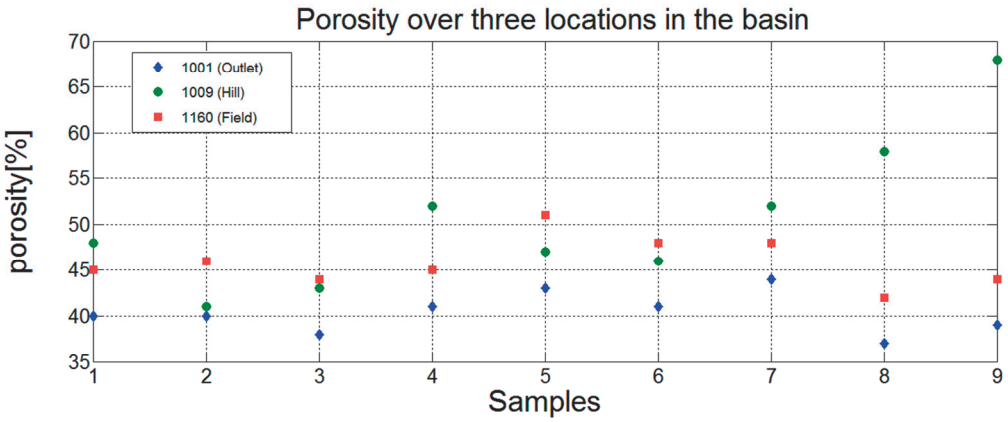

Figure 18: Porosity overall basin

The pore size is larger over the field (red dots) than the agricultural field (green dots), which is also greater than the basin outlet (blue dots). This structure is also validated by the fact the soil is more sandy in the field (sandy with small stone in the upper basin and mainly sandy clay in the outlet). This configuration also explains the pattern of the saturated hydraulic conductivity.

Reference

Constantz, J., Cl Thomas, and G. Zellweger. 1994. "Influence of Diurnal-Variations in Stream Temperature on Streamflow Loss and Groundwater Recharge." *Water Resources Research* 30 (12) (December): 3253–3264. doi:10.1029/94WR01968.

Findell, Kirsten L., and Elfatih A. B. Eltahir. 2003. "Atmospheric Controls on Soil Moisture–Boundary Layer Interactions. Part I: Framework Development." *Journal of Hydrometeorology* 4 (3) (June): 552–569. doi:10.1175/1525-7541(2003)004<0552:ACOSML>2.0.CO;2.

Juang, J.Y.I.H., G.G. Katul, A. Porporato, P.C. Stoy, M.S. Siqueira, M. Detto, H.S. Kim, and R. Oren. 2007. "Eco-Hydrological Controls on Summertime Convective Rainfall Triggers." *Global Change Biology* 13 (4): 887–896.

Muskat, M. 1937. "The Flow of Homogeneous Fluids through Porous Media."

Stull, Roland B. 1988. *An Introduction to Boundary Layer Meteorology*. New York: Springer.

Theophile Mande

mandetheophile@gmail.com
Burkinabe, born 02/12/1977
Languages: Moore (native), French (fluent), English (fluent).

Education

2009-2013 — **Ph.D in Environmental Engineering**
École polytechnique fédérale de Lausanne (EPFL), Switzerland
Hydrology of the Sudanian Savannah in West Africa, Burkina Faso.
Advisor: Marc B Parlange, Co-advisor: Alexandre Repetti

2005-2006 — **MSc, Specialization in Environmental Engineering**
International Institute for water and Environmental Engineering (2iE), Burkina Faso

2000-2005, 2006 — **Postgrad graduate (DEA) in Mathematics, operational research**
University of Ouagadougou, Burkina Faso.
Laboratory of Numerical Analysis Informatics and Biomathematics

Professional summary

2006-2008 — **Research assistant, CIRAD-2iE**
Teaching Assistant at 2iE, Statistic and Water resources management

2008-2009 — **Consultant-CIRAD**
Modeling risk in agriculture: case of Tougou in Burkina Faso
Design a model technical-demographic of Burkina Faso
Teaching professionals, GAMS General Algebraic modeling System

2007-2009 — **Consultant, BEM –Ingénieur conseil, Burkina Faso**
Tasks: Design of dams and irrigated perimeters

Publications

Mande et al, (2014) Toward a new approach for Hydrological Modeling: A tool for Sustainable Development in Savanna Agro-system. Technologies for Sustainable Development, J-C. Bolay et al (eds), 85-98, Springer International Publishing. DOI: 10.11007/978-3-319-00639-0_8
Mande et al (in prep), Suppressed convective rainfall by agricultural expansion in southeastern Burkina Faso. For submission in Nature
Mande et al (in prep) Stream response to a rain event in semi-arid region, Burkina Faso. For submission in Journal of hydrology
Mande et al (in prep) Two drivers for diurnal streamflow cycles in an ephemeral stream in West Africa, Burkina Faso. For submission in Water resource Research

Skills

Hydrological processes and water resources management. Designing of Dam and irrigated perimeter.

Software : ArcGIS, QGIS, MATLAB, GAMS, FLUENT, HYDRUS.

Mathematics: Operational research, Statistic and numerical analysis, EDP.

Field campaigns: Hydrometric and meteorological data observations and collect, experience inTougou (northern of Burkina Faso), Tambarga (south-east of Burkina Faso).

Personal interest

Football, Basketball, Dance and traveling.